TARGETING NANOPARTICLES TO TUMOR VASCULATURE

APPROVED BY SUPERVISORY COMMITTEE

Philip E. Thorpe, Ph.D

Michael Bennett, M.D.

E. Sally Ward, Ph.D.

Christoph Wülfing, Ph.D.

Rolf A. Brekken, Ph.D.

DEDICATION

To my parents for their support and to my friends who made me feel like I am at home in Dallas: Laurentiu, Alex, and Talabera

ACKNOWLEDGEMENTS

I would like to thank my mentor, Dr. Philip Thorpe, for supporting me and my research for the last six years. He taught me how to think as a researcher and to aim for the important findings. He tried to stimulate my imagination by always approaching me with the most unexpected questions. He tried to instill into me the most important quality of a pharmacologist: the ability to foresee a potential new drug.

I would like to thank to everybody in my lab for creating such a pleasant and productive environment to work in. Most significantly to Linda, who does everything from keeping the lab organized to remembering our birthdays; Xianming, who always has a solution for any experimental problem; and Shuzhen, for helping me with more columns and purifications than I can remember.

Last, but not least, I am thankful to Nancy McKinney in the Division of Basic Science who has provided solace on many occasions and to Karen Kazemzadeh for orchestrating the Immunology program and keeping everything on track

TARGETING NANOPARTICLES TO TUMOR VASCULATURE

by

ANDREI MARCONESCU

DISSERTATION / THESIS

Presented to the Faculty of the Graduate School of Biomedical Sciences

The University of Texas Southwestern Medical Center at Dallas

In Partial Fulfillment of the Requirements

For the Degree of

DOCTOR OF PHILOSOPHY

The University of Texas Southwestern Medical Center at Dallas

Dallas, Texas

June, 2008

TARGETING NANOPARTICLES TO TUMOR VASCULATURE

Andrei Marconescu, M.D., Ph.D.

The University of Texas Southwestern Medical Center at Dallas, 2008

Philip E. Thorpe, Ph.D.

Targeting tumor vessels represents an indirect therapeutic approach in oncology by shifting the treatment away from the tumor cells themselves. Endothelial cells are generally considered genetically stable and do not use escape mechanisms against chemotherapeutic agents as frequently as tumor cells do. Also, a very large number of tumor cells can be killed by ischemia if a single vessel is occluded.

Tumor vascular markers have been identified and monoclonal antibodies targeting them have been constructed in my laboratory. There are numerous

approaches to make antibodies more effective in cancer treatment. One option we have investigated is to use them for liposomal targeting to tumor vessels. Nanoparticles, and liposomes in particular, are extremely versatile because they can be adapted to carry drugs, imaging agents, or energy capture agents.

In my project, I have constructed liposomes targeted to three molecules identified as tumor vascular markers: VEGFR-2, phosphatidylserine (PS), and phosphatidylethanolamine (PE). To target VEGFR-2, I have used Fab' fragments derived from a series of rat monoclonal antibodies (RAFL) that bind to the extracellular domain of the receptor. For PS targeting, I used Fab' fragments derived from an anionic phospholipid binding antibody (bavituximab) and also a serum protein, beta-2-glycoprotein 1 (β2GP1). PE was targeted using a small antibiotic peptide, duramycin. All the liposome constructs bound to the purified target, as tested by solid phase assays. VEGFR-2 targeted liposomes bound to and were internalized by mouse endothelial cells expressing VEGFR-2. PS and PE targeted liposomes bound to endothelial cells that were subjected to stress factors that mimic the conditions encountered in the tumor environment. All the liposomes were also detected on the surface of endothelial cells inside tumors.

The tumor treatment potential was assessed by loading the liposomes with doxorubicin and treating mice in an orthotopic breast cancer model. The therapeutic benefit was also assessed for its ability to prolong survival in a lung pseudometastatic model. The tumor growth in the orthotopic model was not

inhibited by any of the constructs compared with control liposomes, but VEGFR-2 targeted liposomes extended the survival in the pseudometastatic model. These data suggest that VEGFR-2 targeted liposomes could potentially be used as an antimetastatic agent in combination with treatments that would target the tumor of origin.

PS and PE binding liposomes were also used as probes for describing the membrane localization and exposure dynamics of PS and PE on the surface of irradiated cells. I have shown that PS and PE follow a similar exposure time course and they colocalize on the cell surface. PS and PE positive membrane patches appear to detach from the cytoskeleton and bud out from the cell surface. These findings suggest that PE and PS share common regulatory mechanisms of membrane translocation.

Long circulating liposomes provide benefit through passive targeting to the tumor environment. My findings imply that active targeting by adding a ligand should be done with care, so as not to impede the passive targeting effect. Compared to other vascular targeting agents, liposomes require targeting to molecular markers that are more selective for tumor endothelial cells and also trigger internalization. Ideally, liposomes would encapsulate cell impermeable drugs for which intracellular delivery critically accounts for the cytotoxic effect.

TABLE OF CONTENTS

PRIOR PUBLICATIONS

A. Marconescu, P.E. Thorpe, Coincident exposure of phosphatidylethanolamine and anionic phospholipids on the surface of irradiated cells. Biochim Biophys Acta. 2008 in press - published online ahead of print (PMID: 18570887)

LIST OF FIGURES

10

LIST OF TABLES

LIST OF ABREVIATIONS

2-IT, 2-iminothiolane

ABAE, Adult aortic bovine endothelial cells

β2GP1, Beta-2-glycoprotein 1

bEnd.3, Mouse brain endothelial cells

DSPE, 1,2-Diostearoyl-sn-Glycero-3-phosphoethanolamine

DSPE-PEG-Mal, DSPE-polyethylene glycol - maleimide

DTT, Dithiothreitol

DXR, Doxorubicin

EC, Endothelial cell

ELISA, Enzyme linked immunosorbent assay,

$F(ab')_2$, An immunoglobulin molecule without the Fc fragment

Fab', A single monomer of the antigen binding fragment of an immunoglobulin

FBS, Fetal bovine serum

Flk-1, Fetal liver kinase 1, mouse homologue of VEGF receptor 2

IgG, Immunoglobulin type G

IHC, Immunohistochemistry

i.v., Intravenously

MFI, Mean fluorescence intensity

MFP, Mammary fat pad

MS1, Mouse pancreatic islet endothelial cells

MT1-MMP, membrane type 1-matrix metalloproteinase

VCAM-1, Vascular cell adhesion molecule 1

PC, Phosphatidylcholine

PE, Phosphatidylethanolamine

PEG, Polyethylene glycol

PG, Phoshphatidylglycerol

PI, Phosphatidylinositol

PL, Phospholipid

PS, Phosphatidylserine

RAFL, Rat anti Flk-1 immunoglobulin

sFlk, Soluble Flk, the extracellular domain of Flk-1

SM, Sphingomyelin

SSL, Sterically stabilized liposomes

TGFβ, Transforming growth factor β

VEGF, Vascular endothelial growth factor

VEGFR-1, VEGF receptor 1,

VEGFR-2, VEGF receptor 2

VLA-4, Very Late Antigen-4

CHAPTER I

INTRODUCTION

Tumor vascular targeting

A limiting factor for the growth of solid tumors is the development of functional blood vessels. Therefore, interfering with the blood supply has long been proposed as an alternative strategy in the arsenal of antitumor treatment methods [1]. Conceptually this can be done either by inhibiting the formation of new vessels, i.e. antiangiogenic therapy, or by destabilizing the already formed vessels, i.e. vascular targeting. The first proof of principle that vascular targeting can lead to complete destruction of a solid tumor was brought by Burrows and Thorpe in 1993, with the use of an immunotoxin targeted to a protein expressed on tumor endothelial cells [2]. The strategy for developing new vascular targeting agents is directed toward identifying specific molecular markers of the tumor blood vessels and developing effectors suitable for targeting those markers.

A good tumor endothelial marker is a molecule that is expressed either solely or at a higher level on the endothelial cells within tumors, as compared to normal vasculature. A variety of tumor endothelial cell markers have been described until now:

- molecules involved in angiogenesis and tissue remodeling: VEGF and its receptors [3-7], roundabout-4 (ROBO-4) [8], fibronectin extra-

domain B (EDB) [9-12], endosialin (TEM1) [13], integrin $\alpha_v\beta_3$ [14, 15], prostate-specific membrane antigen (PSMA) [16, 17], endoglin (CD105) [18]; CD44 variant 6 [19, 20], aminopeptidase N [21]

- molecules induced by hypoxia: endothelial-specific protein disulphide isomerase (*Endo*PDI) [22];
- adhesion molecules: VCAM-1 [23];
- molecules involved in coagulation homeostasis: phosphatidylserine (PS) [24-26], annexin A1 [27];
- molecules with yet unknown function: an orphan receptor (TEM5) and an anthrax-toxin receptor (TEM8) [28].

Ligands able to bind to these tumor endothelial markers have been developed. Monoclonal antibodies are the primary tool used for this purpose, offering a high specificity and also having an intrinsic effector activity through the Fc region that can trigger antibody-dependent cell-mediated cytotoxicity or complement-mediated cytotoxicity. Another approach was taken by using phage display techniques to find peptides that are able to bind with high specificity to the tumor endothelial cell markers [29]. New methods of screening have tested other classes of molecules for detecting specific ligands: random DNA oligonucleotides (aptamers) which have a theoretically huge number of sequence combinations as a pool of possible ligands [30, 31] and small molecule chemical libraries which offer the advantage of finding a ligand with high affinity and low

immunogenicity [32, 33]. Beside these screening based methods for finding ligands, other strategies have used the natural molecules that physiologically bind the tumor endothelial cell markers. VEGF has been conjugated to gelonin toxin for targeting to the tumor vasculature [34, 35].

To create the vascular targeting agents these ligands have been fused chemically or by recombinant expression to a variety of effector molecules that could damage the tumor vessels after homing to the tumor endothelial cells. The most used effector molecules are cytotoxic agents, toxins, coagulation factors, cytokines, and radioactive isotopes.

Liposomes

A separate approach in the field of the vascular targeting agents is represented by the vascular targeting nanoparticles. Nanoparticles are small particles with sizes ranging from 10 to several hundred nm. A particular type of nanoparticle is represented by liposomes, which are enclosed phospholipid bilayers, entrapping an aqueous compartment and suspended into an aqueous buffer. Liposomes conjugated to a ligand for a tumor vascular marker become vascular targeted liposomes. Conceptually, vascular targeted liposomes are an unusual type of vascular targeting agents, because the liposomes themselves are not the effector part per se, but only serve as carriers for other molecules with effector function. The classic application of liposomal carriers is the entrapment

of water soluble drugs in the internal aqueous compartment of the liposomes. Other methods of association of a load to the liposomes have been tested, such as insertion of hydrophobic molecules in the liposomal bilayer or chemical conjugation of small molecules and proteins to the liposomal wall [Fig. 1_1].

The first proof of principle for liposome use as a carrier for other molecules was brought more than 30 years ago by Gregoriadis and Ryman who managed to entrap an enzyme (amyloglusosidase) and albumin in liposomes formed by phosphatidylcholine and cholesterol and to deliver the load to rat hepatocytes *in vivo* [36, 37].

There are a number of benefits of using liposomes as drug carriers, part of them being related to the modification of the basic pharmacology of the drug. By encapsulation, the drugs loose most of their own pharmacokinetic parameters and borrow the parameters of the liposomes. These new parameters are completely different, since the liposome has a theoretical molecular mass that can be more than $2x10^5$ times larger than the one of the drug. The half life and area under the curve of the drugs from the anthracycline family (daunorubicin, DXR) can be increased by 27 fold when a liposomal form is used instead of the free drug. At the same time, the volume of distribution is decreased by approximately 40 times [38-41]. The combination of increased half life and decreased volume of distribution is translated into an increased accumulation at the tumor site and a decreased toxicity because the drug is not distributed into organs that are

responsible for toxicity [42]. The decrease of toxicity, quantified as a decrease of the maximum tolerated dose (MTD), allows the use of higher doses of cytotoxic agent [43]. Also, enclosing a drug inside a liposome allows it to travel through circulation without being subjected to early degradation and maintaining its activity until it is released at the tumor site.

Other factors that contribute to the enhanced accumulation of the liposomal formulation of drugs at the tumor site are the particularities of the tumor blood circulation. Unlike normal tissues, tumors have highly disorganized and convoluted vessels, with frequent shunts and irregular flow that can be very slow and occasionally reversed [44-47]. This produces a longer circulation time of the liposomes in the tumor vasculature relative to the normal organs, allowing longer contact with the tumor endothelial cells and longer time to diffuse into the extravascular space. Tumor vessel leakiness is another factor that enhances the escape of liposomes from the bloodstream into the interstitium. The tumor capillaries have defective endothelial monolayer, with a decreased association between the endothelial cells due to the, presence of interendothelial and transcellular openings and the absence of tight junctions. The size of these openings has been estimated to 100-600 nm, an ideal dimension for liposome extravasation. Furthermore, the material accumulates in the tumor insterstitium due to deficient lymphatic drainage [48-50].

Tumor vascular targeted liposomes

Targeting represents a very promising application of liposomal technology. Compared with other types of targeting agents, targeted liposomes offer an unmatched ratio of ligand/load; several thousand drug molecules can be targeted using only ten or twenty ligand molecules. A variety of targets and ligands have been employed for targeting liposomes to tumor vasculature [Table 1_1].

Cationic Liposomes

The simplest targeting method uses the positive electrical charge of the liposome surface instead of a specific ligand. Cationic liposomes are prepared so that 10% to 15% of the phospholipids have a positive electrical charge. There is a general tendency of the endothelial cells to uptake positively charged particles, this process is accentuated in certain organs: ovary, lung, hypophysis, and lymph nodes [51]. Angiogenic endothelium was studied in RIP-Tag2 transgenic mice and in a chronic inflammation model of infection with *Mycoplasma pulmonis*. In these two models, the activated endothelium presented a 15-33 fold higher uptake of cationic liposomes (containing 1,2-dioleyl-3-trimethylammonium-propane, DOTAP) compared with normal endothelium. More than half of the liposomes associated with the angiogenic endothelial cells were also internalized [52-54]. In spite of several successful therapeutic experiences with paclitaxel loaded cationic

liposomes it is still not clear what the precise target is on the endothelial cells [55-57]. Several hypotheses have been proposed and it is possible that more than one target cooperates for trapping the cationic liposomes: tumor endothelial cells have PS (negatively charged) externalized on the outer leaflet of the plasma membrane bilayer [24]; activated endothelial cells *in vitro* and also endothelial cells from the physiological angiogenesis in the corpus luteum have hyperglycosylation and hypersialyation of the membrane proteins, which present negative charge [58].

Ligand targeted liposomes

Most methods for liposomal targeting use a chemical conjugation to specific ligands. There are a series of defined molecular targets toward which liposomes have been targeted in this way, such as: α_v integrins, aminopeptidase N, membrane type 1-matrix metalloproteinase (MT1-MMP), VCAM-1, and endoglin (CD105).

Integrins are cell surface glycoproteins which are responsible for attachment of cells to the extracellular matrix. They present as non-covalently associated heterodimers with intracellular signaling upon engagement by ECM proteins or immunoglobulin superfamily ligands [59]. $\alpha_v\beta_3$ and $\alpha_v\beta_5$ integrin subclass expression is increased on the surface of endothelial cells during angiogenesis and remodeling. Ruoslahti and Pasqualini have used *in vivo* phage display and determined that peptides containing the sequence RGD have a high

affinity for angiogenic endothelium, binding to $\alpha_v\beta_3$ integrins [29]. Targeting with RGD peptides has since become the most widely applied method for liposomal tumor targeting applications, with almost 30 published studies being listed on PubMed. Both linear and cyclic RGD containing peptides have been used. A supplemental advantage of this approach is that RGD targeted liposomes are also internalized into endothelial cells after integrin binding [60, 61]. Drug loaded liposomes, as well as radio-sensitizers, have been successfully targeted to the tumor endothelial cells using RGD conjugated liposomes [61, 62].

Another molecular target identified by phage display techniques is aminopeptidase N (CD13). The same authors who identified the RGD peptides, Ruoslahti and Pasqualini, also found that peptides containing the sequence NGR home to endothelial cells within tumors by binding to aminopeptidase N [63, 64]. This protein is a cell surface attached protease with functions in tumor invasion and vascular mediated metastasis [65]. DXR loaded liposomes conjugated to NGR peptides were better than control liposomes at prolonging the survival of mice in an orthotopic model of neuroblastoma [66].

Another target, MT1-MMP, is an enzyme involved in angiogenesis. This enzyme is attached on the surface of endothelial cells by a transmembranar domain. MT1-MMP participates in the degradation of the extracellular matrix by cleaving collagen, fibrin, and laminin, and also by activating other matrix metalloproteinase (MMP-2 and MMP-13) [67-69]. MT1-MMP was shown to be

upregulated on the surface of tumor endothelial cells [70-72]. Small peptides with the sequence matching the substrate of the enzyme (GPLPLR) have been conjugated to liposomes to increase their homing to the tumor endothelial cells by about 4 times compared with control liposomes and provided tumor growth suppression in Colon 26 NL-17 carcinoma-bearing mice [60, 73]. The same target was used in a similar approach in which Fab' fragments of an anti MT1-MMP was conjugated to liposomes. These immunoliposomes bound to activate endothelial cells and brought a small improvement of the antitumor effect of the liposomal DXR [74].

VCAM-1 is an adhesion molecule belonging to the immunoglobulin superfamily. It is expressed on the surface of activated endothelium where it is engaged by VLA-4 molecules ($\alpha_4\beta_1$ integrins) on the surface of activated T and B cells to accommodate their extravasation [75]. VCAM-1 is not expressed on resting endothelium while it is found on the surface of endothelial cells in a diversity of solid tumors, such as lung, gastric, breast, and renal carcinomas [76-79]. Liposomes conjugated with an anti-VCAM monoclonal antibody (mAb) presented homing to activated endothelial cells *in vitro* and to endothelial cells within tumors [80, 81]. No tumor treatment with drug loaded liposomes targeted to VCAM-1 has been yet described.

Another molecule which has been tested as a target for liposomes is endoglin (CD105). Endoglin is a glycoprotein receptor that binds transforming

growth factor β (TGFβ) and is upregulated on the surface of endothelial cells during activation and during angiogenesis [82]. Endoglin is essential for proliferation and migration of endothelial cells, partially by negative regulation of TGFβ [83, 84]. A single-chain Fv fragment against endoglin was obtained by screening an antibody phage library and it was conjugated on the surface of PEG coated liposomes. The targeted liposomes showed specific association with activated endothelial cells *in vitro* and were also internalized. When the pharmacokinetics of these liposomes was assessed, they were cleared from the circulation extremely quickly (the circulating half-life being approximately 3 minutes, compared with 1.5 hour for control liposomes), suggesting that interaction with endoglin greatly impedes the long circulating qualities of the liposomes and limits their use *in vivo* [85].

The phage display techniques used as a tool for finding new tumor endothelial cell markers only lead to the identification of peptides that home to the tumor vessels. It takes an extra series of biochemical approaches in order to identify the molecular target of these peptides. Even if the second part of the process is not successful, one can use the identified peptide for tumor vessel targeting without the accurate knowledge of the target itself. Oku et al. found that peptides containing proline-arginine-proline (PRP) sequence or tryptophan-arginine-proline (WRP) sequence have an enhanced tumor vascular homing. A related peptide has been constructed (alanine-proline-arginine-proline-glycine;

APRPG) and was conjugated to liposomes. The targeted liposomes showed an increased accumulation in the tumor compared with control liposomes. Also, drug loaded liposomes targeted with APRPG peptides showed improved control of tumor growth in several tumor mouse models [86-88]. The target of PRP peptides is still unknown.

Recently, Roth et. al. tried to target liposomes to the tumor vessels by using Fab' fragments derived from DC101 monoclonal antibody, which binds VEGFR-2. The targeted liposomes were able to deliver DXR to the tumor site and to decrease the tumor growth compared with untreated animals, but no control liposomes were used. The specificity of the effect is therefore inconclusive [89].

These studies show that targeting liposomes to the tumor vasculature is a promising field, with some of the approaches leading to a good control of tumor growth. The endothelial cells are in direct contact with the blood and thus they are the most accessible target inside a tumor. The rate limiting factor for developing new tumor vessel targeting liposomes is the availability of new molecular markers for the tumor endothelial cells. Our laboratory is focused on the identification of such molecular markers and ligands for targeting them. The objective of my thesis project was to use newly developed tumor endothelial cell targeting molecules for creating vascular targeting liposomes.

Two classes of targets were used: VEGFR-2 and "inside out" phospholipids, each approach will be described in the following chapters. VEGFR-2 is already a classical player in the vascular targeting field with both antibodies and small molecules that bind it being developed [5, 90, 91]. For VEGFR-2 targeting, I used Fab' fragments derived from monoclonal antibodies, rat anti Flk (RAFL), previously developed by our lab [92]. The second class of targets, "inside out" phospholipids, encompasses phospholipids that are specifically exposed on the surface of tumor endothelial cells, PS and phosphatidylethanolamine (PE). These phospholipids are physiologically confined inside the cell, on the inner leaflet of the plasma membrane. It was shown that tumor endothelial cells expose these phospholipids on their surface due to the tumor environment rich in free oxygen radicals, cytokines, and also due to the hypoxia. Monoclonal antibodies have been developed that target PS and one of them (bavituximab) is currently undergoing clinical testing [25, 26]. Bavituximab binds PS containing membranes using a serum cofactor protein, beta-2-glycoprotein 1 (β2PGP1) [93]. Targeting liposomes to PS was done with two targeting ligands: Fab' fragments of bavituximab and β2GP1. For PE targeting liposomes, a small peptide (duramycin) that was previously shown to bind this phospholipid was used [94].

The liposomes were constructed either for detecting cell association or for testing the therapeutic benefit of the targeting. *In vitro* and *in vivo* binding to

endothelial cells was tested using fluorescent or biotinylated liposomes. Tumor growth inhibition in animal models was tested using liposomes loaded with a chemotherapeutic drug (DXR).

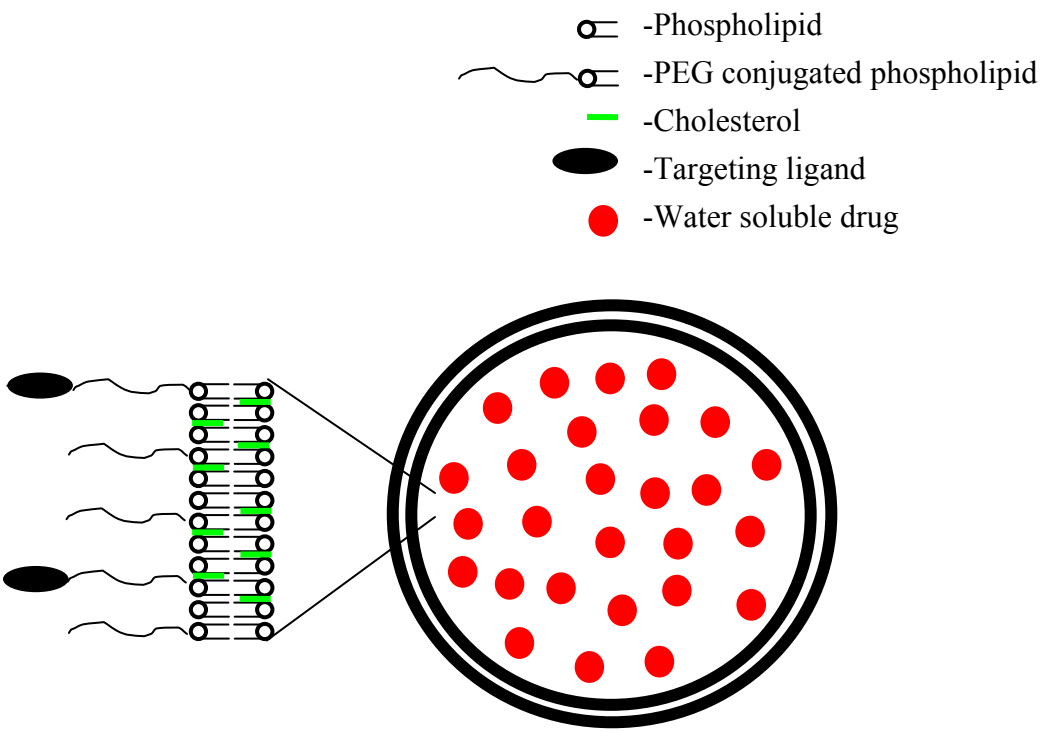

Fig 1_1: Schematic presentation of a targeted liposome
A liposome is a phospholipid vesicle enclosing an aqueous compartment and suspended into an aqueous buffer. The liposomal shell is formed by phospholipids and cholesterol arranged into a bilayer. A minority of the phospholipids carry PEG attached on their headgroup. Water soluble molecules can be trapped inside the liposome.

Table 1_1: Tumor vascular targeting liposomes			
Ligand/Targeting Method	Target	Results	Reference:
Cationic liposomes	PS Hyperglycosylated and hypersyalyated cell surface proteins	*In vitro* *In vivo* tumor localization, Tumor growth inhibition and prolonged survival	[55-57]
RGD peptide	α_v Integrins	*In vitro* *In vivo* tumor localization, Tumor growth inhibition and prolonged survival	[61, 62]
NGR peptide	aminopeptidase N (CD13)	*In vitro* *In vivo* tumor localization, Tumor growth inhibition and prolonged survival	[66]
GPLPLR or Fab' fragment	Membrane type 1-matrix metalloproteinase	*In vitro* *In vivo* tumor localization, Tumor growth inhibition	[60, 73, 74]
Antibody	VCAM-1	*In vitro* *In vivo* tumor localization	[80, 81]
Single chain Fv fragment	Endoglin (CD105)	*In vitro* only	[85]
PRP sequence containing peptide	Unknown	*In vitro* *In vivo* tumor localization and tumor growth inhibition	[86-88]
Fab' fragment of DC101 antibody	VEGFR-2	*In vitro* *In vivo* localization No proven therapeutic benefit	[89]

CHAPTER II

MATERIALS & METHODS

MATERIALS

Dulbecco's modified Eagle's medium (DMEM) and trypsin/EDTA were obtained from Mediatech, Inc. (Herndon, VA). Fetal bovine serum (FBS) was obtained from Biomeda (Foster City, CA). Bovine serum albumin (BSA), duramycin from *Streptoverticillium cinnamoneus*, pyranine (8-Hydroxypyrene-1,3,6-trisulfonic acid), pepsin and o-Phenylenediamine dihydrochloride (ODP) were obtained from Sigma-Aldrich (St. Louis, MO). Lipids for liposome preparation [Cholesterol (Ch), hydrogenated soy phosphatidylcholine (HSPC), 1,2-Distearoyl-Glycero-3-Phosphoethanolamine-N-[Methoxy(Polyethylene-Glycol)-2000] (DSPE-PEG), 1,2-Distearoyl-Glycero-3-Phosphoethanolamine-N-[Maleimide(Polyethylene Glycol)2000] (DSPE-PEG-Mal), 1,2-Distearoyl-Glycero-3-Phosphoethanolamine-N-[Biotinyl(Polyethylene Glycol)2000] (DSPE-PEG-Biotin)], and lipids for ELISA [phosphatidylcholine (PS), phosphatidylethanolamine (PE), phosphatidylglycerol (PG), phosphatidylinositol (PI), Sphingomyelin (SM)] were obtained from Avanti Polar Lipids (Alabaster, AL). Alexa-Fluor 594 and Alexa-Fluor 700 conjugated streptavidin was obtained from Molecular Probes (Invitrogen, Carlsbad, Ca). Horseradish peroxidase conjugated streptavidin was obtained from Jackson ImmunoResearch Labs (West

Grove, PA). 96-well Immulon-1B microtiter plates were obtained from Thermo LabSystems (Franklin, MA). Glass Bottom culture plates were obtained from MatTek Corporation (Ashland, MA). Adult bovine aortic endothelial cells (ABAE) were obtained from Clonetics (Walkerville, MD). NSO mouse myeloma cells were obtained from Sigma. Sephacryl S-300, and Sephadex G-25 were obtained from Pharmacia Biotech (GE Healthcare, Piscataway, NJ). The liposome extruder and polycarbonate membranes were purchased from Northern Lipids Inc (Vancouver, British Columbia, Canada). Iodogen and Sulfo-NHS-LC-Biotin was purchased from Pierce (Rockford, IL). ^{121}I was purchased from Amersham Biosciences (GE Healthcare, Piscataway, NJ).

LIPOSOME PREPARATION

All liposome types were initially prepared by using the lipid film hydration method, as previously described [95]. This step is used to obtain a homogeneous population of liposomes of ~ 100 nm which will be further processed or conjugated to various ligands as needed. The liposome shell is formed by a mixture of HSPC/Cholesterol/M-PEG-PE/Mal-PEG-PE at a molar ratio of 2/1/0.08/0.02, unless otherwise specified. All aqueous buffers were deoxygenated by argon flushing through a gas dispersion tube and all columns were washed with such buffers. The liposomes were coated with PEG in order to assure minimal unspecific binding. The ligands were conjugated on the surface of

the liposomes by a thioether bond. A fraction of the liposomal PEG molecules has maleimide moieties, which reacts with free SH groups of the Fab' fragment or of a thiolated protein or peptide.

Dry lipid film preparation

The lipid stock was kept at -80 °C and dissolved into a mixture of chloroform/methanol: 1/1. Each phospholipid or cholesterol solution was measured using a Hamilton syringe and mixed in a glass bulb with schlenk adapter. The lipid film was obtained by drying the mixture using a vacuum rotary evaporator (BÜCHI Rotavapor R-114, BÜCHI Labortechnik AG, Switzerland) with a water bath at 65 °C. To remove any trace of chloroform and methanol, the lipid film was kept in a vacuum overnight at room temperature.

Lipid film hydration and extrusion

The lipid film was hydrated by adding a warm aqueous buffer (65 °C) and vigorous vortexing. To obtain a large unilamellar vesicle suspension, the solution was sonicated for 10 minutes in a water bath sonicator. The suspension was subsequently extruded 20 times at 65 °C using LIPEX extruder with thermo-barrel (Vancouver, British Columbia, Canada) attached to a pressurized argon tank and loaded with a polycarbonate membrane with 100 nm pores. Extrusion decreased the opacity of the solution and the liposomes size to ~ 100 nm. After extrusion, the different types of liposomes were subsequently conjugated or underwent a separation process.

Biotinylated liposomes

Biotinylated liposomes had a slightly modified lipid mixture, HSPC/Cholesterol/M-PEG-PE/Biotin-PEG-PE/Mal-PEG-PE at a molar ratio of 2/1/0.06/0.02/0.02, respectively. The hydration was done using HEPES buffer (20 mM Hepes, 150 mM NaCl, pH: 7.4). After extrusion, the liposomes were directly used for conjugation reactions.

Fluorescent liposomes

Fluorescent liposomes were composed from a standard lipid mixture. The hydration buffer was HEPES buffer supplemented with either 5 mM pyranine (8-Hydroxypyrene-1,3,6-trisulfonic acid) or Sulphorhodamine 101 (2 mM concentration). After the extrusion, the liposomes were separated from un-encapsulated dye on a G-25 column and subsequently used for conjugation.

DXR loaded liposomes

The liposomes for DXR loading have a standard lipid mixture. For the hydration, an ammonium sulphate buffer was used ($(NH_4)SO_4$ 155 mM, pH=5.5). After the hydration and extrusion, the liposomes were cooled at the room temperature and a pH gradient between the inside and the outside of the liposomes was generated. The extraliposomal buffer was exchanged to the loading buffer (sodium citrate 123 mM, pH=5.5) using a G-25 column. The DXR was dissolved into the same loading buffer and added to the liposome suspension, in a DXR / PL ratio of 2 mg / 10 mg. The total volume of the loading solution was

adjusted for obtaining a PL concentration of 5 mg / ml. The suspension was maintained at 65 °C for 1h, with occasional mixing. After the DXR was loaded into the liposomes, the solution was brought to room temperature and the liposomes were separated from non-encapsulated DXR, using a G-25 column and HEPES buffer. Free DXR has a small affinity for the G-25 resin, therefore it's retarded on the column and very large sample volumes can be used (50 ml sample can be separated very well on a 130 ml column). After separation, the DXR-loaded liposome suspension was concentrated using a pressure Amicon concentrator with a 500 KDa MW cutoff. The concentrated suspension was used for conjugation to thiolated protein and peptides. At the end of the conjugation reaction, the total DXR encapsulated in the final product was quantified by dissolving the liposomes into a Triton X-100 solution, measuring the optical density of the DXR at 482 nm, and comparing it to a standard curve of free DXR in the same solvent.

PREPARATION OF THE THIOLATED LIGAND

Fab' Preparation

Antibody producing hybridoma cells (RAFL 1, RAFL 2, MAC 157, MAC48) were expanded in DMEM supplemented with 10% FBS, 1 mM Na pyruvate, non-essential aminoacids, and 2-mM L-glutamine and maintained until exhaustion of medium. Medium was harvested, cells were removed by

centrifugation. Antibodies were purified on a protein G immobilized column using low pH elution method (pH=2.8). After purification, the antibodies were dialyzed in PBS and the concentration was adjusted to ~ 1 mg/ml. The pH was decreased using citric acid, pepsin was added and the solution was incubated at 37 °C for 30-70 minutes. The pH, pepsin concentration and the length of incubation for each antibody was previously established [Table 3_2]. After digestion, the pH was elevated to 7.5 and the $F(ab')_2$ were purified using FPLC on S200 column. The $F(ab')_2$ was concentrated to 2.5 – 5 mg/ml.

For a better quantification of the subsequent conjugation reaction with liposomes, the proteins were radiolabeled. A 50 µl aliquot of the $F(ab')_2$ was radiolabeled using ^{125}I, before doing a reduction reaction to Fab'. The radiolabeled protein was mixed with the cold protein, in a ratio which provides ~ 1000 cpm / µg $F(ab')_2$. The mixture of hot + cold protein was reduced using DTT. After reduction any DTT trace was removed using a G-25 column, and the Fab' was reacted with maleimide containing liposomes, as described.

Protein/Peptide Thiolation

β2GP1 and BSA were thiolated using Traut's reagent (1-iminothiolane). The pH of the protein solution was raised to 8 – 8.1, using tri-ethyl-ammonium and Traut's reagent was added at a 3-5 X excess molar ratio. For the thiolation, peptides (Duramycin), were dissolved in 0.1 m NaHCO3 (pH 8.1) before adding

Traut's reagent. The reaction incubated for 30' at RT and the protein was used for conjugation to liposomes.

CONJUGATION TO LIGANDS

For the conjugation reaction, the maleimide containing liposomes were mixed with freshly thiolated ligands (Fab' fragments, other proteins, or peptides). The mixture was kept under argon, at room temperature for 48h, with continuous stirring. The reaction was stopped by blocking the free maleimide groups with cysteine (adjust the solution to 1 mM cysteine for 1h). Once the reaction was complete, the liposomes were separated from unconjugated ligands. When the ligands were proteins (e.g. Fab' fragments, BSA, β2GP1), the liposomes were separated using an S-300 gel filtration column; when the ligands were peptides (e.g. duramycin) the liposomes were separated from unreacted peptide using a G-25 column. Before the conjugation reaction, the proteins were radiolabelled with ^{125}I as described in the following section. The conjugation efficiency, the amount of free protein, and conjugated protein were quantified by measuring the radioactivity of each fraction collected from the gel filtration columns.

SOLID PHASE ASSAY FOR TARGET BIDING OF LIPOSOMES

Bavituximab and duramycin conjugated liposomes were tested by this method for binding to various PL. RAFL 1 and RAFL 2 conjugated liposomes

were tested for binding to the sFlk. BSA, Rituxan, or MAC157 conjugated liposomes, as well as non-conjugated liposomes were used as controls.

For the PL binding assays, the different PLs were dissolved in n-Hexane (100 μg/ml). 50 μl of this solution was added to each well of a 96 well plate. The solvent was evaporated at RT and the plates were blocked with 10% FBS in Hepes buffer for 2 hours at 37 °C. For sFlk immobilization, the protein was coated on the plate using carbonate buffer followed by blocking. The liposomes were diluted in the same buffer and incubated on the plates for 2h, at 37 °C, starting with 0.25 mg phospholipid/mg. Because a liposome suspension contains mostly phospholipids and the targeting agent (Fab' or peptide) represents just a minority of the total mass (~ 1% protein), the solution was normalized for phospholipid concentration. For the experiments using biotinylated annexin V, this was diluted in the same buffer, supplemented with 5 mM CaCl2, at an initial concentration of 10 μg/ml, and incubated for 2 hours at 37 °C. After washing, different types of liposomes were detected using specific methods:

a) biotinylated liposomes, or biotinylated annexin V: HRP conjugated streptavidin (1:2000 dilution in the same buffer) followed by ODP developing reagent were used. The plates were read at 490 nm using a microplate reader, 7525 Microplate Reader, Cambridge Technology, Lexington, (MA).

b) fluorescent liposomes and DXR filled liposomes: triton X-100 solution (0.02 %) in 0.01 M HCl was used to dissolve the pyranine filled liposomes

attached to the wells and Triton X-100 (0.02%) in water was used for sulphorhodamine or DXR filled liposomes. The fluorescence was detected using 96 well plate reader fluorimeter . For pyranine, the excitation and emission filters used were 360 nm and 520 nm, respectively. For sulphorhodamine, excitation filter was at 544 nm and emission filter was 590 nm. DXR was detected using excitation at 485 nm and emission at 590 nm.

INDUCTION AND DETECTION OF PS AND PE ON IRRADIATED CELLS

PS and PE quantification on the surface of irradiated endothelial cells

ABAE cells were plated on glass bottom dishes (35 mm) at a density of 80.000 / dish, and maintained in DMEM supplemented with 10% FBS, 1 mM Na pyruvate, non-essential aminoacids, and 2-mM L-glutamine. The cells were γ-irradiated and stained 24 hours later using PS or PE detecting liposomes. The liposomes were filled with pyranine and conjugated to Fab'of bavituximab or to duramycin, for detection of PS and PE, respectively. The cells were imaged using a TE2000-U Nikon inverted microscope, equipped with a 10x objective and a Roper Scientific ccd camera. The images were analyzed using ImageJ software. For each image, the integrated intensity value was normalized for the number of cells.

PS and PE colocalization studies

For double staining, z-sectioning and 3D reconstruction, endothelial cells grown in glass bottom plates were stained 24 hours after 5 Gy γ-irradiation. For PS I used one step labeling with pyranine filled liposomes conjugated with Fab' of bavituximab. For PE I used a two step staining method, with biotinylated liposomes conjugated to duramycin, than Alexa Fluor 495 conjugated streptavidin. The cells were imaged using Applied Precision Deltavision RT deconvolution microscope, equipped with Olympus, oil immersion 40x and 60x objectives. The images were processed and the 3D reconstruction was done using Imaris software (Bitplane Inc.).

Induction and Detection of PS and PE on Myeloma Cells

NS0, mouse myeloma cells were maintained in the same medium as ABAE cells and irradiated with 5 Gy. At various time points later, the cells were harvested by tapping the flask. Cells were stained with pyranine filled liposomes for PS and biotinylated liposomes followed by Alexa Fluor 700 conjugated streptavidin for PE. Dead cell nuclei were stained using propidium iodide. The cells were analyzed using BD LSR II flow cytometer (BD Biosciences). Pyranine was detected on FL4 channel (excitation: Violet (405), Emission: 515/20) while Alexa Fluor 700 was detected on FL11 (excitation: Red (625), Emission: 730/45) and propidium iodide on FL2 (excitation: Blue (488), emission: 675/40. The data was analyzed using FlowJo software (Tree Star, Inc.).

BINDING AND INTERNALIZATION OF VEGFR-2 TARGETED LIPOSOMES TO MOUSE ENDOTHELIAL CELLS

Cell imaging

Mouse endothelial cells (bEnd.3, MS-1) were plated in the same medium as ABAE cells in 8 well chamber slides (BD Biosciences), at a concentration of 20000 cells / well. Fluorescent, RAFL conjugated liposomes were incubated in the chambers for 1h at 37 °C, followed by washing, fixation with 4% PFA, nuclear staining with Hoechst 33342, and mounting in Vectashield mounting media (Vector Laboratories). The slides were imaged using Nikon Eclipse E6000 microscope with a Coolsnap digital camera (Photometrics, Tucson, AZ).

Flow-cytometry

The mouse endothelial cells were grown in T175 flasks and detached using Trypsin EDTA. Equal numbers of cells were placed in 12 x 75 mm FACS in 100 µl and incubated with 5-10 µl liposome suspension for 1-3 h. The cells were washed, stained with propidium iodide and the FACS data was acquired on a BD LSRII flow cytometer using BD FACS DIVA software.

TREATMENT OF ORTHOTOPIC BREAST CANCER MODEL

Human breast cancer cells (MDA-MB-231) were implanted into the MFP of athymic female mice (Ncr nu/nu). Mice were anesthetized and a 3-5 mm incision was made on the skin of the right side of the thorax. $4x10^6$ cells were

injected into the MFP and the skin was closed with a metallic staple. The mice were randomized in the treatment and control groups. Liposomal DXR, free DXR or HEPES control was administered by i.v. injection, every 5 days. DXR was administered at a dose of 3-5 mg/kg, each injection. Tumors were measured using a caliper and the tumor volume was estimated as (small diameter x large diameter^2)/2. Mice were assessed for toxicity by monitoring the weight.

TREATMENT OF PSEUDOMETASTATIC BREAST CANCER MODEL

For the pseudometastatic animal model MDA-MB-231 human breast cancer cells and nude mice (Ncr nu/nu) were used. $1x10^6$ cells were injected i.v. into the tail vein of female mice. Liposomal DXR, non-liposomal DXR, or HEPES buffer was administered each 5 days, starting 10 days after cell injection. DXR was used at a dose of 3 mg / kg / injection. Mice were monitored for weight and sacrificed when showed sign of disease (decrease of weight with > 20%). The anesthetized mice were perfused with saline solution and organs were harvested and fixed in Bouin's fixative solution for later counting of metastatic colonies.

BIODISTRIBUTION OF BIOTINYLATED LIPOSOMES

MFP tumors were grown in nu/nu mice, as previously described. 100 μl of liposomal suspension (0.1-0.2 mg PL total) was administered into the tail vein. At various time points afterward, the mice were heparinized (1000 u of heparin i.p.)

followed at 30 min by anesthesia and perfusion with saline solution. Tumors, kidney, liver and spleen were harvested, frozen in liquid nitrogen and stored at -80 °C. The liposome binding to the vessels in various organs was detected by immunohistochemistry. 10 μm thick sections were cut using a cryostat (Leica CM3050S). The liposomes were detected using streptavidin conjugated fluorophores or horseradish peroxidase. The vessels were detected by staining with an anti CD31 antibody

.

CHAPTER III

MANUFACTURE AND CHARACTERIZATION PROCESS OF TARGETED LIPOSOMES

INTRODUCTION

Liposomes are nanoparticles formed by an enclosed phospholipid bilayer. The phospholipids have an amphipathic character; the fatty acid residues are hydrophobic while the ionized head-groups are hydrophilic. This dual affinity for different types of solvents makes them organize spontaneously in the presence of polar or nonpolar solutions. In aqueous buffer, the hydrophilic fatty acid residues are clustered together while the ionized headgroups are exposed to the water molecules. The conformations that can be obtained in such conditions are micelles or bilayers; this depends on the size of the head-group and the length of the fatty acid chains. For certain phospholipids, such as phosphatidylcholine, the most favorable conformation taken is an enclosed membrane bilayer, i.e. a liposome.

Lipid composition

The lipid composition for the liposomal shell is optimized for assuring minimal unspecific interaction in circulation, high stability, and low spontaneous release of the encapsulated drugs. Phosphatidylcholine is the most widely used

phospholipid for constructing targeted liposomes due to the overall neutral charge at physiologic pH. Saturated fatty acids are preferred, since they have a higher phase transition temperature and help the formation of a more rigid liposomal shell [96]. The presence of cholesterol contributes to the decrease of drug leakage and an increase in the stability of the liposomes [97-99].

The introduction of the concept of sterically stabilized liposomes (SSL) was a very important advancement in the nanoparticle field. Covering the surface of the liposomes with a hydrophilic polymer provided a colloidal stabilization of the particles [100-103]. Compared to the conventional liposomes, the SSL are more stable and do not aggregate. The unspecific interaction with plasma proteins and blood cells is decreased and the circulation half-life is increased [102, 104-106]. The most frequently used method for liposome stabilization is coating with PEG. A variety of PEG molecules of different lengths are available, already conjugated to a lipid anchor (PE). 5% PE-PEG(2000) molar ratio of PL in the liposomal composition confers an optimal stabilization of the liposomes without impeding the drug loading efficiency [107, 108]. The liposomes used in our experiments were all formed by a mixture of HSPC / Cholesterol / PE-PEG(2000) = 2 / 1 / 0.1, molar ratio.

Construction of the liposomes

The final product used for drug targeting in an animal model is obtained in a multistep process: formation of the liposomes shell, loading with the drug, preparation of the reactive ligand, conjugation of the ligand with the liposomes, and final purification of the targeted liposomes [Fig. 3_1].

Regardless of the particular method used to obtain the liposome shell, similar steps are employed in all processes: 1) the lipids are mixed in an organic solvent, 2) the solvent is replaced with an aqueous buffer, and 3) the vesicles are processed for decreasing their size and obtaining a homogeneous population.

The first step is similar for most methods, and involves mixing the different phospholipids used for liposome preparation, as well as cholesterol, into an organic solvent; usually a 1/1 chloroform/methanol solution. The solvent is then evaporated and the lipids form a thin film which is adherent to the walls of the recipient. Various methods have been used for hydration of the lipid film: reverse phase evaporation, detergent depletion, and direct hydration. For the reverse phase evaporation, the lipid film is solubilized using a very volatile solvent (such as diethyl-ether). A small amount of aqueous buffer is added while the organic solvent evaporates. This is a very good method when a high efficiency of aqueous buffer encapsulation is needed [109]. The detergent depletion method involves solubilization of the lipid film using a detergent solution in aqueous buffer, followed by the slow removal of the detergent using a variety of methods: detergent absorbing resins, dialysis, or gel filtration. While the detergent is

removed, the phospholipids organize into membrane bilayers [110]. This method is very gentle and useful for the incorporation of transmembrane proteins into the lipid bilayer. For drug targeting purposes, the most widely used method is the direct hydration of the lipid film using the aqueous buffer. Vigorous vortexing and sonication disrupts the lipid film and leads to the formation of a suspension of closed, large multilamellar vesicles with diameters ranging from 0.5 to several microns [111]. The size of the multilamellar vesicles can be decreased using a high pressure homogenization method. The method of choice for the laboratory setting is extrusion. This method uses a high pressure chamber to force the vesicle suspension through a polycarbonate membrane having a defined pore size. Using specific membranes, the size of the liposomes obtained can be controlled between 30 and 400 nm [112, 113].

In my experiments, I used direct hydration of the lipid film followed by extrusion through a 100 nm pore size polycarbonate membrane. This method yields liposomes with an average diameter of 100-150 nm.

The liposomes I constructed were used mainly for two purposes: tumor treatment or detection of cellular association *in vitro* or *in vivo*. For tumor treatment, the liposomes were loaded with DXR. For cell binding experiments, I needed a system for detecting liposomes. Filling the particles with a fluorescent solution was a simple and efficient method for *in vitro* experiments. These liposomes were useful for both fluorescence microscopy and FACS. For tumor

localization experiments and biodistribution analysis, the liposomes were biotinylated.

DXR loading

Liposomes enclose an aqueous compartment in which hydrophilic molecules can be trapped. The simplest method for introducing a molecule inside the liposomes is to have it dissolved in the buffer used for lipid film hydration. After the liposomes are formed, the non-entrapped molecules can be removed by gel filtration. Unfortunately, this method has a very low efficiency, with less than 20% of the original amount of drug being captured in the liposomes. Weak bases, like DXR, can be loaded into the liposomes after their formation, using a pH gradient [114, 115]. This method is very efficient, with encapsulation of more than 90% of the drug used. The process is based on the ability of the non-ionized form of the drug to penetrate through the liposomal membrane. A pH gradient is formed between the enclosed liposomal compartment (more acid) and the outside buffer (neutral pH). DXR (pKa = 8.6) is non-protonated in the external buffer and can traverse across the membrane. Inside the liposome, it becomes protonated and subsequently trapped. The loading process is more efficient than the pH gradient would predict. This is due to precipitation of the drug inside the liposomes, which decreases the number of the internal soluble molecules and provides an enhanced

driving force for accumulation [115]. The final intraliposomal DXR concentration is above the aqueous solubility limit of the drug [114].

The particular method I chose for DXR loading is creating the pH gradient using an amine gradient [Fig. 3_2]. The liposomes are formed and extruded in an ammonium sulfate buffer. The external buffer is exchanged for one without ammonia. The ammonia from inside the liposome leaks freely through the membranes, according to its concentration gradient, leaving the inside with an excess of protons thereby creating the pH difference.

For cell association experiments the liposomes were either filled with a fluorescent solution or they were biotinylated. For the fluorescent liposomes, highly hydrophilic fluorophores were used, which do not leak out of the liposomes: 8-Hydroxypyrene-1,3,6-trisulfonic acid (pyranine) and Sulphorhodamine 101. Both flurophores have very good water solubility. Additionally, pyranine has fluorescence at both neutral pH and acid pH, being suitable for detection even if the liposomes are internalized into acidic compartments of the cells [116, 117]. For biotinylation, the lipid mixture of the liposomes contained PE-PEG-Biotin.

Ligand coupling

Targeting liposomes involves a chemical conjugation of the liposome shell to a molecule with high affinity for tumor endothelial cells. The techniques used for the coupling should be efficient and reproducible while the chemical bond should be stable in circulation and lacking toxicity. Because the liposomes are covered in PEG, direct conjugation of the ligand to the liposome surface could lead to an impeded interaction of the ligand to the target [118, 119]. Therefore, the coupling is done on the terminal end of PEG. In this way, the ligands have free access to the target and also the PEG confers a higher mobility. I chose maleimide ending PEG, which is able to react to free thiol moieties on the ligand. PE-PEG(2000)-Mal is commercially available and it was incorporated in the lipid composition of the liposome shell. The maleimide to thiol conjugation confers the advantages that the thioether bond formed with the ligand is stable after injection in circulation and that the thiolation chemistry for proteins and peptides is straightforward and reproducible [Fig. 3_3].

The ligands coupled to the liposomes were Fab' fragments, other proteins, and peptides. For Fab' fragments the coupling chemistry used the endogenous thiol residues of the Fab'. The conversion of an antibody to Fab' fragment is done in two steps: 1) the antibody is digested using pepsin producing $F(ab')_2$ and 2) the $F(ab')_2$ is reduced to Fab' fragment using DTT. The advantage of this method is that the thiol group is generated by reducing the disulfide bonds between the heavy chains and avoids the introduction of additional thiol groups which renders

the risk of multiple thiolation or thiolation on the antigen binding region of the Fab' fragments [120-122]. The endogenous thiol is located in the hinge region of the Fab' fragment which, after coupling with the liposomes, is optimally oriented for antigen binding [Fig. 3_4 A].

Other targeting agents used for liposome conjugation in our experiments were proteins (β2GP1) or peptides (duramycin). The ligands were thiolated at the free amino groups using Traut's reagent. To reduce the chance of multiple thiolation, a low molar ratio of Traut's reagent to the ligand was maintained (3-6 x) [Fig 3_4 B and C].

The results presented in this chapter describe the liposome manufacture process from a biophysical point of view. The size and structure of the liposomes was analyzed by electron microscopy and dynamic light scattering, while the protein conjugation was analyzed by chromatography.

RESULTS

Visualization and measurement of the liposomes

Liposomes were formed by direct hydration of a dried lipid film followed by extrusion through polycarbonate membranes with 100 nm pores. The composition of each liposome type is presented in Table 3_1; 5% of the phospholipids contained PEG, in the form of PE-PEG(2000). 20% of the PEG molecules carry maleimide moieties, which accounts for approximately 2500 molecules on the surface of each liposome. After formation and conjugation to Fab' fragments, the liposomes were visualized using electron microscopy. Liposomes were absorbed on the surface of coated grids and negative staining was done using a vanadate solution. The images show liposomes which appear to be unilamellar. Due to a flattening effect, the measured size of the liposomes was on average 150-160 nm, which is slightly larger than that predicted by the extrusion. The liposomes were separate from one another, and large particles which might have been created by fusion were not observed [Fig. 3_5].

The liposomes were also measured using dynamic light scattering. The results [Fig. 3_6] show a single, homogeneous population of liposomes with an average diameter of 160 nm. There were no large aggregates of liposomes; these would appear as particles with larger diameters.

DXR filled liposomes were visualized using electron microscopy with negative staining. Upon loading into the liposomes, DXR concentration increased above the solubility limit and DXR precipitated, forming crystals which organize in large bundles. The DXR bundles were visualized by EM inside the liposomes. The DXR filled liposomes maintain better their shape on the grid, compared to the empty liposomes, possibly because the DXR bundles offer a support for the liposomal membrane [Fig. 3_7].

Fab' fragment preparation for conjugation to liposomes

Using intact antibodies for targeting liposomes was proven to be less beneficial than Fab' fragments. The presence of the Fc fragment of the antibody made the targeted liposomes bind to cells with Fc receptors. To eliminate the Fc fragments, the antibodies were digested to $F(ab')_2$, using pepsin, as described in Table 3_2. The digestion process decreased the molecular weight of the antibody from 150 KDa to approximately 110 kDa for $F(ab')_2$ [Fig. 3_8]. The most physiological manner for chemical conjugation of an Fab' fragment to a liposome is to use the intrinsic thiol group from the hinge region. The disulfite bond between the heavy chains was reduced using DTT [Table 3_3], before conjugation to the maleimide containing liposomes. The Fab' molecular weight is approximately 55 kDa [Fig. 3_8]. In this way, the hinge region will be oriented toward the liposome, while the antigen binding part is oriented toward target.

Introducing a supplemental thiol group on the molecule would be a less challenging method, but it would pose the risk of uncontrolled positioning and orientation of the Fab' fragments.

After the conjugation reaction, the targeted liposomes were separated from the unconjugated protein, using gel filtration. A high molecular weight resolution resin was chosen (Sephacryl S-300). The liposomes are above 100 nm in size, while the maximal cut-off size for the molecules resolved on this resin is 12 nm. In this way, the liposomes exit the column with the void volume, while the unconjugated proteins are delayed [Fig. 3_9]. Because the presence of phospholipids and DXR does not allow a colorimetric detection of the proteins, the method used for quantification of the conjugation efficiency was to radiolabel the $F(ab')_2$ before reduction and conjugation. The amount of conjugated protein and free protein was assessed by measuring the radioactivity in each chromatographic fraction.

DISCUSSION

The data presented in this chapter represent the key elements in the manufacturing process of the liposomes used for vascular targeting of DXR. These are: the formation of the liposome shell, loading of the liposome with DXR, formation of the thiol containing Fab', and assessment of the conjugation reaction.

The hydration of a dried lipid film results in a variety of large vesicles which are broken into smaller particles by extrusion. In spite of the fact that the extrusion was done through membranes with 100 nm pores, the final size of the liposomes measured by both EM and DLS was around 140-160 nm. It is likely that the real dimension of the liposomes is smaller than these values. For the EM imaging, the liposomes absorbed on the grid are dried and flattened. This would make them appear larger than the real dimension in water suspension. The second measurement technique (DLS) is based on the change in the light scattering pattern by the particles undergoing a Brownian movement. The liposomes constructed have 5% PE-PEG(2000). At this concentration the PEG molecules are straight, in a "brush"-like conformation on the surface of the liposome, increasing the apparent radius by at least 4.5 nm [123]. PEG also is highly hydrophilic, approximately 210 water molecules are bound to a PEG(2000) chain [124]. These water molecules form an adherent "coat" around the liposome surface, the effect

of which will be a decrease of the liposomal mobility, which will lead to an apparently larger volume as measured by DLS. Therefore it is likely that the real dimension of the liposomes is smaller than the measured one (of approximately 140-160 nm). Still, the size can be larger than 100 nm, because the extrusion is done at 65°C, which is above the phase transition temperature of HSPC. This temperature allows the phospholipid membrane to undergo deformation and particles larger than the pore size to form [123].

After liposome formation, the DXR loading into the liposomes was done using an ammonium sulfate gradient. The loading efficiency was assessed spectrophotometrically, by comparing the DXR optical density in the liposomal fraction with a standard curve of solubilized DXR. The results show that 1 μg DXR corresponds to approximately 6.2 μg phospholipids. Based on the surface area of each phospholipid molecule on the liposome membrane it was assessed that there are approximately 7.8×10^{12} liposomes for each micromole of PL [119]. By extrapolation, we can conclude that there are approximately 25000 DXR molecules enclosed in each liposome [Table 3_4].

The ligand conjugation on the surface of the liposomes involved either the used of intrinsic thiol group of the Fab' fragments, or introducing a supplemental thiol group for β2GP1 or duramycin. The most difficult method is the first one, because the reduction process of the $F(ab')_2$ to Fab' is never perfect; one has to compromise between too much reducing agent, which leads to total reduction to

heavy and light chains, or too little reducing agent which is not enough for obtaining sufficient Fab' fragment. The reduction efficiency to Fab' is rarely higher than 50%. The under-reducing reaction pose a lesser danger for the quality of the final product, because intact $F(ab')_2$ fragments will not be able to enter conjugation reaction. The over-reducing reaction is less desirable because free heavy and light chains have available thiol groups that will react with the liposomal maleimide without being able to contribute to targeting. RAFL antibodies are rat IgG_{2a} while bavituximab is a human IgG1. These antibodies have a hinge region containing 3 cysteine residues. When $F(ab')_2$ fragments are reduced, all three disulfide bonds must be reduced in order to obtain Fab'. The successful preparation of the conjugated particles suggests that maleimide moieties on the liposomes surface reacts with one to three free SH groups on one Fab'. Conjugation of one Fab' to multiple liposomes is unlikely to occur since this would lead to large complex formations and precipitation of the suspension.

Conjugation efficiency was easily assessed by radiolabeling the proteins (β2GP1 or Fab') before conjugation. Because of the accuracy of the radioactivity measurement I was also able to calculate the approximate number of targeting molecules on each liposome; the numbers obtained in different liposome types were consistently between 30 and 70. These values show the excellent load/ligand ratio obtained with drug targeting liposomes; 25000 DXR molecules are targeted using approximately 50 ligand molecules [Table 3_4]. For duramycin, the

radiolabeling was not an option; therefore I was not able to quantify the conjugation reaction and the final duramycin content. The duramycin-liposomes were only qualitatively tested for binding to PE on solid phase assay; this will be described later.

After the manufacture process, the liposomes were used *in vitro* and *in vivo*, for antigen binding, cell association, cell cytotoxicity, and tumor growth inhibition. The use of liposomes targeted to VEGFR-2 and to phospholipids is described in the next two chapters.

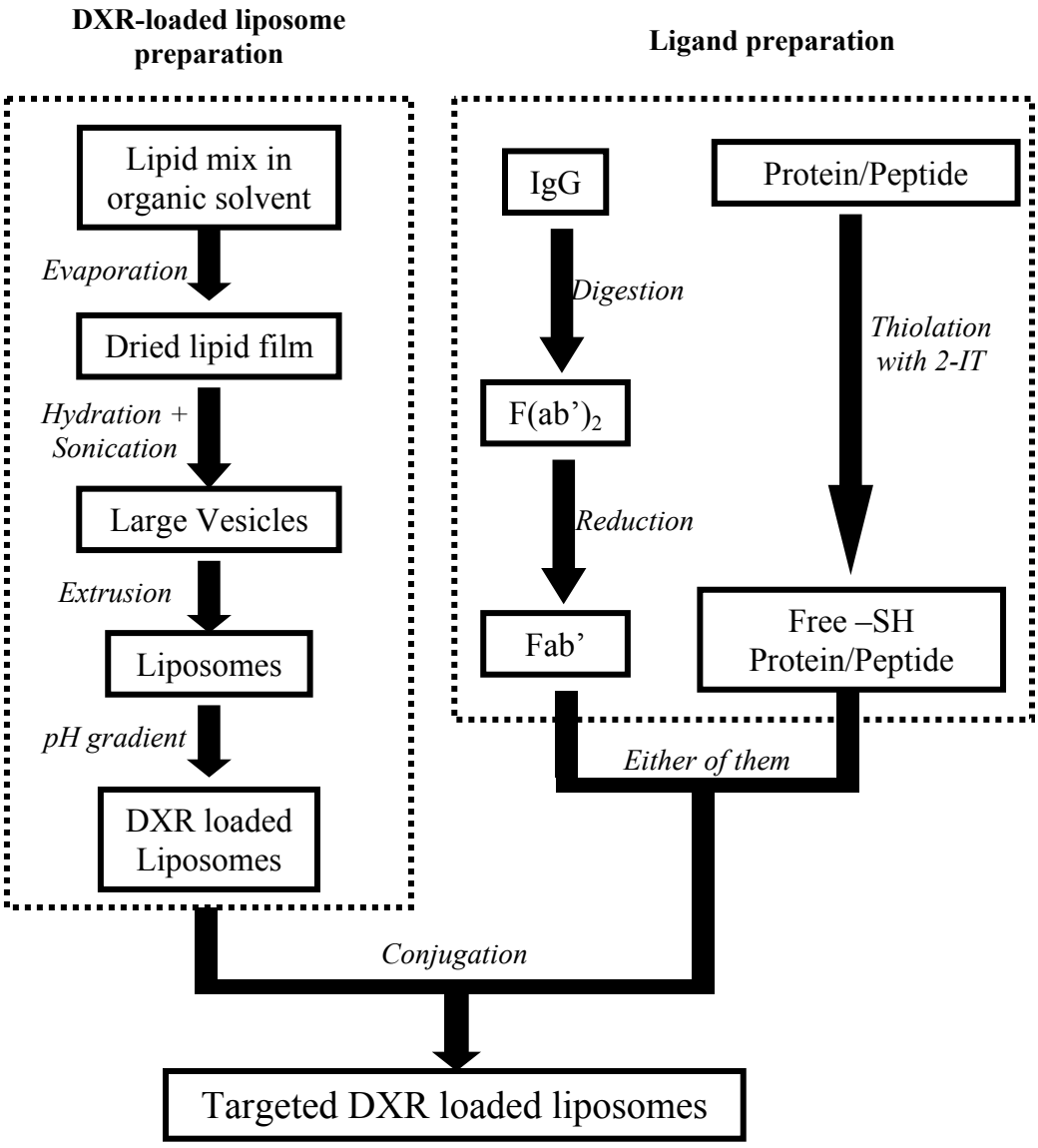

Fig. 3_1: The manufacture process of targeted liposomes

Targeted liposomes are prepared by conjugation of the thiol containing ligands with the drug loaded liposomes than present maleimide on their surface. The left side of the figure represents the steps of the liposome preparation from phospholipids and loading with the DXR. The right side of the figure represents the steps of obtaining the free thiol containing ligand. Either Fab' fragments or thiolated protein/peptide are used in one conjugation reaction.

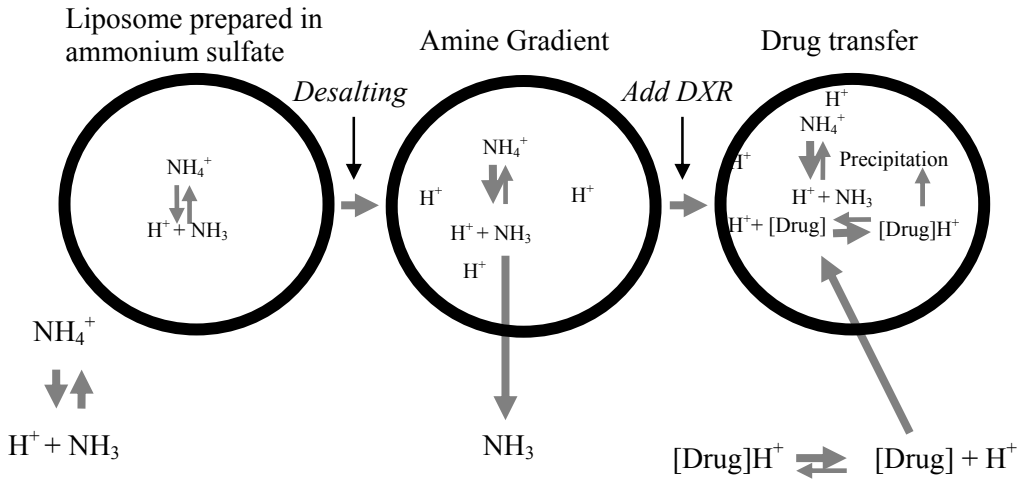

Fig. 3_2: DXR loading by ammonium sulfate gradient

The DXR is loaded into liposomes by creating a pH gradient between the internal compartment of the liposome and the surrounding buffer. The process has 3 steps:
1) The liposomes are prepared in $(NH4)_2SO_4$. In this step the concentration of ammonium ions is equal between inside and outside liposomes
2) The outside buffer is exchanged for an ammonia free buffer (citrate). The ammonium molecules equilibrate between the inside and outside buffers because they can cross freely through the liposomal bilayer. The protons are left inside
3) DXR is added in the solution outside liposomes. The liposomal membrane is permeable for the nonprotonated form of the drug which equilibrates between inside and outside buffers. Inside the liposomes, the equilibrium between the nonprotonated and protonated DXR is pushed toward protonated form due to the proton excess. Because the $[DXR]H^+$ precipitates, its concentration is constantly decreasing as a free solute promoting the equilibrium of the reaction toward formation of new $[DXR]H^+$

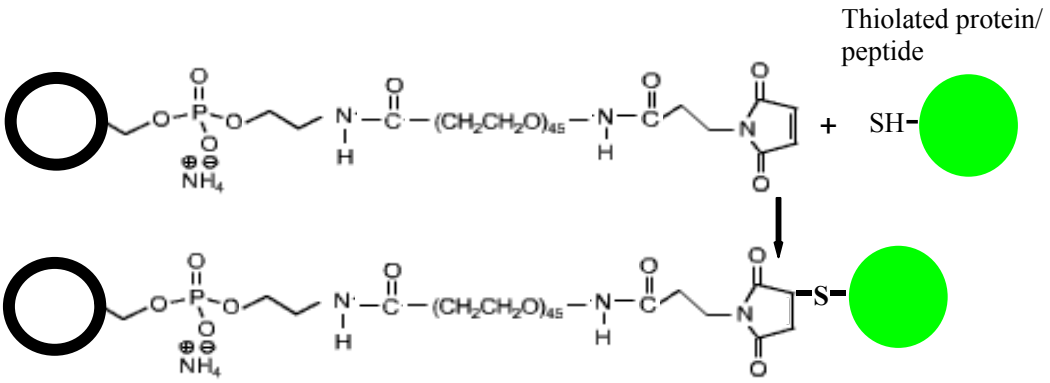

Fig. 3_3: Conjugation of thiolated ligands with liposomes

1% of the phospholipids from the liposome composition are PE-PEG(2000)-Maleimide. After extrusion and DXR loading, the liposomes are able to react with a free –SH containing ligand forming a thioether bond which is stable after injection in circulation. The ligands can be either Fab' fragments or thiolated proteins/peptides. The reaction is allowed for at least 24h at pH 7.4 and at room temperature.

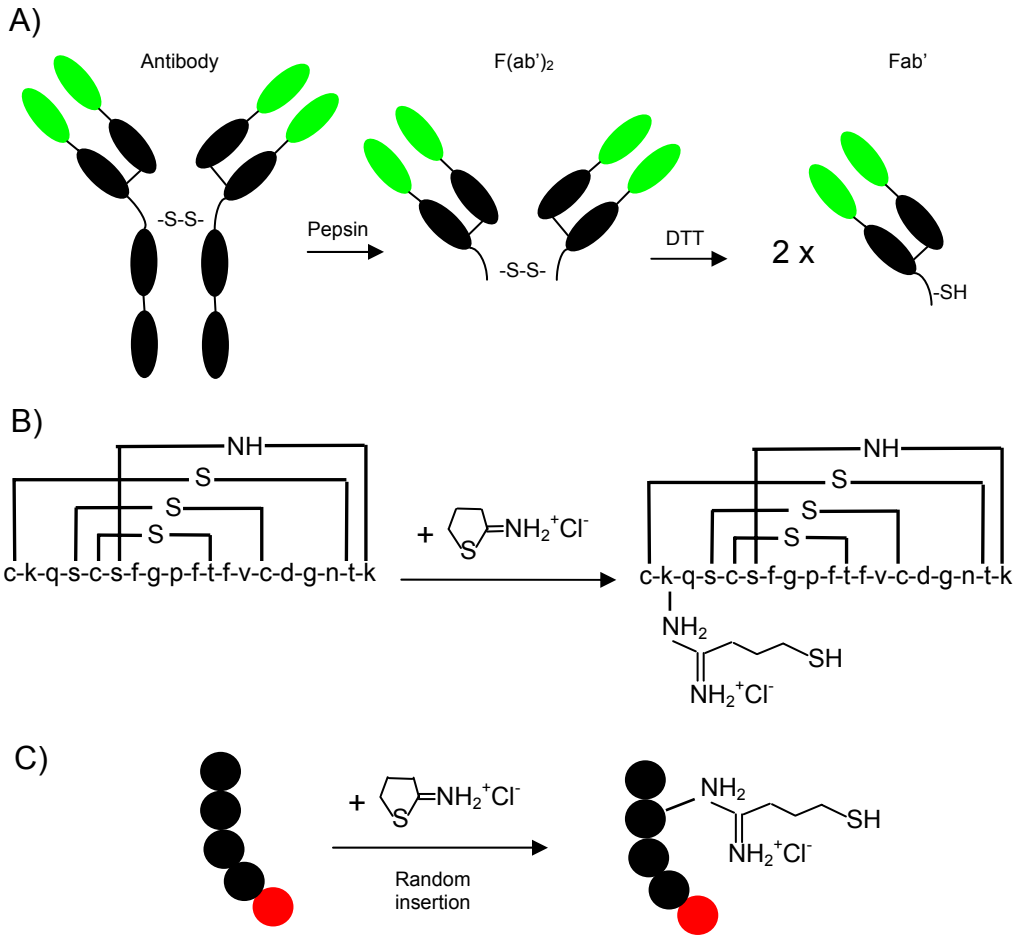

Fig. 3_4: Thiolated ligand preparation:

A) Preparation of Fab' with endogeneous free –SH group. Whole IgG purified from hybridoma supernatant are digested using pepsin. The $F(ab')_2$ are purified and reduced to Fab' fragments using DTT (dithiothreitol). The free –SH groups are placed on the hinge region of the Fab' fragment allowing a proper orientation on the liposomal surface with the hinge region toward the liposome and the antigen binding part toward exterior (green = variable regions of the IgG, black= constant regions of the IgG).

B) Preparation of duramycin with a supplemental –SH group. Duramycin sequence is presented with the posttranslational modification bonds above. The lysine from position 2 presents an amino group which can react with 2-

iminothiolane (2-IT). A new –SH group is introduced in the molecule which can react with the liposomes.
C) Preparation of β2GP1 with supplemental –SH group. β2GP1 has 5 domains, with domain 5 (red) being responsible for phospholipid binding. 2-IT reacts with random lysine in the sequence of the protein. The human homolog has 30 lysine and the reaction is not specific to any of them. After the thiolated β2GP1 reacts with the liposomes, the whole construct maintains phospholipid binding activity suggesting that domain 5 is still available for interaction with the target.

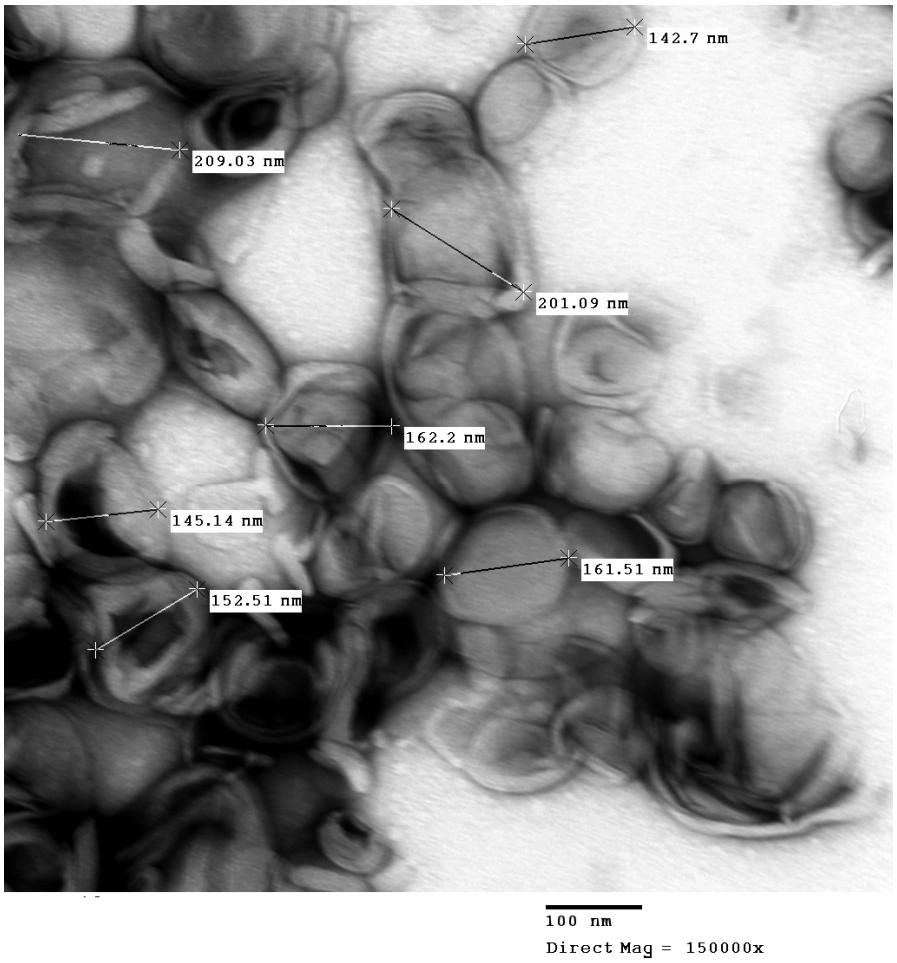

Fig. 3_5 Electron microscopy images of empty liposomes with negative stain

Empty liposomes coated with PEG were absorbed on Formvar coated grids and negatively stained with methylamine vanadate (Nanovan). The grids were visualized using a JEOL 1200 EX electron microscope equipped with a ccd camera. The images show liposomes adhering to the grid. The real dimension of liposomes is smaller than the measured 140-170 nm, due to a flattening effect on the EM grid. Most of liposomes appear to be unilamellar. The PEG prevents the fusion of liposomes into large vesicles.

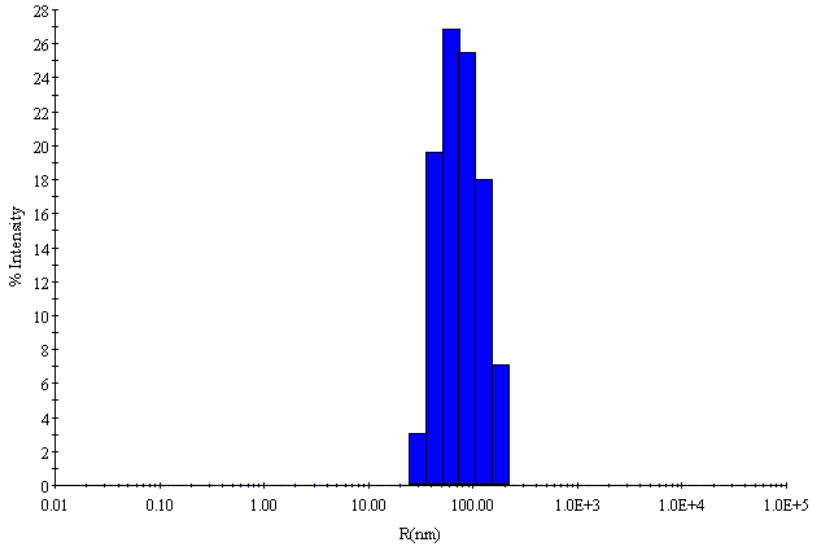

Fig. 3_6 Evaluation of liposome size by dynamic light scattering

PEG coated liposomes were diluted to 3.7 µg PL/ml in Hepes buffer and the size was evaluated using a DynaPro dynamic light scattering machine. The plot represents a histogram of the average radius of the particles in the suspension. The liposome population size has a radius of 80 nm, in average. PEG prevents the formation of large aggregates of multiple liposomes or liposome fusion into larger particles which would appear as a supplemental population.

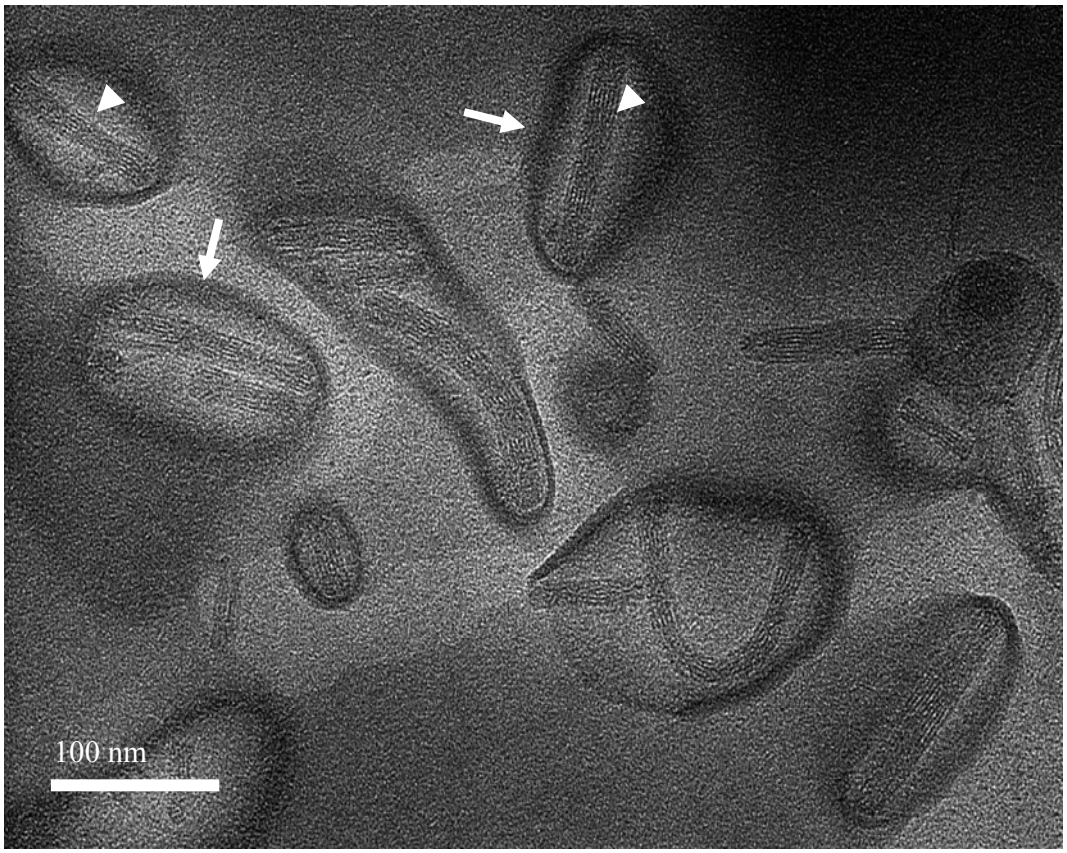

Fig. 3_7: Electron microscopy images of DXR filled liposomes with negative stain

Liposomes coated with PEG and filled with DXR were absorbed on carbon coated grids and negatively stained with methylamine vanadate (Nanovan). The grids were visualized using a JEOL 1200 EX electron microscope equipped with a film camera. The images show liposomes filled with bundles of precipitated DXR (arrowheads). The liposome membrane is visualized by the negative staining (arrows). Each liposome contains one to two bundles which do not break the liposome wall. Due to the rigidity of the DXR bundles, the liposomes maintain their round shape in spite of drying the sample during grid preparation. There are no empty liposomes visualized.

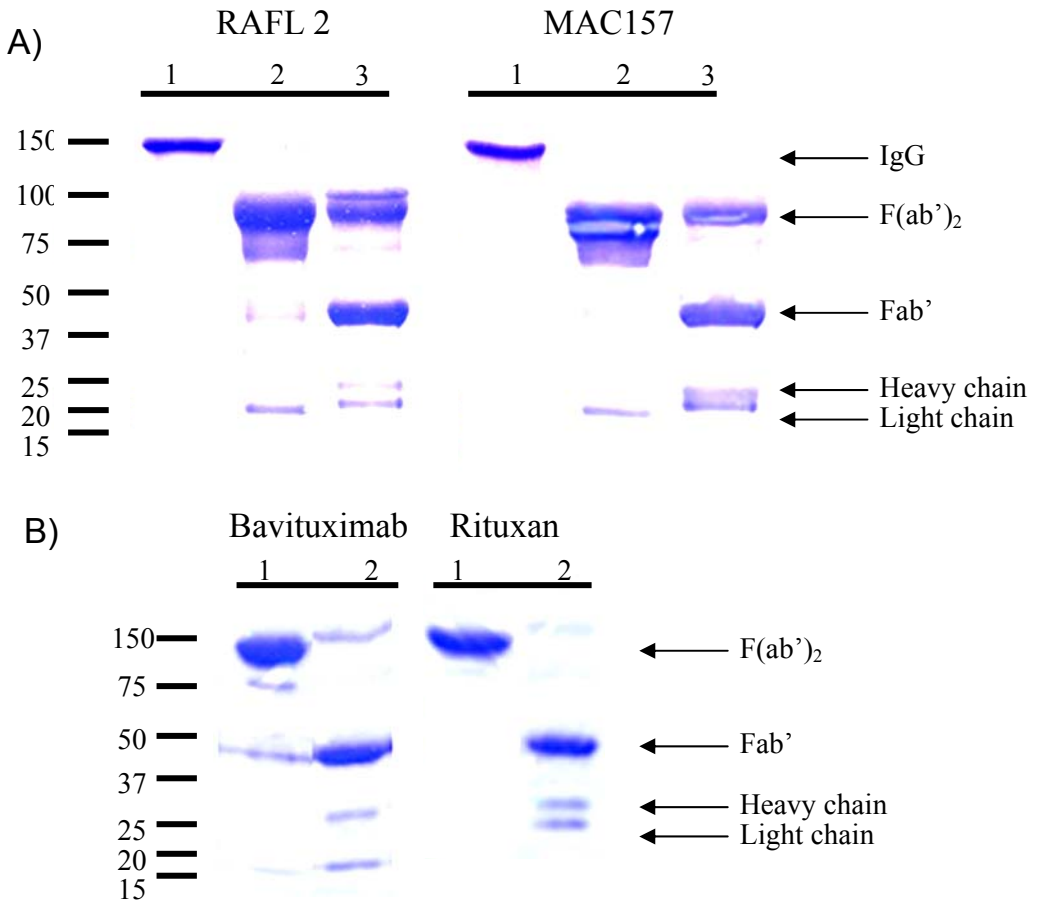

Fig. 3_8: Preparation of Fab' fragments of RAFL2, Bavituximab, MAC157 and Rituxan antibodies.

Whole IgG, F(ab')2, and Fab' fragments are compared by SDS gel electrophoresis

A) RAFL2 and MAC157 antibodies (rat IgG2a class) were purified from hybridoma cell medium by affinity chromatography on immobilized protein G (lane 1 for each antibody). Lane 2 presents the $F(ab')_2$ after digestion of the IgG and purification on size exclusion S200 column. Lane 3 shows the product obtained at reduction of F(ab')2 with DTT. The reduction result is a mixture of whole $F(ab')_2$, Fab', and heavy and light chains.

B) Similar comparison for bavituximab and rituxan. The starting material was $F(ab')_2$ previously obtained from whole IgG. Lane 1 = $F(ab')_2$; Lane 2 = product obtained at reduction with DTT, a mixture of Fab' fragments and heavy and light chains

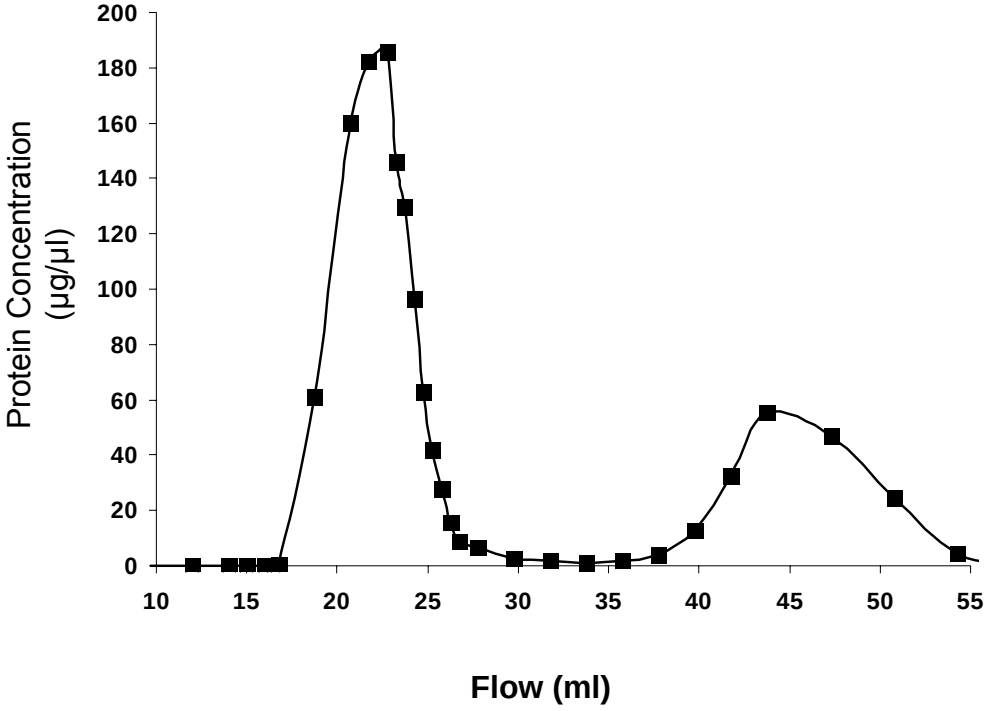

Fig. 3_9: Separation of liposomes conjugated to radiolabeled ligand from unconjugated ligand

Chromatography graph for the purification of proteoliposomes. After the conjugation reaction of the liposomes with the thiolated ligand, the reaction mixture is run on a Sephacryl S300 column. The proteoliposomes are larger than the cut-off size for the resin (12 nm) and exit the column with the void volume (first peak). Unconjugated protein is delayed in the column (second peak). The protein concentration is calculated by measuring the radioactivity (cpm) in each fraction and dividing the value with the specific activity of the radiolabeled ligand.

Table 3_1: Liposome composition (molar ratio)					
	HSPC	Cholesterol	PE-PEG	PE-PEG-Mal	PE-PEG-Biotin
Empty Liposomes DXR-Liposomes Fluorescent Liposomes	2	1	0.08	0.02	-
Biotinylated Liposomes	2	1	0.06	0.02	0.02

Table 3_2: Digestion conditions for different antibodies			
	pH	Pepsin mass ratio (%)	Incubation time (min)
RAFL 1	3.1	2.8	35
RAFL 2	3.8	1.2	70
MAC 157	3.4	1.25	30

Table 3_3: Reduction conditions for different $F(ab')_2$.		
	DTT/$F(ab')_2$ molar ratio	Incubation time (min)
RAFL 1	10	180
RAFL 2	6	180
MAC 157	6	210
Bavituximab	6	210
Rituxan	10	120

Table 3_4: Composition of DXR filled liposomes			
	DXR	Phospholipids	Fab'
Mass Ratio	1	6.2	0.2
Molar Ratio	511	2260	1
1 Liposome (# of molecules)	25000	100,000	46

CHAPTER IV

VEGFR-2 TARGETED LIPOSOMES

INTRODUCTION

Tumor growth and metastasis are dependent on angiogenesis. Tumor foci that enter a transition from a dormancy phase to a positive growth phase undergo an angiogenic switch. For this to happen, new vessels are needed to be formed or recruited. Among the determinant factors for angiogenesis VEGF plays a primary role [125, 126]. VEGF stimulates the proliferation and migration of endothelial cells and enhances the permeability of blood vessels. There are two receptors for VEGF: VEGF-R1 (FLT-1 in humans/Flt-1 in mice) and VEGFR-2 (KDR in humans/Flk-1 in mice). VEGFR-2 appears to be responsible for most of the angiogenic effects of VEGF and it has been found to be upregulated on the surface of tumor endothelial cells or tumor cells [127, 128].

Various approaches have been employed to inhibit either the interaction of VEGF with VEGFR-2 or the intracellular signaling through the receptor, some examples are: antibodies against VEGF or VEGFR-2, soluble VEGF-R1 receptors, or small molecule inhibitors of the tyrosine kinase. Our lab previously developed a panel of rat IgG_{2a} monoclonal antibodies against mouse VEGFR-2, named rat anti Flk (RAFL) [92]. Three of them, RAFL-1 to 3, have been shown to

partially inhibit VEGF binding to VEGFR-2 and also to localize *in vivo* to tumor vessels. Treatment with RAFL-1 was able to decrease the vessel density within tumor.

I used RAFL antibodies to prepare Fab' fragments for liposome conjugation. The VEGFR-2 targeted liposomes designed in this way would be able to bind to the endothelial cells in the tumors. Another advantage of using this targeting system is the possibility of cross-linking several receptors on the cell surface thereby stimulating the receptor mediated endocytosis; this would provide an entry way for the liposomes and the drugs they transport into endothelial cells.

I have constructed the RAFL Fab' conjugated liposomes and showed that they are able to bind to the VEGFR-2 *in vitro* and *in vivo*. The liposomes bound to the extracellular domain of VEGFR-2 in solid phase experiments. *In vitro*, the liposomes bound to and were internalized by mouse endothelial cells expressing VEGFR-2. I have loaded the liposomes with DXR and tested the advantage brought by VEGFR-2 targeting for treating breast cancer in mouse models.

RESULTS

Binding of RAFL Fab' conjugated liposomes to sFlk

I used 2 RAFL antibodies to generate Fab' fragments: RAFL-1 (9G10) and RAFL-2 (2D6). The Fab' fragments were conjugated on the surface of various types of liposomes (biotinylated, fluorescence filled, or DXR filled). The liposomes were tested on a solid phase assay for the ability to bind to the target antigens. All types of liposomes yield similar results. Fig 4_1 shows the binding of pyranine filled liposomes to sFlk immobilized on the surface of ELISA plates. The bound liposomes were quantified by detecting the fluorescence of the pyranine released using a solution of Triton X-100. RAFL liposomes bound to sFlk while control liposomes did not. The binding of RAFL-liposomes to sFlk was specifically inhibited by an excess of free RAFL antibody, but not by an excess of control antibody.

Binding and internalization of RAFL conjugated liposomes to mouse endothelial cells

The ability of RAFL conjugated liposomes to bind to mouse endothelial cells was tested using fluorescence microscopy and flow cytometry. For microscopy, fluorescent liposomes were incubated with live or fixed cells that had been grown on chamber slides. The liposomes were observed to be bound to the

cells. The image pattern of the cell staining differs depending on whether the cells are alive or fixed before adding the liposomes. When incubated with live cells, the liposomes were clustered into strongly fluorescent speckles that are mainly found on the cell body, in the perinuclear area. On the dendritic extensions of the cells, the liposomes were also detected in clusters. [Fig 4_2]. The fixed cells had a completely different appearance, with the liposomes spread homogeneously on their surface, without enhanced fluorescence on the perinuclear area of the cells. These images suggest that the liposomes had been internalized into endocytic vesicles. The liposomes each carry 10-40 Fab' fragments and can crosslink numerous receptors on the cell surface. This triggers a receptor-mediated endocytosis. This process is precluded by cell fixation.

I confirmed the internalization by incubating live endothelial cells with fluorescent liposomes at 37 °C and at 4 °C, followed by flow cytometry assessment. The liposome association with the cells was quantified by calculating the MFI [Fig 4_3]. The MFI of the cells incubated at 37 °C was at least 10 times higher than MFI of cells incubated at 4 °C. The increase in MFI was decreased by different methods which are known to inhibit internalization: sodium azide or cytochalasin B. NH_4Cl, which only inhibits acidification of the endosomes, had a more limited effect. An inhibitor of PI3K, LY294002, did not significantly decrease the MFI. These experiments confirm the internalization process observed

by microscopy and suggest that the mechanism of internalization is not by macropinocytosis, but by a receptor mediated phagocytosis.

Minimal increase of toxicity by the internalization of doxorubicin loaded liposomes

Binding and internalization of liposomes to endothelial cells could be used to deliver drugs targeted to these cells. I tested if DXR loaded liposomes have enhanced cytotoxicity toward endothelial cells. Cells were grown in 96 well plates and incubated with serial dilution of DXR loaded liposomes conjugated to Fab' of a RAFL antibody or control antibody. As an additional control, I used free, non-liposomal DXR. As was widely described in the literature liposomal DXR has a much higher IC50 compared to free DXR. Among the two liposomal formulations, those conjugated to RAFL had only a marginally increased toxicity (maximum 2 folds) [Fig. 4_4]. The results are consistent with other internalizing liposomes which also have only a small increase in cytotoxicity [129, 130].

Localization of VEGFR-2 targeting liposomes to tumor endothelial cells

It was shown that RAFL antibodies can localize to tumor endothelial cells when injected into circulation. They can also be detected on the surface of capillaries in the kidney glomeruli [92]. I tested if liposomes conjugated to a RAFL Fab' can reproduce the finding described for the naked antibody.

Biotinylated liposomes were injected i.v. and 4 hours later the mice were perfused, and the tumors, liver, spleen, and kidneys were harvested. The liposomes were detected by IHC, using either fluorescent or HRP conjugated stretpavidin. RAFL liposomes were detected on the surface of tumor capillaries, while control liposomes were not [Fig. 4_5]. Both types of liposomes were detected in the liver and spleen, which are organs that have the ability to trap liposomes [Table 4_1]. Only RAFL liposomes were detected in the kidney glomeruli, which confirms previous findings that these endothelial cells are VEGFR-2 positive [92].

Testing the therapeutic benefit of VEGFR-2 binding liposomes

The end point of designing VEGFR-2 targeted liposomes is to deliver a drug to the tumor endothelial cells leading to their destruction. We tested the ability of RAFL Fab' conjugated tumors to inhibit the tumor growth of an orthotopic breast cancer. Human MDA-MB-231 breast cancer cells were injected into the MFP of female nude mice. The tumors were allowed to grow until reached a volume of 100 μl, when treatment was started. The treatment groups were: RAFL targeted liposomal DXR, control targeted liposomal DXR, soluble DXR, or buffer control. DXR was administered at a dose of 4 mg/ml/injection, every 5 days. All treatments were intravenous. The liposomal DXR had a better control of the tumor growth compared with both buffer control and soluble DXR.

However, there was no significant difference between the RAFL targeted or control targeted liposomes [Fig. 4_6].

VEGF and VEGFR-2 are key factors in the initial steps of tumor development, when 1-2 mm tumor foci need to trigger an angiogenic switch and stimulate the formation of new vessels or recruitment of neighboring vessels [125]. I tested the therapeutic benefit of RAFL targeted liposomes against smaller tumors, for which VEGF has a higher role than in the large tumors with already established vasculature. I used the same tumor model as in the previous experiment, but I did not allow the tumors to grow before initiating the treatment. 5 days after tumor cell injection into the MFP the mice were randomized into the four treatment groups and followed for tumor growth. The experiment was stopped after 6 treatment sessions, when tumors treated with RAFL targeted liposomes grew larger than control treated tumors. This difference was statistically significant ($p = 0.01$) [Fig. 4_7].

I tested the benefit of targeting DXR to VEGFR-2 expressing endothelial cells in a lung pseudometastatic model of human breast cancer cells (MDA-MB-231). Mice were injected with $1x10^6$ cells and 10 days later the mice were randomized to receive liposomal DXR targeted with either RAFL2 Fab' fragment or control Fab'. Another group was treated with buffer only. DXR was administered at a dose of 3 mg/kg every 5 days, for 5 times. RAFL-2 targeted

liposomes prolonged the survival of the mice with 34 days [Fig. 4_8]. Control targeted DXR liposomes did not have any significant survival benefit compared with buffer control.

DISCUSSION

I have successfully designed and manufactured VEGFR-2 targeted liposomes. These liposomes are binding to purified extracellular domain of VEGFR-2 and to endothelial cells expressing VEGFR-2. Upon binding to the receptor on the cell surface they are internalized. The liposomes are also binding to tumor endothelial cells when injected into the blood stream. In spite of these findings, VEGFR-2 targeting only minimally increased the cellular toxicity of DXR loaded liposomes and was unsuccessful in delaying the growth of tumors in a mouse model of breast cancer. But, when used in a lung pseudometastatic model, the targeted liposomes were able to extend the survival of mice with more than 50% compared to control liposomes.

The liposomes were conjugated to the hinge part of the Fab' fragment allowing a free access of the antigen binding part to VEGFR-2. In this way, the particle was able to adhere to immobilized extracellular domain of VEGFR-2 and also to cells expressing the receptor. In our system, RAFL conjugated liposomes showed a very strong internalization into endothelial cells after binding to the receptor on the cell surface. The internalization is sustained by the fluorescence microscopy images with the characteristic enhancement in the perinuclear area in contrast with the diffuse staining on the surface of dead-fixed cells. I studied the mechanism of internalization using inhibitors of different cell-entry pathways.

The liposomes I constructed are more than 100 nm in diameter; therefore it is unlikely to be internalized by a caveolin mediated mechanism or clathrin and caveolin independent endocytosis, which are able to uptake particles of up to 60 - 90 nm. A PI3K inhibitor prevented only minimally the liposome uptake while inhibitor of actin fibers polymerization inhibited this process strongly. These findings suggest that the liposomes enter into the cells not by a macropinocytosis process, but by a receptor mediated phagocytosis.

Internalization of liposomes after cross-linking receptors on the cell surface was previously shown to bring an added benefit to simple targeting. In comparison to non-internalizing targets (CD20), the internalizing ones (CD21) lead to an increase in cytotoxicity and antitumor effects of the DXR loaded liposomes [130]. Liposomes conjugated to scFv A5, targeting human endoglin (CD105), bound and were subsequently internalized into endothelial cells [85]. A small molecule inhibitor of neuropeptides (antagonist G) which binds to multiple receptors on the surface of small-cell lung cancer cells was conjugated to liposomes and also led to their internalization into H69 cells [131-133]. One successful targeting method of liposomes to endothelial cells uses peptides binding to α_v-integrins. $\alpha_v\beta_3$ and $\alpha_v\beta_5$ are integrins which have an increased expression on the surface of dividing endothelial cells, endothelial cells in tumors, and some tumor cells [59, 76, 134, 135]. Using phage display methods a series of peptides containing RGD was discovered to bind with high affinity to these

integrins and were conjugated to liposomes [29]. The RGD-targeted liposomes bound to tumor endothelial cells and were internalized, providing an enhanced anti-angiogenic effect [60-62].

In spite of a strong internalization, I was not able to detect a large increase in the toxicity of the targeted DXR filled liposomes compared with untargeted ones. This is not very different from findings by other groups regarding liposomal DXR toxicity. Internalizing, anti-disialoganglioside liposomes only decreased the IC50 of DXR 2.5 to 4 times compared with untargeted liposomes [129]. In another comparison of internalizing CD19 targeted compared with non-internalizing CD20 targeted DXR liposomes, the IC50 was decreased only from 5 μM to 3 μM [130]. These small differences in the cytotoxicity in the *in vitro* conditions were enough to obtain a therapy benefit when they are combined with the *in vivo* targeting abilities of the liposomes; all the examples presented above led to an increase of the animal survival, or inhibition of tumor growth.

When tested for tumor growth inhibition, the RAFL Fab' conjugated liposomes proved to be not better than control liposomes. When treatment started at 100 μl tumor volume, the average tumor growth was equal in targeted and control liposomes. When treatment started immediately after injection of cells, the average tumor volume in RAFL targeted liposomes was significantly larger than the average volume of control liposomes. MDA-MB-231 tumors responded to both free DXR and liposomal DXR. Our results suggest that conjugation to RAFL

Fab' fragments may lead to a decreased accumulation of liposomes into the tumor environment, probably due to trapping in other organs. VEGFR-2 has been described to be upregulated on the surface of tumor vessels but it was also found to be present in several organs or structures in normal adult mice. Due to the polyvalent nature of the liposomes used in our experiments their avidity for the receptor may be very high; therefore liposomes can bind very well even toward low density receptors. Using immunohistochemistry methods, it was found that VEGFR-2 is expressed in the intima of the aorta. Extracts of liver, kidney, adipose tissue, and lung tissue were positive for VEGFR-2 on westernblot experiments [136]. In terms of the density of the receptors, the expression of VEGFR-2 on each of these structures is not very high, but due to the large volume of these organs, and rich vascularization, the total amount of the receptor may be large. The scattered VEGFR-2 molecules from the organs other than tumor may create a sink which absorbs a significant amount of the injected dose of the liposomes.

Another explanation for the decreased effect of RAFL targeted liposomes may reside in the modifications induced by their anti VEGF effects. RAFL-liposomes are binding to VEGFR-2 on the endothelial cell surface in the tumors and may block the VEGF-VEGFR-2 interaction therefore decreasing the signaling downstream of the receptor. It was shown that inhibition of the VEGF signaling via two different methods (tyrosine kinase inhibitor AG013736 or VEGF-Trap)

leads to rapid changes in the architecture of tumor endothelial cells with disappearance of the endothelial fenestrations, inhibition of vessel sprouting and decrease of the vascular blood flow [137]. All these changes are, of course, desired as an antiangiogenic treatment, but in the same time they can lead to an impairment of the non-targeted, spontaneous accumulation of liposomes in the tumor. PEG covered liposomes are a good tool for tumor treatment especially because of their accumulation in the tumor environment, even without the need for targeting. Endothelial fenestrations play an important role in this spontaneous accumulation and if they disappear then liposomes lose an important advantage. It could be possible that interfering with VEGF signaling may pose a problem for the VEGFR-targeted liposomes.

Contrary to the effects obtained in the orthotropic breast cancer model, the RAFL-2 targeted liposomes prolonged survival in the lung pseudometastatic model. Angiogenesis is an essential factor for the development of the metastatic foci above 2 mm diameter. Small foci may be different in tissue organization compared with established tumors. The characteristics of the tumor vascularization, with disorganized vessels, abundant leakage, and necrotic areas are not yet established in the small foci. The PEG coated liposomes do not have a passive targeting at the same extent encountered in larger tumors. Additionally, the VEGFR-2 may be expressed at a higher level on the endothelial cells in the early stages of development of tumor foci [138]. In these conditions, targeting

liposomes to VEGFR-2 may be optimal because the disadvantages brought by interfering with the passive targeting of liposomes into the tumor environment are avoided, while binding and internalization into VEGFR-2 expressing cells is maximal. The number of receptors expressed on a target cell is critical for success of a targeted liposome. It was shown that HER2 targeted liposomes are not effective in a tumor model when the cancer cells expressed a low number of HER2 receptors ($2x10^4$) and are effective only when the receptors are at high density ($1x10^5$) [139]. In my hands the mouse endothelial cells bEnd.3 express between $2x10^4$ and $4x10^4$ receptors. This is not a very large number and it could explain why there was very little improvement in the IC50. The endothelial cells in the vessels at the early developmental stages of metastatic foci may have a high enough number of receptors that would enhance the cytotoxic effect of the targeted liposomes.

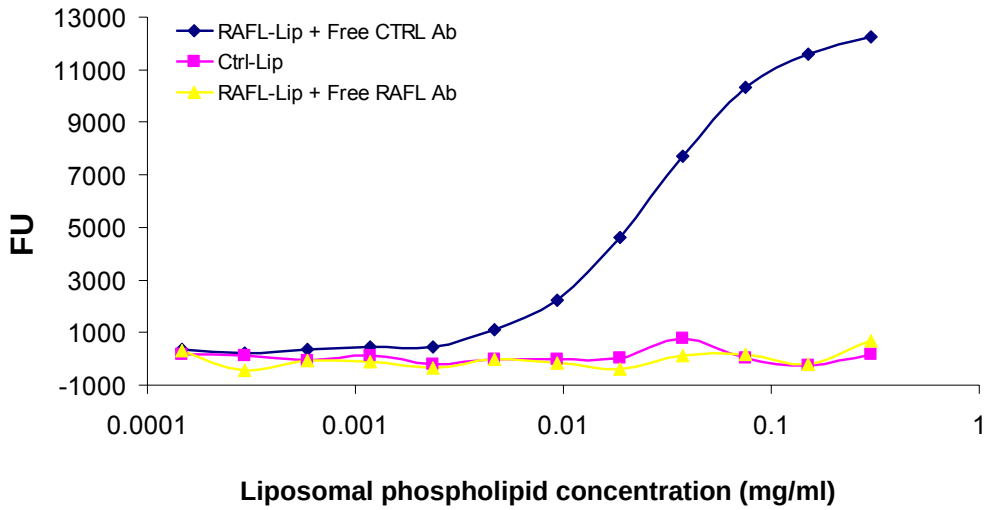

Fig. 4_1: RAFL targeted liposomes bind to sFlk
The wells of ELISA plates were coated with sFlk and incubated with serial dilutions of pyranine filled liposomes conjugated to Fab' fragment of RAFL or control antibodies. The RAFL liposomes were incubated in the presence of an excess of free RAFL antibody or control antibody. The liposomes were detected by reading the fluorescence after sulphorhodamine was released from the liposomes using 0.2% triton X-100. RAFL-liposomes bound sFlk while control liposomes did not. The binding curve is inhibited by an excess of free RAFL antibody, but not by the excess of control antibody.

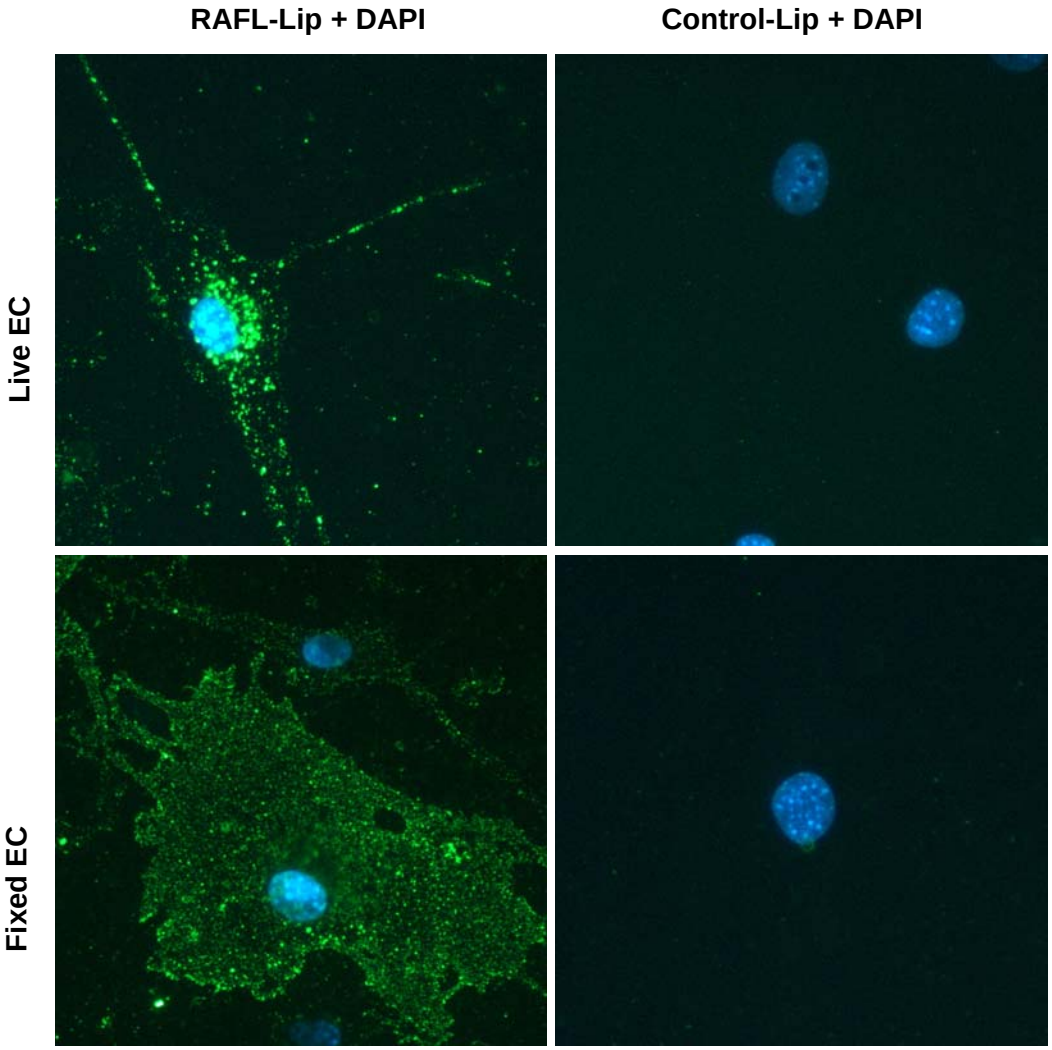

Fig. 4_2: Binding and internalization of RAFL conjugated liposomes to mouse endothelial cells

Mouse endothelial cells (bEnd.3) grown on chamber slides were incubated with pyranine filled liposomes conjugated to RAFL or control Fab' fragments. The cells were either alive of fixed with PFA. The images are obtained by merging the nuclear staining (DAPI) with the green fluorescence of pyranine liposomes. The staining pattern suggests that RAFL liposomes are binding to the cells and are clustering and internalizing in endocytotic vesicles enriched in the perinuclear area. The fixed cells have the VEGF-R2 homogeneously distributed on the cell surface, with a uniform binding of the liposomes.

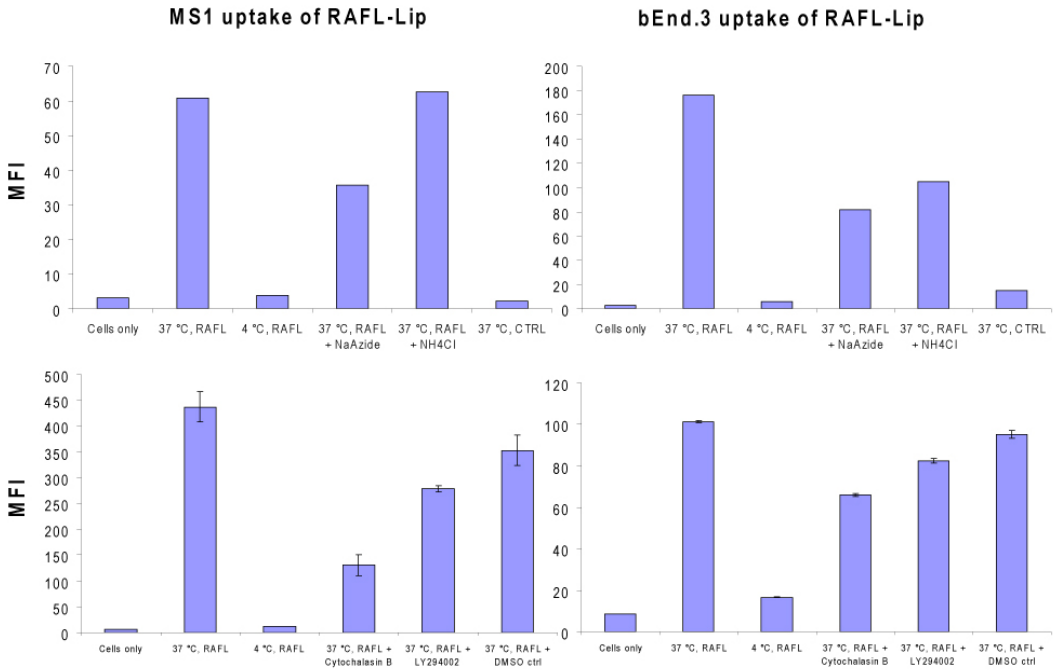

Fig. 4_2: Binding and internalization of RAFL conjugated liposomes to mouse endothelial cells

Mouse endothelial cells (bEnd.3 and MS-1) were trypsinized and incubated with RAFL Fab' conjugated liposomes or control Fab' conjugated liposomes filled with pyranine. The liposomes association with the cells was assessed by flow-cytometry. The incubation was done at 4 °C or 37 °C in the presence or absence of various inhibitors on internalization (Na azide, Cytochalasin B, LY294002). The graph represents the MFI of the cells in each condition.
Fluorescence of endothelial cells is significantly increased when incubation is at 37 °C. Na azide inhibits internalization while NH_4Cl has marginal effect. Cytochalasin B inhibits RAFL liposomes internalization while the inhibitor of macropinocytosis has little effect.

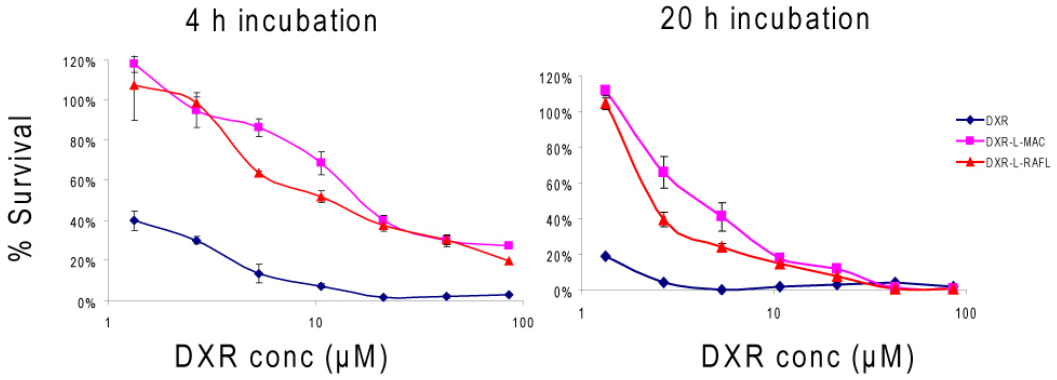

Incubation time	IC50-RAFL-Lip (μM)	IC50-Ctrl-Lip (μM)
4 h	10.7	24.0
20 h	2.3	4.2

Fig. 4_4: **Binding and internalization of DXR loaded liposomes conjugated to RAFL Fab' decreases the IC50**

Mouse endothelial cells (MS-1) grown on 96 well plates were incubated with serial dilutions soluble DXR or liposomal DXR conjugated to Fab' of RAFL or control antibody for 4 or 20 hours. The cell proliferation was assessed 72 h later using a standard MTA assay. The survival percent of cells in each well was plotted for each drug concentration. Liposomal DXR has less toxicity to endothelial cells compared to soluble DXR. RAFL targeted liposomes have a 2 fold decrease in IC50.

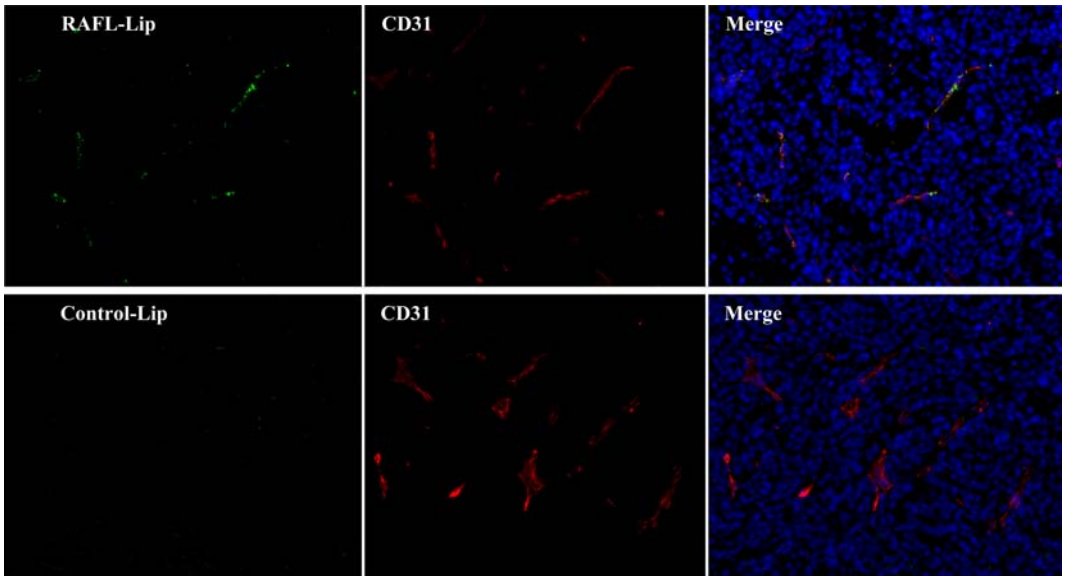

Fig. 4_5 **Tumor endothelial cell localization of RAFL binding liposomes**

Human breast cancer cells MDA-MB-231 were grown in the MFP of nude mice (nu/nu). A suspension of biotinylated liposomes conjugated to RAFL Fab' (0.2 mg phospholipids) were injected i.v. 4 hours later the mice were heparinized and sacrificed by perfusion through the left ventricle after general anesthesia. Tumors were harvested, sectioned followed by IHC. Liposomes were detected with FITC conjugated streptavidin (green) and blood vessels were detected by anti CD31 staining (red). RAFL liposomes were colocalized with endothelial cells on the tumor capillaries.

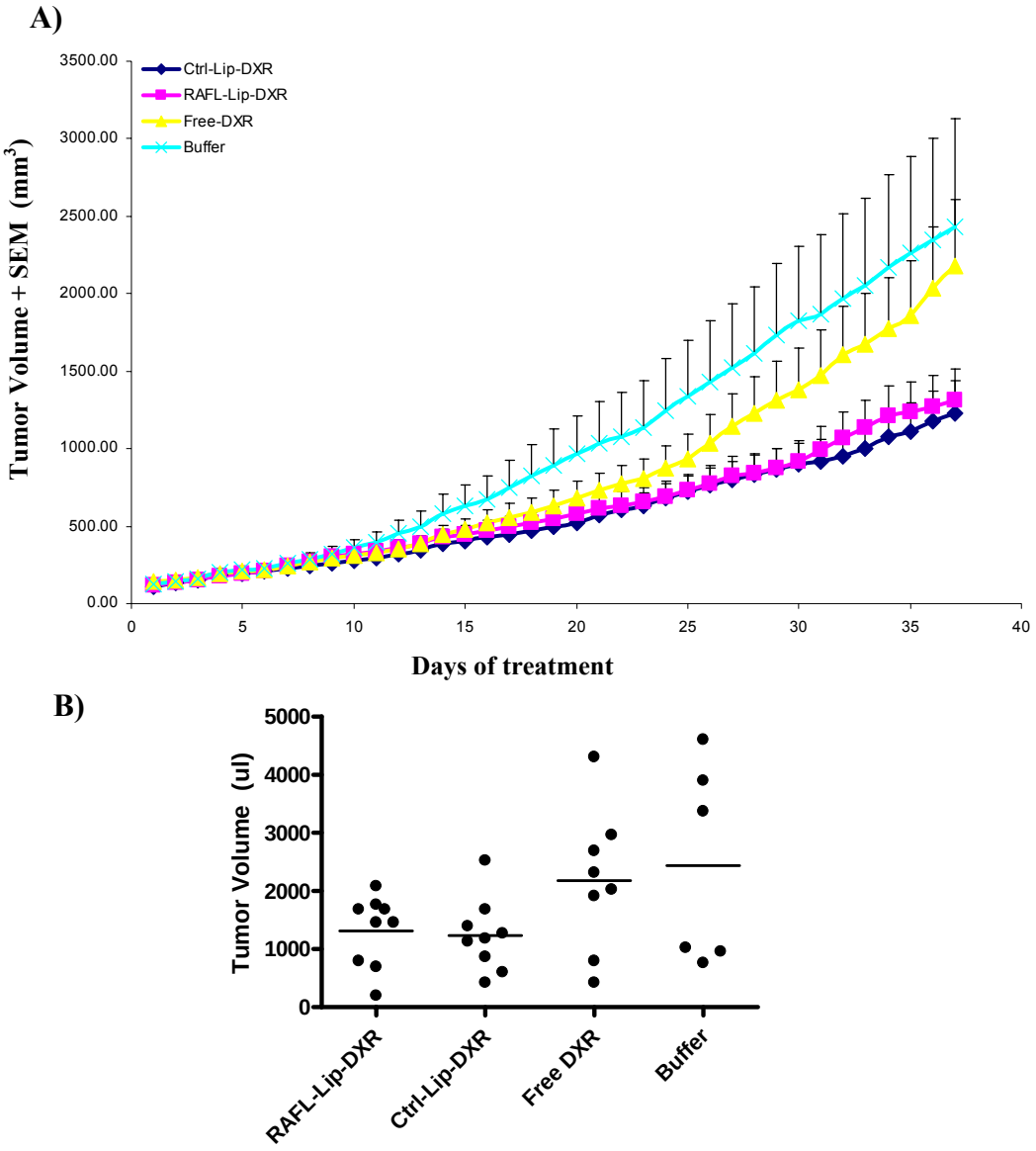

Fig. 4_6: **Lack of therapeutic effect of RAFL-liposomes against MDA-MB-231 tumors in mice**

$4x10^6$ human breast cancer cells (MDA-MB-231) were injected into the MFP of female nude mice (nu/nu). When tumors had grown to a volume of 100 µl, the mice were randomized to receive either RAFL-targeted liposomal DXR, control

targeted liposomal DXR, free DXR, or buffer only. DXR was administered i.v. at a dose of 4 mg/kg/injection every 5 days. The tumors were measured with a caliper and the tumor volume was calculated as (small diameter x large diameter^2)/2. A) The time evolution of the average tumor volume after cell implantation. B) Individual tumor volumes were plotted for each treatment group at the end of the experiment (day 37). The group treated with RAFL targeted liposomes is not different from average in the control liposomes treated group.

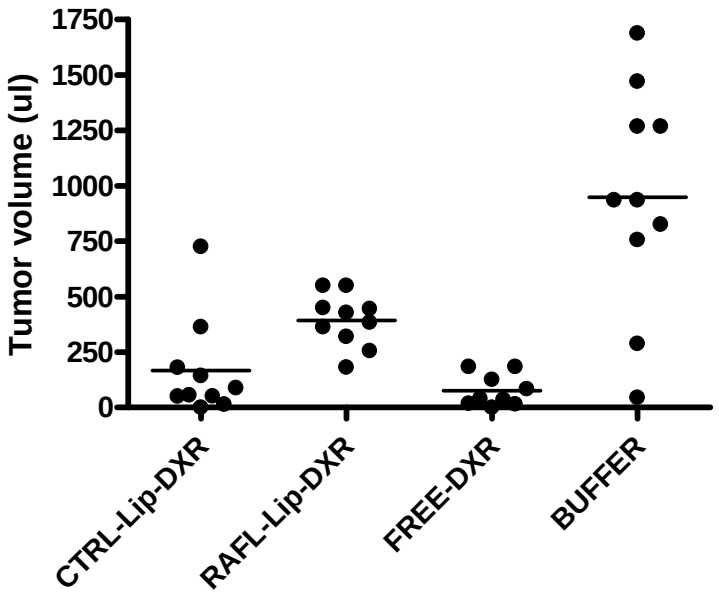

Fig. 4_7: Lack of therapeutic effect of RAFL-liposomes against MDA-MB-231 tumors in mice (early treatment).
$4x10^6$ human breast cancer cells (MDA-MB-231) were injected into the MFP of female nude mice (nu/nu). 5 Days later, the mice were randomized to receive either RAFL-targeted liposomal DXR, control targeted liposomal DXR, free DXR, or buffer only. DXR was administered i.v. at a dose of 4 mg/kg/injection every 5 days. The tumors were measured with a caliper and the tumor volume was calculated as (small diameter x large diameter^2)/2. The experiment was terminated after 6 treatment sessions, when the average tumor volume in RAFL treated animals grew significantly larger than the average tumor volume in control liposomes treated animals.

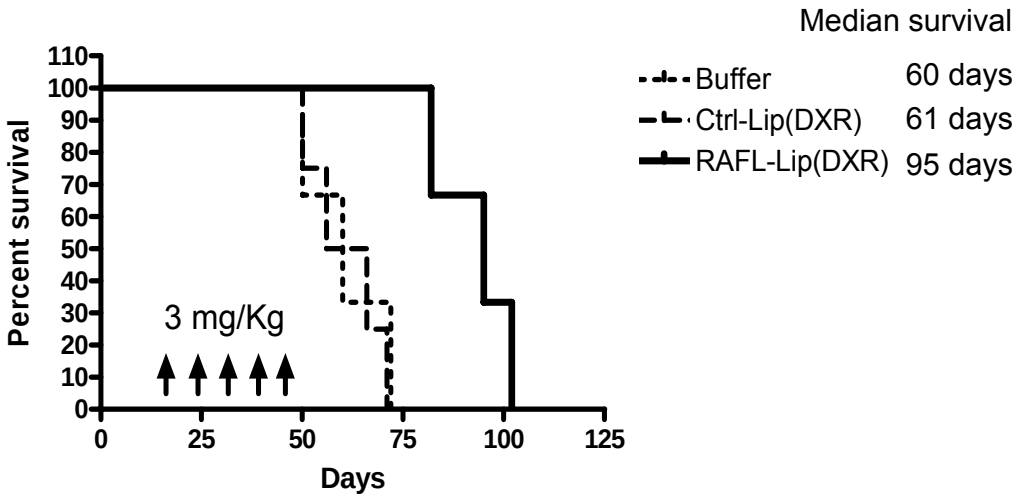

Fig. 4_8: Prolongation of the survival in a pseudometastatic model

$1x10^6$ human breast cancer cells (MDA-MB-231) were injected intravenously into female nude mice (nu/nu). 10 days later, the mice were randomized to receive either RAFL-targeted liposomal DXR, control targeted liposomal DXR, or buffer only. DXR was administered i.v. at a dose of 3 mg/kg/injection every 5 days. The weight of the mice was monitored as a surrogate of disease evolution and mice were sacrificed if the weight decreased with more than 20%. RAFL targeted liposomes prolonged the survival with 34 days compared to control liposomes.

Targeting agent	Spleen	Liver	Kidney glomeruli	Tumor capillaries
9G10-Lip	+ +	+/-	+	+
Control-Lip	+	+/-	-	-

Table 4_1: **Biodistribution of RAFL conjugated liposomes to the capillaries of organs known to trap liposomes.**

Cryosections of tumors, kidney, liver and spleen were obtained during the experiments described in Fig. 4_6. The liposomes were detected with HRP-conjugated streptavidin and developed with DAB. The intensity of the staining was observed under the microscope and quantified as (-) for no clear staining above background, (+) 1-4 scattered, low intensity vessel-like structures, and (++) intensely stained > 5 vessels/field. RAFL liposomes were detected on the tumor capillaries, spleen, liver, and also kidney glomeruli, which are known to express VEGF-R2

CHAPTER V

PHOSPHOLIPID TARGETED LIPOSOMES

INTRODUCTION

Among the molecules regarded as tumor endothelial cells markers, PS distinguishes itself as unusual, being a phospholipid and not a protein. The first observation that PS is present on the surface of endothelial cells within tumors was made by Ran et. al [24]. Monoclonal antibodies binding anionic PL have been developed. These antibodies can be detected on the surface of the tumor endothelial cells after being injected i.v. into tumor bearing animals [25, 140]. The presence of PS on the tumor endothelial cells was also confirmed by localization experiments done using another anionic phospholipid binding molecule (annexin V).

For normal endothelial cells, as well as for most eukaryotic cells, the different species of phospholipids are non-homogeneously distributed between the inner and outer leaflets of the plasma membrane. The choline-containing phospholipids, PC and SM, are segregated to the external leaflet, while the aminophospholipids, PS and PE, are segregated to the inner leaflet, together with the less abundant PI [141-143]. The cell uses several transporter families to maintain or disrupt the segregation of the phospholipids. Unidirectional, inward

transport of phospholipids, from the outer leaflet to the inner leaflet, is performed by aminophospholipid translocases (APTLs). These proteins belong to a group of P-type ATPases, designated P4 ATPases [141, 144, 145]. APTL transport is specific for PS and PE. Based on homology studies, 14 different proteins with this function have been described in mammals [146]. APTLs are ATP and Mg^{++} dependent, and inhibited by Ca^{++}, vanadate, and sulfhydryl reacting compounds [147]. Unidirectional, outward transport of phospholipids is performed by a multitude of proteins from four families (A, B, D, and G) of the ATP-binding cassette (ABC) group of transporters. The ABC proteins are considered unspecific, being able the transport a variety of phospholipids, cholesterol, or cytotoxic xenobiotics. Unlike APTLs, the ABC proteins are activated by an increase in intracellular Ca^{++} concentration [143, 148, 149]. Bidirectional transport is performed by phospholipid scramblases (PLSCRs). In humans, there are 4 proteins, members of this family; two of them have been extensively studied (PLSCR1 and 3). As with the ABC proteins, the PLSCR are activated by Ca^{++} [150]. The activation related PS expression has been described in certain cell types, e.g. thrombocytes, erythrocytes, and lymphocytes [151, 152].

Various cellular events, including cell activation and apoptosis, malignant transformation and cell injury influence the activity of the phospholipid transporters. In the tumor environment, the endothelial cells are exposed to a variety of factors that can lead to cell injury or activation. Among these, cytokines

and ROS play an important role. Cytokines, like IL-1α, IL-1β, IL-6, and TNF- α are secreted both by cancer cells and by host cells as a response to the presence of the malignant cells [153, 154]. ROS are secreted either directly by the tumor cells, or by the leukocytes which adhere to the activated endothelial cells expressing adhesion molecules [155].

Therapeutic interventions used in oncology can accentuate the stress factors already present in the tumor environment. Cytotoxic drugs like docetaxel can induce the generation of ROS. Radiotherapy also induces ROS which can cause peroxidation of membrane phospholipids and local phase transitions that allow calcium influxes and release of calcium from intracellular stores [156, 157]. All these events lead to a change in the physiologic equilibrium of the plasma membrane composition and to the exposure of PS on the surface of the endothelial cells.

Much less information is available about PE translocation during cell activation or apoptosis. A reason for this may be the scarcity of good and specific detection systems for discriminating between PE and PS or other phospholipids. Using biochemical labeling it was shown that PE is externalized on the sarcolemma of ischemic cardiomyocytes [158, 159]. Emoto et al. have described that late apoptotic cells can be stained with a PE binding antibiotic peptide (Ro09-0198) and that PE is enriched on the surface of apoptotic blebs [94]. Correlations have not been made between the exposure and colocalization of PE and PS on the

surface of intact cells after activation or early apoptosis. Most studies use annexin V, which binds both PS and PE with similar affinity in the presence of physiological concentrations of calcium [95, 160].

One of the antibodies developed against anionic phospholipids (including PS), 3G4, proved to be a good agent used as a single drug for delaying tumor growth in various animal models and cancer types. The tumor growth inhibition varies from 50% to 90% in mouse models of: breast tumors (MDA-MB-435, MDA-MB-231), fibrosarcoma (Meth A), Hodgkin (L540). 3G4 was used in combination regimens with docetaxel for treatment of human breast cancer in mice, both orthotopic models and metastatic models. 3G4 acted synergistically with the cytotoxic drug, enhancing the tumor growth control without an increase of toxicity [140]. The antitumor activity of 3G4 is also increased by association with local radiotherapy. The combination regimen lead to a 90% control of the tumor growth in a human lung cancer model in nude mice [161].

This experience led us to hypothesize that using the Fab' fragment of a 3G4 derived antibody (bavituximab) a liposomal nanoparticle could be targeted to the endothelial cells within solid tumors. I obtained the Fab' fragment of bavituximab (a human chimeric version of 3G4 antibody) and I conjugated it to a variety of liposome types: fluorescent, biotinylated, and DXR loaded. I showed that the particles bound to the target *in vitro* as designed and that they can also be

detected on the surface of tumor endothelial cells *in vivo*. I also tested to therapeutic benefit of these liposomes for delaying tumor growth in mouse animal models.

Since the translocation mechanisms which lead to the exposure of PS on the surface of mammalian cells are also able to transport PE, I hypothesized that exposure of PS on the surface of endothelial cells within tumor will be coincident with PE. Therefore, I created an additional targeting system for PE. I used a small antibiotic peptide, duramycin (from *Streptoverticillium cinnamoneus*) belonging to a family of tetracyclic polypeptides. Peptides from this family have previously been used to detect PE on cell surfaces [162, 163]. I chemically conjugated duramycin on the surface of liposomes and I used this product to demonstrate that PE and PS are coincidentally exposed on the plasma membrane. I tested the PE targeting liposomes in the same systems used for bavituximab targeted liposomes: endothelial cell targeting and tumor growth delay.

RESULTS

Phospholipid specificity of bavituximab targeted liposomes

Bavituximab Fab' fragments were conjugated on the surface of liposomes. The binding spectrum of the naked bavituximab antibody to different phospholipids was previously described, with similar affinity for PS, PI, CL, and PA and no binding to neutral PE, PC and SM [25]. The binding properties of the bavituximab-liposomes were determined for each phospholipid and were shown to reproduce with fidelity the binding of the whole bavituximab antibody. The binding was determined on purified phospholipids in a solid state experiment. Every type of liposomes (biotinylated, fluorescent, or drug loaded) can be tested in this assay, but the best signal vs. noise ratio was obtained using the biotinylated ones. Different purified phospholipids were immobilized on 96 well plates. The liposomes were allowed to bind to the target and the amount of attached liposomes was detected using HRP conjugated streptavidin and subsequently with standard colorimetric methods used for ELISA.

Bavituximab-liposomes bound to anionic phospholipids PS, PI, and PG, but not to neutral phospholipids PE, PC, and SM [Fig 5_1]. The binding strength for PI and PS was equal and slightly smaller that that for PG. This proved that Fab' fragments maintain their target specificity after being separated from an antibody and attached on the surface of a liposome. The targeting properties of the

Fab' were extended to the whole particle. We confirmed that the liposomes need the presence of β2GP1 for their binding to PL. After PS was absorbed on the surface of 96 well plates, we used different blocking and incubation buffers. The bavituximab-liposomes bind to PS only when serum was added to the system, regardless of the time of the addition. The binding to PS is similar whether the serum is added as a blocking agent or as an incubation agent. Incubating the liposomes on the immobilized PS in the presence of ovalbumin leads to complete loss of binding affinity [Fig 5_2].

Phospholipid specificity of duramycin targeted liposomes

After thiolation with 2-iminothiolane, duramycin was conjugated on the surface of liposomes. Duramycin was shown to have a high specificity to PE [162]. I tested if thiolation and conjugation to large particles impedes PE binding ability of the peptide. Biotinylated liposomes were incubated on phospholipids immobilized on 96 well plates. PE stands out as the only phospholipid to which the liposomes are bound. Low background binding was seen to all other phospholipids tested [Fig 5_3].

I tested if the binding of the duramycin conjugated liposomes can be inhibited by an excess of free duramycin. I incubated the liposomes on the immobilized PE in the presence of at least 200 times more free duramycin. I repeatedly observed an enhancement of the binding affinity of the liposomes [Fig.

5_4]. This suggests that in the presence of PE, duramycin molecules can associate among themselves and the complex increases the total binding strength.

Coincident PS and PE exposure on stressed mammalian cells can be detected with bavituximab and duramycin liposomes

I created the PS and PE binding liposomes in order to target the endothelial cells within tumors. PS exposure on the tumor endothelial cells was previously described, but so far there is no data regarding a possible coincidence with PE. The bavituximab and duramycin conjugated liposomes thus retained the same binding specificity as the unconjugated ligands and they also provide a tool for mutually exclusive detection of PS and PE. To validate our methods of specific phospholipid detection I confirmed the binding spectrum of annexin V, which bound to anionic phospholipid (PS, PI, PG) and also to neutral PE. It did not bind to PC or SM [Fig. 5_5]. This results are in agreement with the previous published data of annexin binding to PL in the presence of physiologic concentrations of calcium [160].

It is difficult to reliably reproduce *in vitro* the conditions from the tumor environment. I tried to mimic the stress on the cells by using ionizing irradiation which is known to produce ROS and led eventually to apoptosis. I used two different types of cells and I shown that after irradiation they express PS and PE coincidentally.

Pyranine filled liposomes were used to detect PS and PE exposure on the surface of adherent ABAE cells after irradiation (5Gy). Non-irradiated adherent ABAE cells showed no detectable surface staining for either PS or PE apart from the occasional disintegrating cells [Fig 5_6]. Irradiation (5 Gy) induced exposure of PS and PE on approximately 50% of the cells. The fluorescence intensity of the entire cell population was quantified by Image J software and normalized for the number of cells in each field. Irradiation increased the level of staining for PS and PE by about 4 fold relative to the levels on non-irradiated cells. The control liposomes did not produce detectable staining under any conditions.

Using flow cytometry, the semiadherent cell line, mouse myeloma NS0, was assessed for PS and PE exposure after irradiation. Having low adherence, the cells do not require trypsinization, which can change the cell shape and possibly influence the plasma membrane organization. PS was detected with pyranine filled bavituximab-liposomes, while a two step staining with biotinylated duramycin liposomes and Alexa 700 conjugated streptavidin was used to detect PE. Propidium iodide permeable cells were excluded from the quantification. NS0 cells showed increases in both PS and PE staining after irradiation [Fig. 5_7 A]. The majority of the cells shifted from being negative for both markers to being positive for both markers. Cells that were positive for PS, but not for PE and vice versa were rarely observed. Cells stained with control liposomes had only background levels of staining in all conditions. To obtain further evidence that

cells have coincident exposure of PS and PE, I gated NS0 cells for low PS, medium PS, or high PS and I found the gated populations had low PE, medium PE, and high PE, respectively [Fig. 5_7 B]. This finding indicates that the level of externalization of the two phospholipids on the cell surface follow similar trends.

To determine the time course of PS and PE exposure, NS0 cells were irradiated and stained for both markers at various time-points over a 48 hour period. After irradiation, the cells shifted slowly from being double negative toward being double positive [Fig. 5_8]. The percentage of PS and PE positive cells and the mean fluorescence intensity (MFI) started to increase after 4-5 hours, reached a transient plateau around 16 hours and further increased at 48. These findings indicate that PS and PE gradually accumulate on the cell surface after irradiation. The levels of both markers increase coincidentally over time.

The dynamics of PS and PE exposure areas are similar

I observed the dynamics of PS and PE exposure areas on the surface or irradiated ABAE cells by staining with bavituximab or duramycin liposomes and imaging repeatedly the cells for a 30 h period. The PS and PE positive areas are initially located on various areas on the cell body. In time, these areas congregate in blebs located toward the periphery of the cells. Often, the blebs remained attached to the cell by thin strands of membrane. I repeatedly observed that

membrane blebs were left behind the cell bodies as the cells advanced on the culture plate [Fig. 5_9].

PS and PE are colocalized on cell membrane patches and blebs

The spatial distribution of PS and PE on the surface of individual irradiated cells was analyzed by double staining live irradiated ABAE cells and imaging them using a deconvolution microscope. PS and PE were not expressed uniformly on the cell surface. The positive cells displayed discrete areas with strong intensity. Some were small scattered punctuate areas, but most of the staining was clustered into larger patches with high colocalization of both PS and PE [Fig. 5_10 - A]. These larger areas had the appearance of membrane blebs where regions of the plasma membrane had escaped anchorage from the cytoskeleton and appear to be protruding outside the. Clusters of blebs were frequently observed on the cell surface.

Maintenance of PS and PE colocalization over time and clustering at the cell periphery

The evolution of the staining pattern was observed for up to 12 hours. The cells were stained and imaged over several hours without re-staining. The PS and PE remained colocalized even when the positive areas moved around on the cell surface, as the cells change their position and shape on the chamber slide [Fig.

5_10 - B]. The PS/PE positive areas freely slide on the cell surface, as I noted with the single positive staining. Some of the double positive blebs drift on the cell surface and remain on the rear part of the cell relative to the moving direction [Fig. 5_11].

Alternative PS targeting using β2GP1 conjugated liposomes

Bavituximab-liposomes bind to PS indirectly by bridging β2GP1 molecules. I tried an alternative approach for PS targeting by directly conjugating the β2GP1 molecules on the surface of the liposomes. In this way I avoid the use of an intermediary molecule and the variability of bavituximab interaction with β2GP1 from different species. I thiolated β2GP1 molecules using 2-IT and I conjugated it to liposomes. β2GP1-liposomes were tested side by side with bavituximab-liposomes for binding to PS [Fig 5_12]. Both liposomes have similar affinity to PS immobilized on 96 well plates and much lower binding to PE.

β2GP1-liposomes bind to PS induced endothelial cells

I tested if β2GP1-liposomes can bind to PS on the surface of endothelial cells. To induce PS, I have treated the endothelial cells with a membrane destabilizing compound, l-PC, as previously published [93]. I observed a strong staining with β2GP1-liposomes compared with control liposomes [Fig. 5_13]. These findings show that β2GP1-liposomes have the same similar binding

abilities as bavituximab-liposomes and set the basis for an alternative method for targeting PS on the tumor endothelial cells.

Localization of PS targeting liposomes to tumor endothelial cells

It was shown that bavituximab antibodies injected i.v. into a tumor bearing mouse can be detected on the surface of the endothelial cells of the tumor capillaries [25, 140]. I tested if the two different types of PS binding liposomes (bavituximab or β2GP1) can bind to the tumor endothelial cells *in vivo*. Detection of liposomes by IHC of tumor sections was a very difficult process. Fluorescent liposomes, which were very good for *in vitro* experiments, proved to completely loose their fluorescence during the tissue preparation. Therefore I used the biotinylated liposomes and standard streptavidin detection methods. The liposome suspension was injected i.v. and 2-4 hours later the mice were perfused, tumors and organs harvested and tissue prepared for IHC. I specifically looked for the presence of the liposomes on the capillaries within tumors, not in the large vessels at the periphery of the organ. Both bavituximab and β2GP1 conjugated liposomes were detected on the intratumoral capillaries [Fig. 5_14]. The control liposomes were detected only on the large vessels at the periphery of the tumors or in the peritumoral mammary fat pad. I performed IHC on sections obtained from other organs which are known to trap the particles in the 100 nm size range: liver, kidney and spleen. Bavituximab liposomes were very scarcely detected in the

liver, kidney and spleen. β2GP1 liposomes were strongly present in the spleen and liver, as the control ones as [Table5_1].

Lack of therapeutic effect of Bavituximab-targeted liposomes against MDA-MB-231 tumors

The main purpose of designing liposomes with affinity for PS was to obtain a drug delivery system for targeting cytotoxic drugs to the tumor endothelial cells. I chose to test the advantages of PS targeted liposomes on a tumor model which was known to respond at bavituximab. Human MDA-MB-231 breast cancer cells injected into MFP of nude mice form tumors that grow above 2000 μl in approximately 40 days. Bavituximab as single agent decrease the tumor growth by 75%. I tested the drug loaded liposomes conjugated to bavituximab on this model. The cells were implanted into the MFP and when the tumor reached 100 μl the mice were randomized into 4 groups: untreated (buffer only administration), free DXR, DXR loaded liposomes conjugated to a control Fab' (Rituxan), and DXR loaded liposomes conjugated to bavituximab Fab'. All treatments were administered i.v. to mimic the administration route used in human clinical setting. DXR was normalized for a dose of 4 mg/kg, administered every 5 days.

The bavituximab targeted liposomal DXR treated mice presented with a significantly increased tumor size compared to control liposomes (mean tumor

size = 2108 μl compared to 1085 μl). [Fig. 5_15] The difference between the tumor size was statistically significant (p = 0.019). DXR loaded control liposomes were only marginally better in controlling the tumor growth compared to free DXR, without statistical difference.

Lack of therapeutic effect of β2GP1-liposomes against MDA-MB-231 tumors

I also tested the alternative PS targeting strategy using DXR loaded liposomes conjugated to β2GP1. The tumor model and treatment regimens were the same as those used for bavituximab liposomes. β2GP1 targeting produced no treatment improvement compared to control liposomes. The mean tumor size was for β2GP1 group (1067 μl) was not significantly smaller than the mean tumor size in the control liposomes (1374 μl [Fig. 5_16].

Lack of therapeutic effect of duramycin targeted liposomes against MDA-MB-231 tumors

It was already proven that local irradiation of the tumors produce an increase on the PS expression on the endothelial cells [161]. Our findings described above demonstrate that PS and PE are coincidentally expressed on the surface of the endothelial cells. These are findings that suggest that ionizing irradiation may lead to an increased expression of PE on the surface of tumor

endothelial cells. In the light of these findings, the association of local radiotherapy with PE targeting liposomes could bring a benefit. I used the same tumor model, MDA-MB-231 cells in nude mice. The mice received 5 sessions of 5 Gy in combination with either duramycin targeted DXR-liposomes or non-targeted DXR-liposomes. At 50 days after cell implantation the mean tumor size in the duramycin group was 4 times higher than the tumor size in the control liposomes ($p = 0.0003$) [Fig. 5_17]. This proves that PE binding properties of DXR-liposomes brings a disadvantage for tumor targeting; even in conditions known to increase the level of PE on tumor capillaries.

DISCUSSION

The results presented in this chapter describe the design and construction of liposomes which bind to anionic phospholipids and liposomes that bind to PE. These liposomes bind to irradiated cells *in vitro* and to endothelial cells within tumors. I am demonstrating that PS and PE are colocalized on the cell surface, with clustering on membrane blebs. When testing the drug targeting properties of the liposomes I observed a decrease of the therapeutic benefit, suggesting a miss-targeting outside of the tumor side.

The mechanism of binding of bavituximab antibody to phospholipids is indirect, by using an intermediate serum protein, β2GP1. Each of the antibody's Fab' arms binds to one β2GP1 molecules. In the presence of a lipid membrane, each of the two β2GP1 molecules binds to the membrane. Each β2GP1 molecule by itself has a low affinity for PS [164, 165]. Crosslinking the β2GP1 molecules using the antibody forms a tri-molecular complex (bavituximab + 2 β2GP1) that is stabilized on the membrane surface. The avidity of the multi-molecular complex can increase by ~1000 times compared to the affinity of the single β2GP1 molecule [166]. Separating the Fab' fragments from the natural antibody structure and rejoining them on the surface of a large particle can lead to a complex of much more molecules. The liposomes I constructed carry between 20 and 70 Fab' fragments on each particle. Theoretically, this structure can lead to an

even higher avidity, but also poses the risk of not being able to reproduce the multi-molecular complex needed for attaching on the membrane surfaces. The Fab' are differently positioned on the liposomal surface compared the antibody. The distances between the Fab' are much larger on the liposome. The PEG linker from the liposome surface make the Fab' fragment much more mobile. Also it is not known if the location of PE-PEG-Fab' molecule on the surface of the liposome is fixed or it can slide on easily. In spite of all these variables, our experiments demonstrated that the positioning details are not essential for cross-linking β2GP1 between the Fab' and the phospholipid surfaces. I cannot make a formal comparison with regard to the affinity of the Fab'-liposomes versus the antibody, because the liposome is a macromolecular complex out of which the Fab' molecules form only a very small minority. The serum dependence of bavituximab-liposomes for PL binding also confirmed that β2GP1 is needed as an intermediary between Fab' of bavituximab and PS.

A simpler strategy for targeting PS was also used by directly conjugating β2GP1 molecules on the surface of the liposomes. β2GP1 (also known as apolipoprotein H) is a protein found in mammalian plasma. It is a 345 aminoacid protein organized into 5 domains. The C terminal domain (V) has a lysine rich segment and a hydrophobic loop which assures the phospholipid binding [167, 168]. The structure was determined and it was shown that the molecule has the shape of letter "J" with a rigid conformation [169]. The function of β2GP1 is not

completely understood, appearing to have a role in coagulation. It is not essential for normal development and functioning and its absence does not pose a risk in humans or mice [170, 171]. For the chemical conjugation, the use of a small molar ratio of thiolated reagent to β2GP1 assured the addition of s single –SH moiety on each protein and avoided the crosslinking of several liposomes which would lead to precipitation of the particles. The precise location on the β2GP1 molecule where the thiol group was inserted was not determined, but the conservation of the affinity for anionic phospholipids proves that the lipid binding domain is still available for interaction with membranes. The β2GP1 liposomes were comparable with bavituximab-liposomes for PS binding on solid phase experiments and for staining PS expressing endothelial cells. For experimental purposes, bavituximab use in mice is complicated by the lack of interaction with mouse β2GP1 and the need to co-inject the human variant of the protein together with the antibody. The β2GP1 liposomes are not serum dependent and they are also specie independent, therefore they can be used in any animal model.

Another PL which is confined on the inner leaflet of the cell membranes is PE. It was described that the translocation mechanism which regulates PS also acts on PE, but until now there is no direct evidence that PS and PE appear on the cell surface together. I hypothesized that PE could be useful as an alternative molecule for targeting tumor endothelial cells in a similar manner PS is used. I

designed liposomes which target PE and I tested them side by side with bavituximab liposomes for cell binding and drug delivery to tumor vessels.

For PE targeting I used a molecule which was previously employed for PE detection on the surface of cells. Emoto et. al biotinylated duramycin non-covalently associated it with fluorescent streptavidin obtaining a 5 molecule complex [172-174]. The mechanism of PE binding of the lantibiotic peptides is not clearly understood [163]. It is not known if each duramycin molecule binds independently to PE or they must form a multi-molecular complex in order to adhere to PE membranes [162]. On the membrane, duramycin destabilizes the bilayer and increases the permeability to small molecules. Liposome-conjugated duramycin can bind to PE containing bilayers without destabilizing them, because I did not observe any hemolytic activity of the liposomal duramycin up to 10 μg/ml duramycin content. I concluded that chemical conjugation of duramycin does not impede the PE binding function, but only inhibits its permeabilization properties. To our surprise, the addition of free duramycin molecules increases the PE affinity of liposomal duramycin. This signifies that the chemical modification and conjugation to liposomes does not completely inhibit the complex formation between the modified molecules with the free ones. The lack of hemolytic activity was also demonstrated by the completely non-toxic profile at administration into mice. The mice received up to 8 intravenous injections of the liposomal suspension without any weight loss and death. The lack of toxicity of the

conjugated duramycin suggests that it can not form large complexes or ion channels and it can be safely used for drug administration.

Having the PS and PE targeting system, I was able to confirm our hypothesis that these two PL are regulated together and are coincidentally externalized on the surface of cells. I used ionizing irradiation as a stress method for cells and I showed that the externalization of the two phospholipids occurs at the same time, with a similar increase in their staining intensity, and on the same areas of the cell membrane.

Bavituximab-coated liposomes and duramycin-coated liposomes were used to demonstrate that PS and PE become exposed on the surface of adherent ABAE cells and semiadherent NS0 cells after irradiation. These liposomes allow mutually exclusive detection of PS and PE on the cell surface. Both phospholipids became detectable on the cell surface 4-5 hours after irradiation, and thereafter increased in parallel. The phospholipid detected on the cell surface with bavituximab-coated liposomes is most likely to be PS. PS is the most abundant anionic phospholipid and its exposure on the cell surface is known to be regulated by environmental influences or injury [151, 152]. Bavituximab also has affinity for other anionic phospholipids: PI, phosphatidic acid (PA) and phosphatidyl glycerol (PG) [25]. PA and PG are minor constituents of the plasma membrane and are mostly found in the membranes of the intracellular organelles [175]. PI is

a major component of the inner leaflet of the plasma membrane but its distribution is not known to be disturbed by cell activation or stress factors [176]. Still, I cannot exclude the possibility that PI contributes to the signal detected with bavituximab-coated liposomes. Duramycin-coated liposomes detect only PE on the cell surface.

The model I used to determine the exposure of PS and PE on the cell surface was by ionizing irradiation. Irradiation has both direct and indirect effects which can influence the phospholipid distribution. The direct effects are by generation of ROS which can lead to peroxidation of phospholipids and changes the permeability of the membranes. This allows calcium to enter the cells from the interstitial space or to be released from the ER. Additionally, irradiation causes activation of acidic sphingomyelinase (ASMse) and the conversion of sphingomyelin into ceramides [177, 178]. Endothelial cells in $ASMase^{-/-}$ mice are resistant to irradiation induced apoptosis, implying that ceramide production may be of particular importance in the radiation response of this cell type [179, 180]. The ceramides have effects on mitochondria, increasing their outer membrane permeability and causing release of cytochrome c, thereby activating the caspase pathway. At the same time, the ER responds to ceramides by releasing calcium into the cytosol [181]. Elevation of intracellular calcium induced either by lipid peroxidation or by ceramide generation could affect several different lipid transport systems that lead to the coincident appearance of PS and PE on the

surface of the cells: 1) Inhibition of the APTLs, which are the main transport systems for maintaining the segregation of PS and PE on the inner membrane leaflet. Although APTLs have a higher preference for PS than for PE, the transport rate for both of these phospholipids is much higher than for PC, SM, or PI. Inhibition of APTLs may indirectly lead to PS and PE accumulation on the cell surface [145, 182, 183]. 2) Activation of the ABC transporters, which directly transport all phospholipids, including PS and PE, to the external leaflet [141, 149, 150]. 3) Activation of the scramblases which causes intermixing of phospholipids between leaflets, thereby exposing PS and PE [142, 143, 148, 184]. It is not clear which of these three mechanisms is prevalent or if all three are present in all cell types. Aside from these Ca^{2+} triggered phospholipid transport mechanisms, ceramide accumulation in the plasma membrane may cause lamellar to non-lamellar lipid phase transitions that directly facilitate movement of lipids, including PS and PE, across the membrane. Spontaneous, non-enzymatic PS and PE flipping from the inner leaflet to the outer leaflet occurs very slowly in intact bilayers, but the presence of ceramides disrupts the bilayer and accelerates lipid movement across the membrane [185, 186].

PS and PE became exposed non-uniformly on the surface of irradiated cells long before nuclear condensation and fragmentation became visible. 24 hours after irradiation, a fine dynamic array of PS and PE positive patches was visible, some of which consolidated into larger, intensely stained blebs. The blebs

on the surface of endothelial cells occupied a relatively small area of the whole cell. Cells with blebs followed for up to 30 hours were still intact and moving on the surface of the slide. Although many reports have been published on the appearance of PS positive blebs on stressed cells, there is no general agreement on the time when PS first appears on the surface of the cells. Two types of cell blebbing have been described: an early, fine ruffling limited mostly to the cell membrane, and a late blebbing, which coincides with nuclear condensation and fragmentation. Some authors detected PS before early blebbing and some detected it after blebbing [183, 187]. These different findings may be due to the sensitivity of detection and the variation in the order of apoptotic steps among different cell types.

There is a striking resemblance between the blebs I observed on the live cells and the "intramembranous particles" described by electron microscopy on the surface of ischemic cardiomyocytes, with spacing of the plasma membrane from the cytoskeleton [158]. PS participates in the attachment of the plasma membrane to the cytoskeleton, through its interaction with various actin binding proteins, including annexins, spectrin, or protein 4.1 [188, 189]. When lipid asymmetry is lost and PS is evenly distributed between the leaflets of the membrane, the cytoskeletal association with the cell membrane is weakened and the cell can no longer maintain its proper shape [190]. Also, blebs form when the membrane phospholipids locally detach from cytoskeleton. Such regions offer a

weak point on the cell surface where the intracellular content can herniate outward due to intracellular pressure [191, 192]. Without local cytoskeletal reinforcement the cell has difficulty controlling patches of plasma membrane with inverted phospholipids. Therefore, the blebs slide on the cell surface and remain toward the rear of the cell, relative to its direction of movement.

This phenomenon may explain how membrane blebs of endothelial cells or macrophages are at the origin of the circulating microparticles, which were also shown to be positive for PS and PE. The circulating microparticles have been related with the level of coagulation anomalies and with the presence of antiphospholipid antibodies (aPL), pathologic immunoglobulins which target phospholipids [193, 194]. Negatively charged phospholipids like PS or cardiolipin are the most common targets described for aPL, but PE has also been included in this group. They have been correlated to prolonged coagulation time, thrombotic events and pregnancy pathology [195, 196]. Our findings suggest that PS and PE exposure may represent two features of the same type of pathological process which starts with phospholipid translocation imbalance and inappropriately recognized cellular components, and ends with mis-targeting of the immune system and autoimmune diseases.

As far as I am aware, this is the first study to simultaneously visualize and follow the dynamic of PS and PE on the membrane surface of live cells. PS targeting antibodies were proven as useful tools for modulating the immune

system and directing it against tumor vessels and viruses [25]. In spite of the failure of efficient drug delivery by nanoparticle use, the antibody targeting may still lead to alternative approaches for immune modulation and anti-angiogenesis.

I tested the PS and PE targeting antibodies for their ability to localize on the endothelial cells within tumors. I used a tumor model which was previously responsive to the treatment with bavituximab antibody, MDA-MB-231 [25]. I was able to detect both PS and PE liposomes on the surface of endothelial cells of the capillaries within the tumor developed in the MFP. The liposomes were also detected on the capillaries of other organs which are known to trap them (liver and spleen). I was not able to bring any quantification regarding the amount of liposomes localized at the tumor site because the only method suitable for such calculation involves the use of heavily radiolabeled liposomes.

The final end point of developing the PS and PE targeting liposomes is to deliver drugs to the tumor site better than non-targeted liposomes. Bavituximab antibody has therapeutic benefit against a large array of tumor types (breast, lung, prostate). The model I chose for testing (MDA-MB-231) is responsive to both therapy with bavituximab and also to DXR. Bavituximab targeted liposomes loaded with DXR represents a combination of two successful approaches; the result of which could be a synergistical effect. Previously, bavituximab was successfully combined with docetaxel for another breast cancer model (MDA-

MB-435) [140]. The outcome of our experiments with bavituximab targeted liposomal DXR were opposite to our predictions; the tumors treated with the targeted liposomes grew significantly larger than the control-liposomes conjugated to a Fab' fragment not reactive in mice. Similar results were obtained with duramycin targeted liposomes, even if I increased the PE presence on the tumor endothelial cells by combination of the liposomal treatment with local radiotherapy. In both experiments, the difference of the tumor volume increase in the targeted liposome approach was statistically different from the control targeted liposomes. The outcome of the tumors treated with β2GP1 targeted liposomes was not distinct from the tumors treated with control liposomes. All these experiments show that targeting liposomes to PS or PE is not a beneficial strategy to be employed for drug loaded liposomes. The most likely explanation I have for our finding is that the total amount of liposomes that are targeted to the tumor site is lower with the PS/PE binding liposomes. The endothelial cells within tumor are indeed positive for PS and for PE, as shown in the literature and confirmed by our experiments. But tumor endothelial cells are not the only structures that present on their surface these phospholipids. Aged erythrocytes have a decreased activity of APTL and an increase of PS and PE on the surface of the plasma membrane [197, 198]. *In vivo* biodistribution experiments with radiolabeled PS/PE binding annexin V show that a large amount of the tracer accumulates in liver, kidney, and gut [199, 200]. Activated platelets present PS

and use it for regulating coagulation [201-203]. Circulating microparticles from plasma are small cell fragments derived from endothelial cells, thrombocytes, erythrocytes, or macrophages. They have been shown to present PS on their surface and are found in larger amounts in inflammatory states or cancer patients [194, 204, 205]. Together, the PS or PE on other structures than tumor endothelial cells may be sufficient enough to create a sink for skewing the distribution of targeted liposomes away from the tumor site. In the case of an antibody which triggers a change on an immune response toward tumor cells the fraction of the total injected dose that localizes to the tumor may be less important than for a liposomal system.

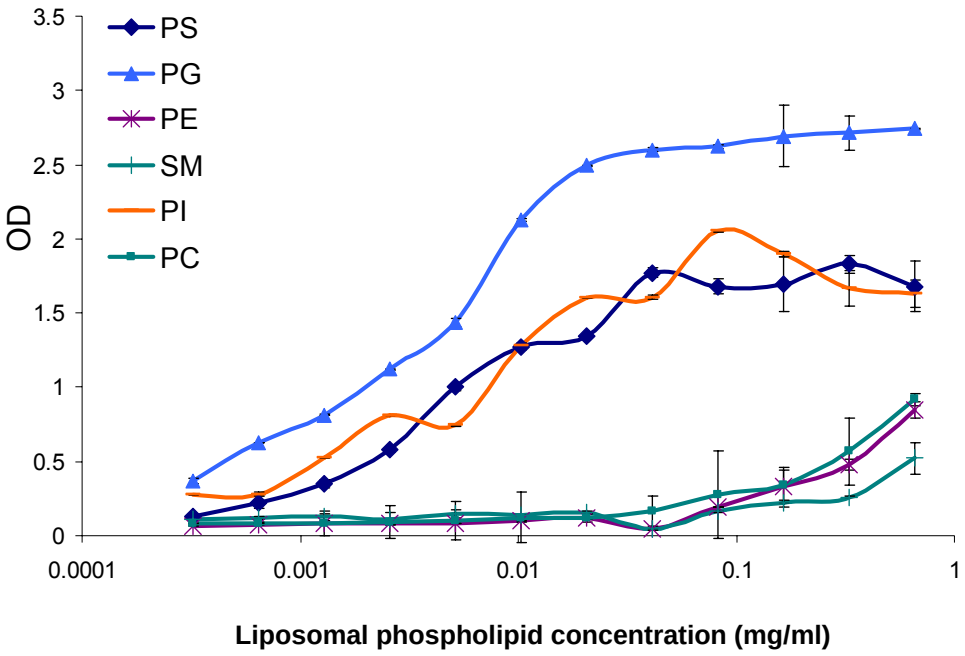

Fig. 5_1: Bavituximab-liposomes bind to anionic phospholipids

The wells of ELISA plates were coated with PS, PI, PG, PE, PC, or SM and incubated with serial dilutions of biotinylated bavituximab conjugated liposomes. The liposomes were detected using HRP conjugated streptavidin. Bavituximab liposomes bound anionic phospholipids (PS, PI, and PG) and not to neutral phospholipids (PE, PC, and SM)

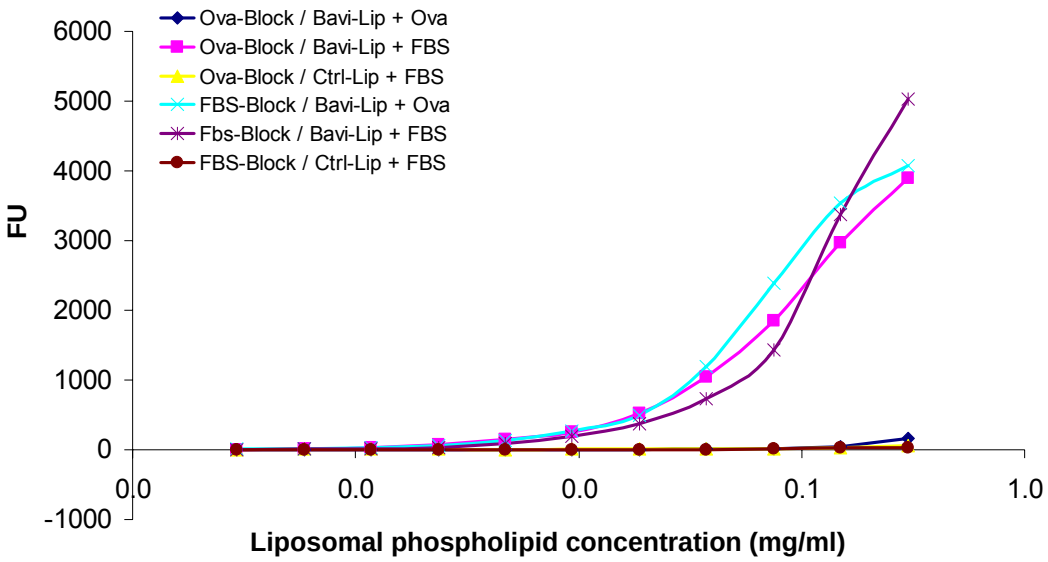

Fig. 5_2: Binding of bavituximab-liposomes to PS is β2GP1 dependent

The wells of ELISA plates were coated with PS and blocked with either 10% fetal bovine serum or with 2% ovalbumin in PBS. Serial dilutions of bavituximab conjugated liposomes filled with 5 mM pyranine solution were incubated on the plate in the buffers specified for each line. The liposomes were detected by reading the fluorescence after pyranine released from the liposomes using 0.2% triton X-100. Bavituximab liposomes bound to PS only when PS was exposed to FBS either in the blocking step of incubation step. There is no binding when both blocking and incubation were done in ovalbumin buffer.

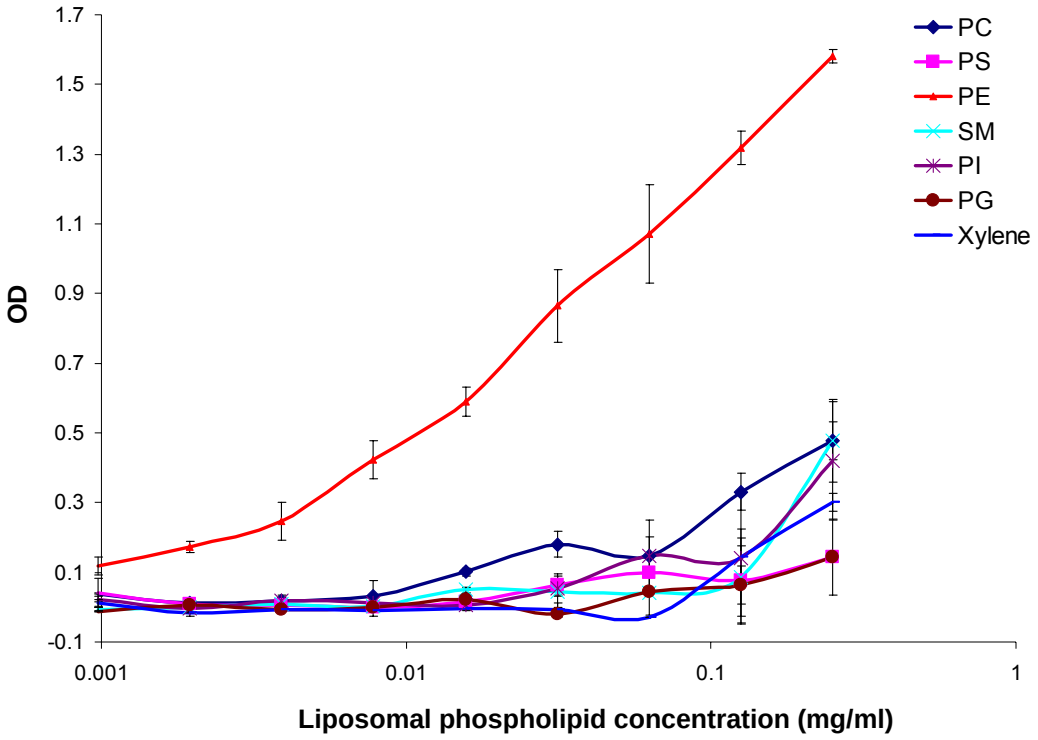

Fig. 5_3: Specific binding of duramycin conjugated liposomes to PE.

The wells of ELISA plates were coated with PS, PI, PG, PE, PC, or SM and incubated with serial dilutions of biotinylated duramycin conjugated liposomes. The liposomes were detected using HRP conjugated streptavidin. The specific binding curve of duramycin liposomes is plotted after the signal of control liposomes was subtracted from the signal obtained with the duramycin liposomes, at each concentration. Duramycin liposomes bound to PE only with no binding above background to any other phospholipids.

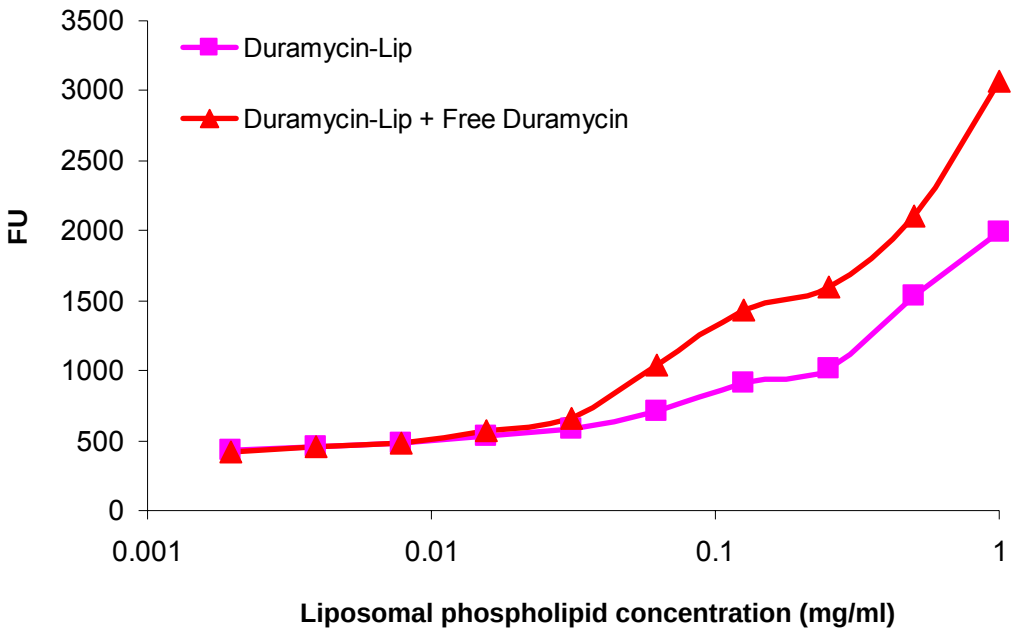

Fig. 5_4: Free duramycin enhances the PE binding activity of duramycin-liposomes

The wells of ELISA plates were coated with PE and blocked with 10% FBS in PBS. Serial dilutions of pyranine filled duramycin liposomes were incubated on the plates in the presence or absence of 200 times free duramycin excess. The liposome binding was quantified by reading the fluorescence of pyranine released using 0.2% Triton x-100 solution. Free duramycin enhances the binding of liposomal duramycin to PE.

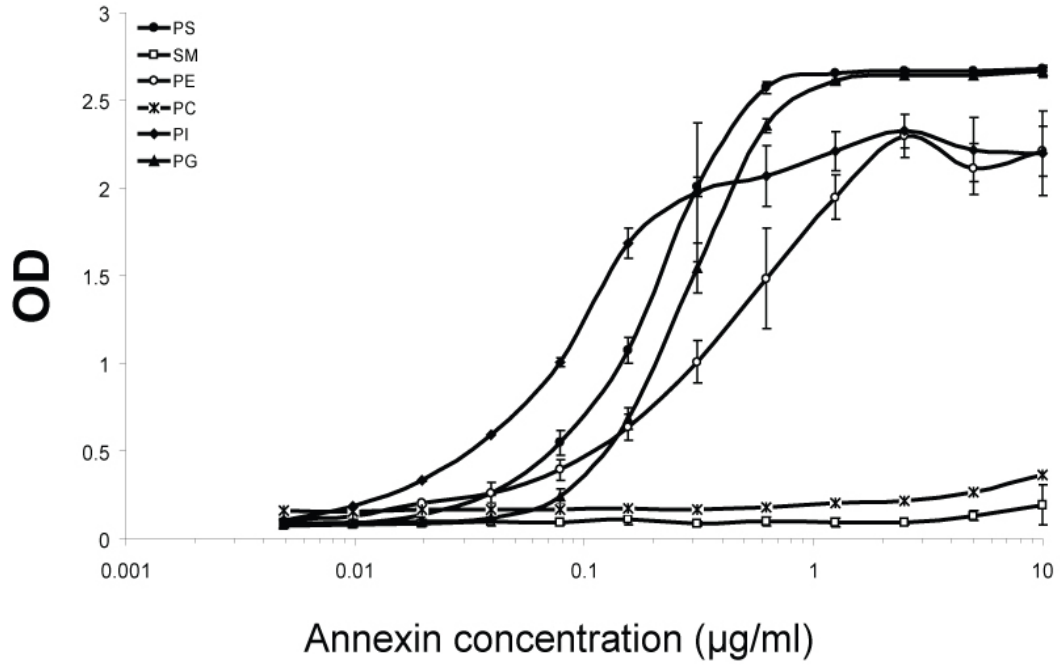

Fig. 5_5: Annexin V binds to anionic phospholipids and to PE

The wells of ELISA plates were coated with PS, PI, PG, PE, PC, or SM and incubated with serial dilutions of biotinylated annexin V. The binding of annexin V was detected using HRP conjugated streptavidin. Annexin V binds to anionic PL (PS, PI, PG) and to neutral PE. There is no binding to PC or SM.

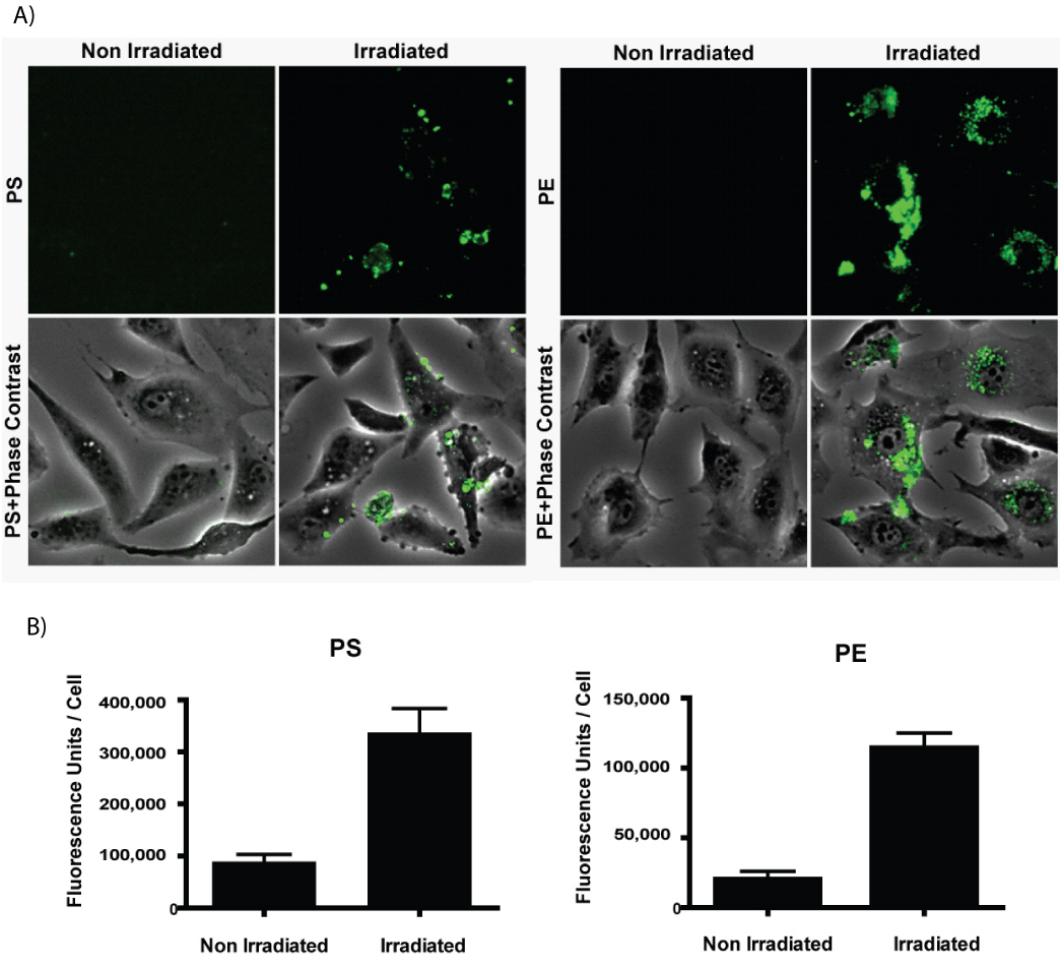

Fig. 5_6: PS and PE become exposed on the surface of irradiated endothelial cells.

A) ABAE cells were irradiated with 5 Gy and stained 24 hours later for PS or PE using pyranine-containing fluorescent liposomes (green). Non irradiated cells were also examined. The live cells were washed and immediately imaged using a fluorescence microscope. Staining is superimposed on phase-contrast images. B) PS and PE exposure on ABAE cells was quantified using Image J software. The histograms show the ratio of fluorescence units / cell +/- SEM. Irradiation significantly increased PS ($p < 0.05$) and PE ($p<0.001$) exposure.

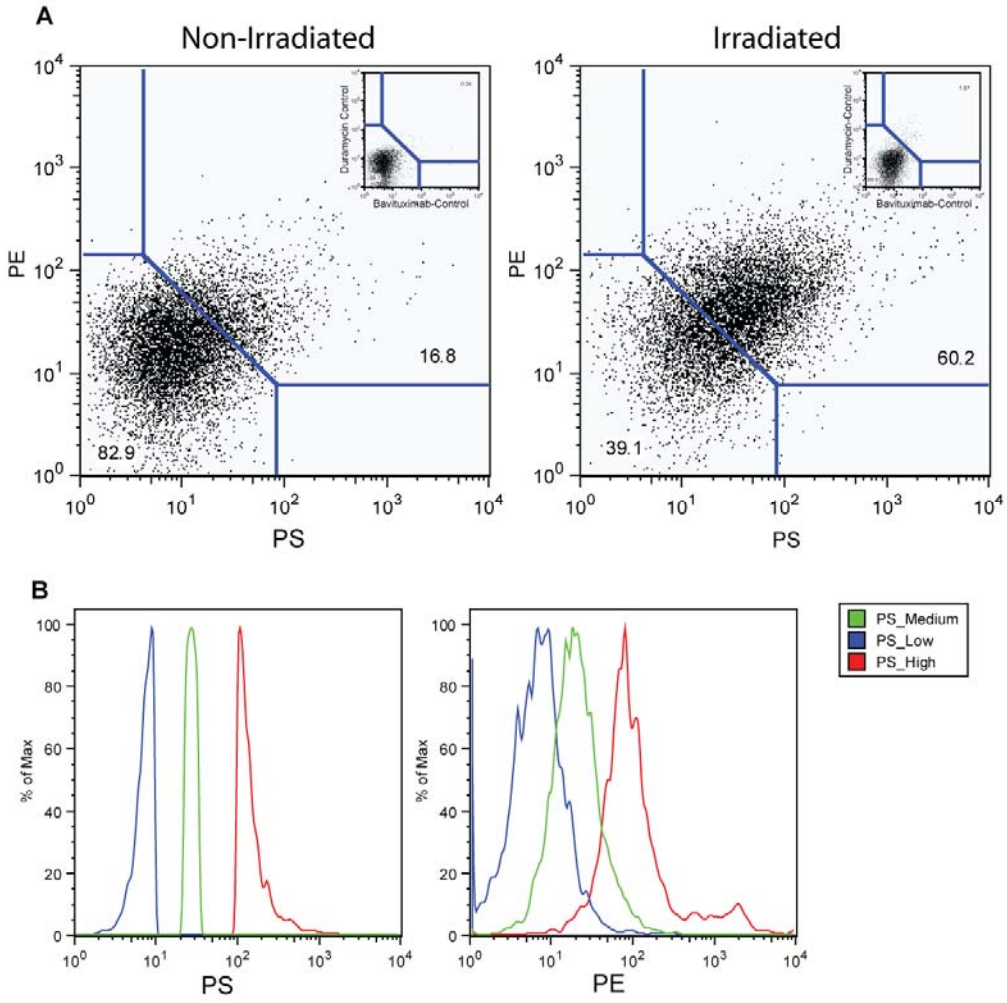

Fig. 5_7: PS and PE are exposed on the surface of myeloma cells after irradiation.

Mouse myeloma cells (NS0) were double stained for PS and PE using fluorescent and biotinylated liposomes and analyzed by flow cytometry. Propidium iodide positive cells were excluded from the data analysis. A) The dot-plot representation of non-irradiated and irradiated NS0 cells shows that after irradiation cells become double positive for PS and PE. The insets show that cells stained with control liposomes are not stained. B) Cells were gated for low, medium, or high PS (blue, green, and red) and each subgroup was analyzed for PE intensity. Cells with low PS also have low PE, cells with medium PS have medium PE, while and cells with high PS have high PE.

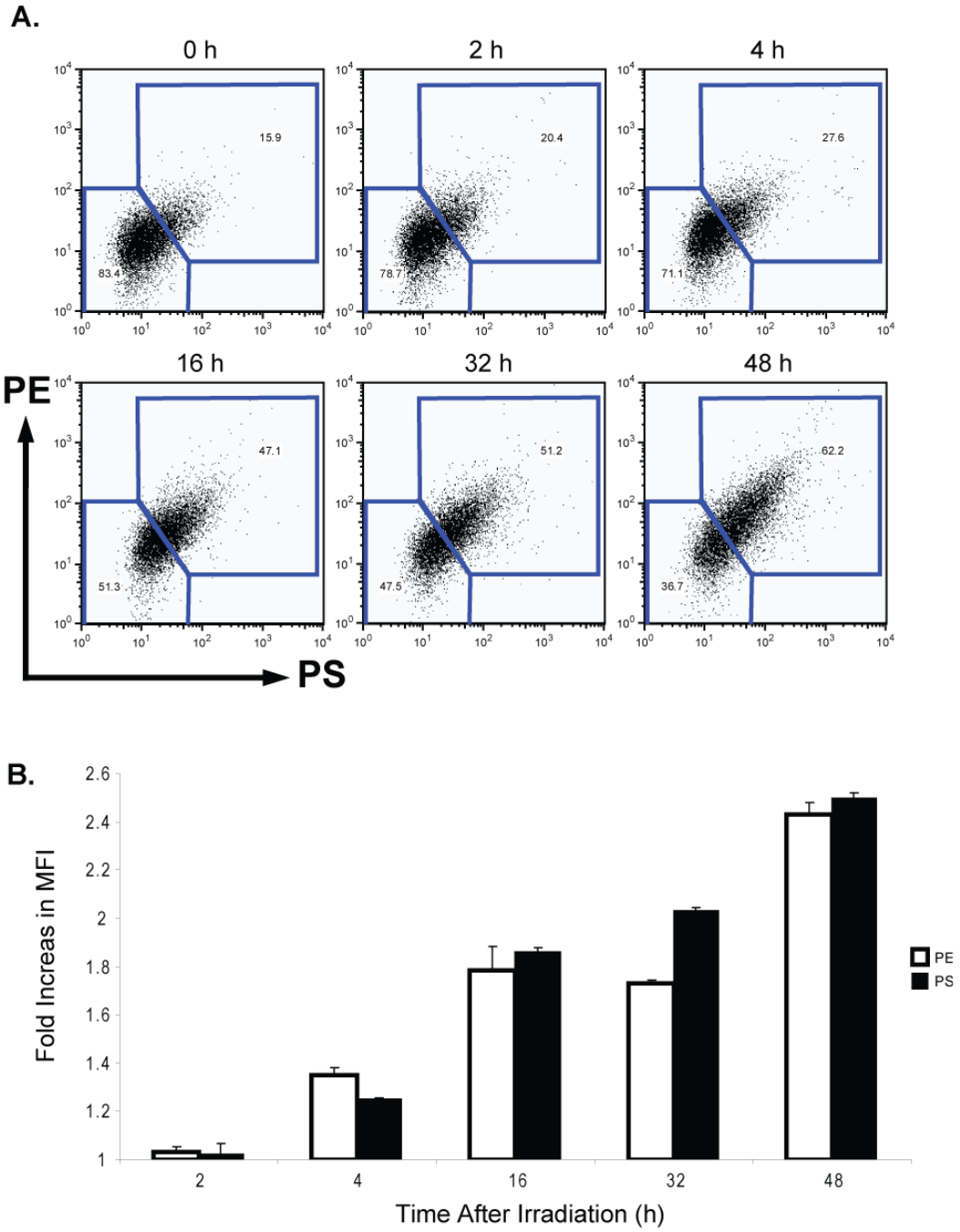
A.
0 h
2 h
4 h
16 h
32 h
48 h
15.9
20.4
27.6
83.4
78.7
71.1
47.1
51.2
62.2
51.3
47.5
36.7
PE
PS
B.
Fold Increas in MFI
2.6
2.4
2.2
2
1.8
1.6
1.4
1.2
1
2
4
16
32
48
Time After Irradiation (h)
PE
PS

Fig. 5_8: Time-course of PS and PE exposure on the surface of irradiated myeloma cells.
NS0 cells were cytofluorimetrically analyzed for PS and PE exposure at various times after irradiation. A) Dot-plot representation of the propidium iodide negative cells. After irradiation, the percentage of the cells positive for both markers gradually increases. B) MFI for PS and PE staining is expressed as a fold increase of that on non-irradiated cells. Significant PS and PE exposure is seen at 4h and progressively increases up to 48 hours after irradiation.

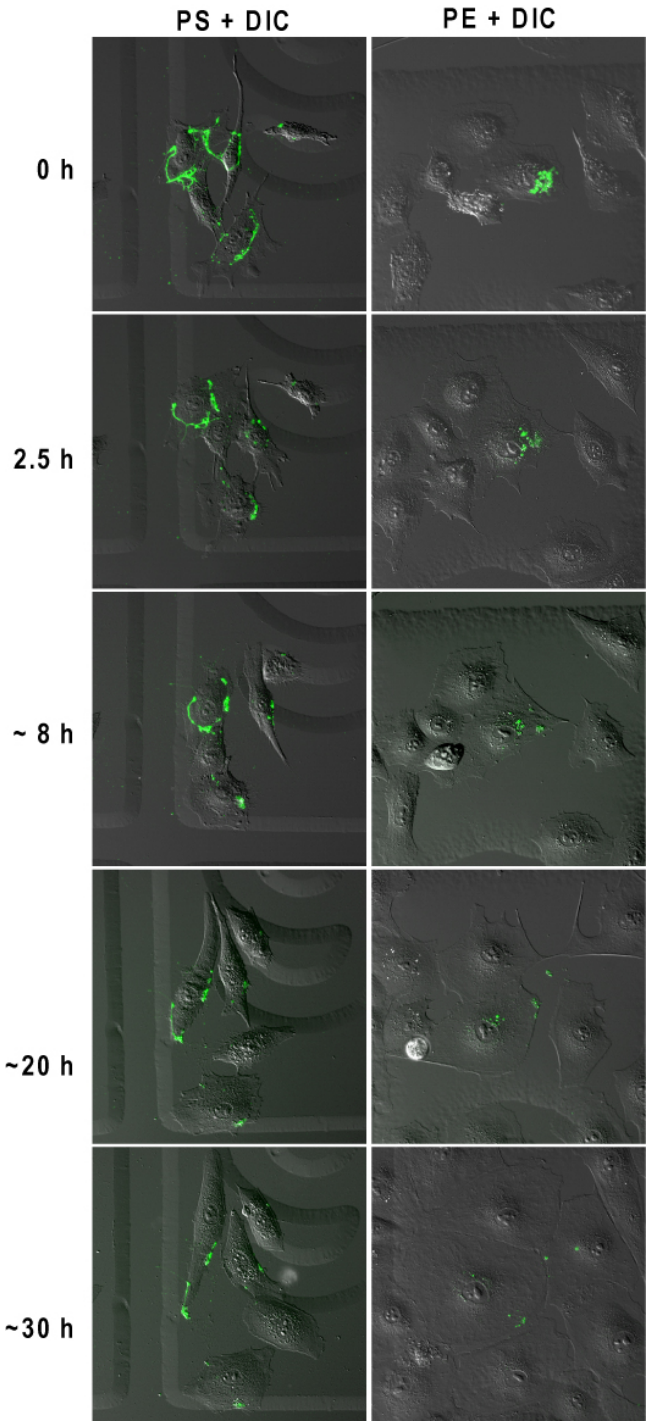

Fig. 5_9: The dynamics of PS and PE exposure areas are similar

The dynamics of PS and PE exposure areas on the surface of irradiated ABAE cells were observed over a 30 h period. The cells were stained with pyranine filled liposomes. We followed the time evolution of the fluorescence. The images are obtained by merging the fluorescence with DIC pictures. PS and PE exposure is concentrated into blebs distributed on various locations on the cell surface. In time the positive areas congregated toward the periphery of the cells. The cells were not in a late stage of apoptosis, since they were intact and moving on the microscope slide.

Fig. 5_10 - A

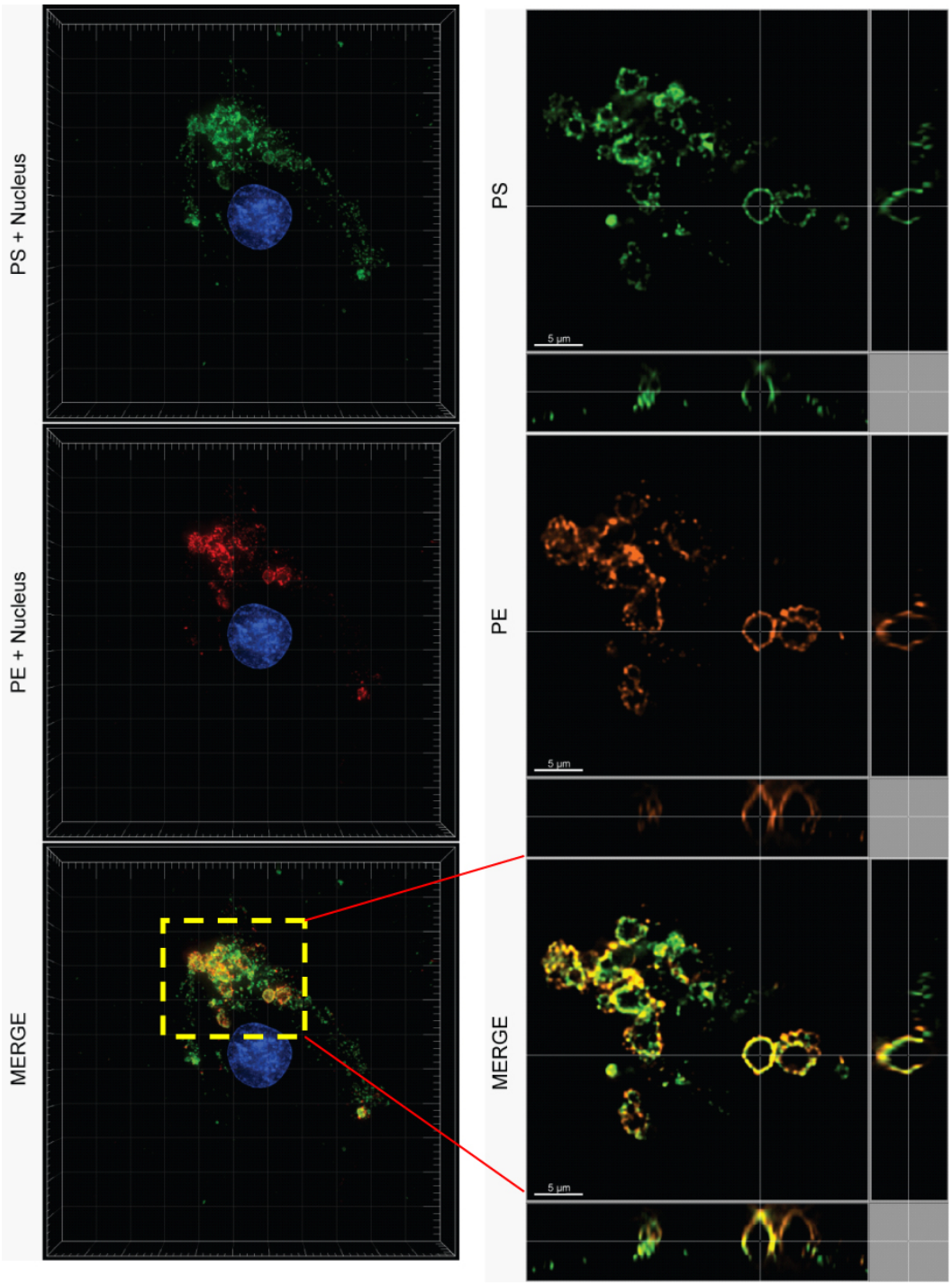

Fig 5_10 -B

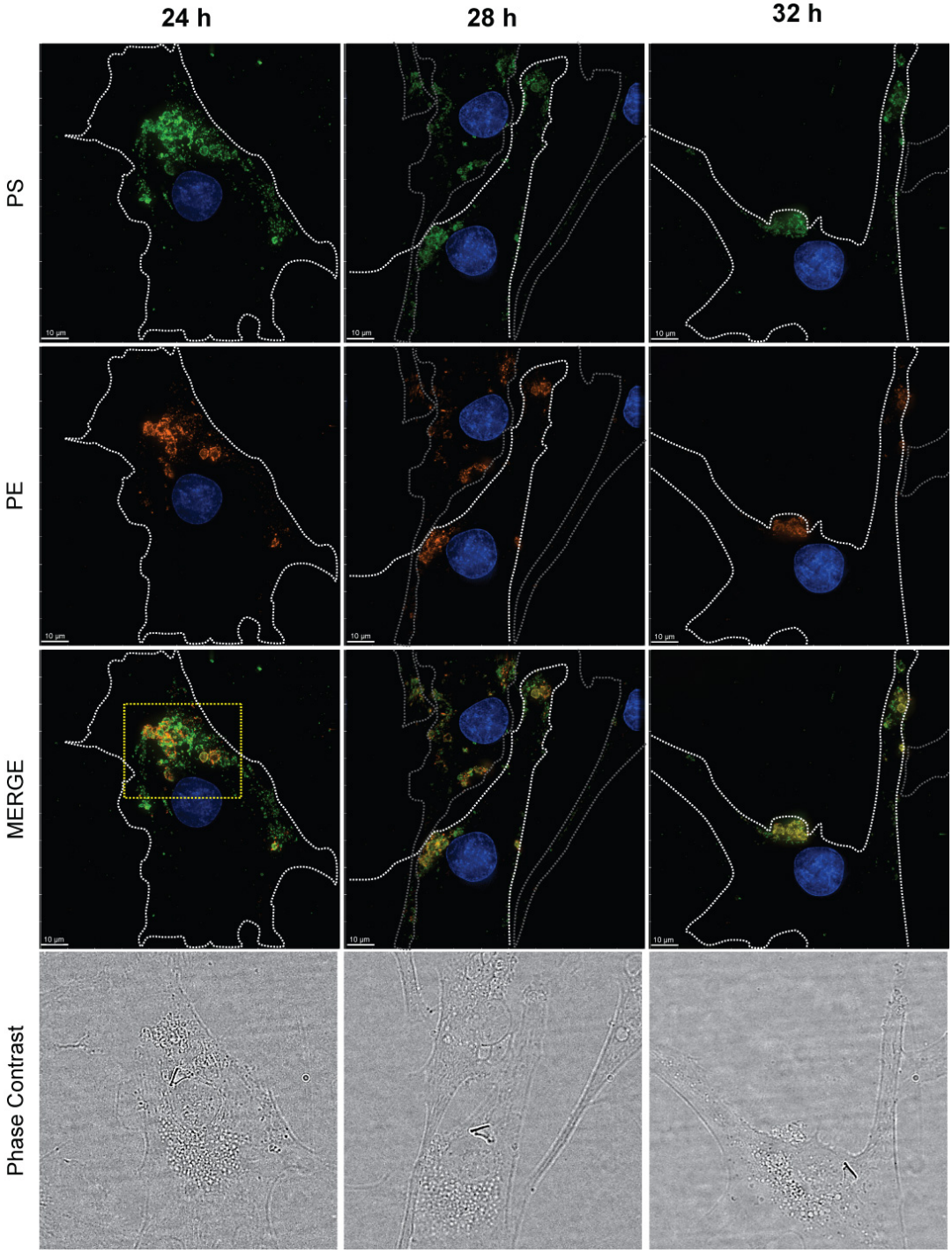

Fig. 5_10: PS and PE are expressed on the same area of the cell and remain colocalized.

ABAE cells were irradiated and stained for PS (green) and PE (red) 24 hours later. The nuclei (blue) were stained with the cell permeable stain Hoechst 33342. The cells were imaged at 24 hours, 28 hours, and 32 hours after irradiation. A deconvolution microscope was used to obtain a z stack of the cells and a phase contrast reference image was taken in the middle of the z stack. The images were used for a 3D reconstruction on Imaris software.

A) The pictures represent a full 3D reconstruction. The PS and PE staining are co-clustered into discrete areas which appear to be cell membrane blebs that protrude from the cell surface. Other positive patches are spread toward the periphery of the cells. A high magnification view of the region of the cell demarked by the yellow dotted rectangle is presented in the right side of the figure as a z stack with 3 orthogonal views. Colocalization of PS and PE to several membrane blebs is visible.

B) The pictures are obtained with the "easy 3D" function of the software. The outer limits of the cell represented in Fig. A were followed by phase contrast in microscopy and are marked with white dotted lines. The grey lines mark two cells which visit the microscope field at 28 and 32 hours. The Pearson correlation factors for PS and PE colocalization are 0.49 (24 hours), 0.5 (28 hours) and 0.54 (32 hours) signifying a high degree of colocalization. The staining pattern and the colocalization are maintained over the 8 h period of examination.

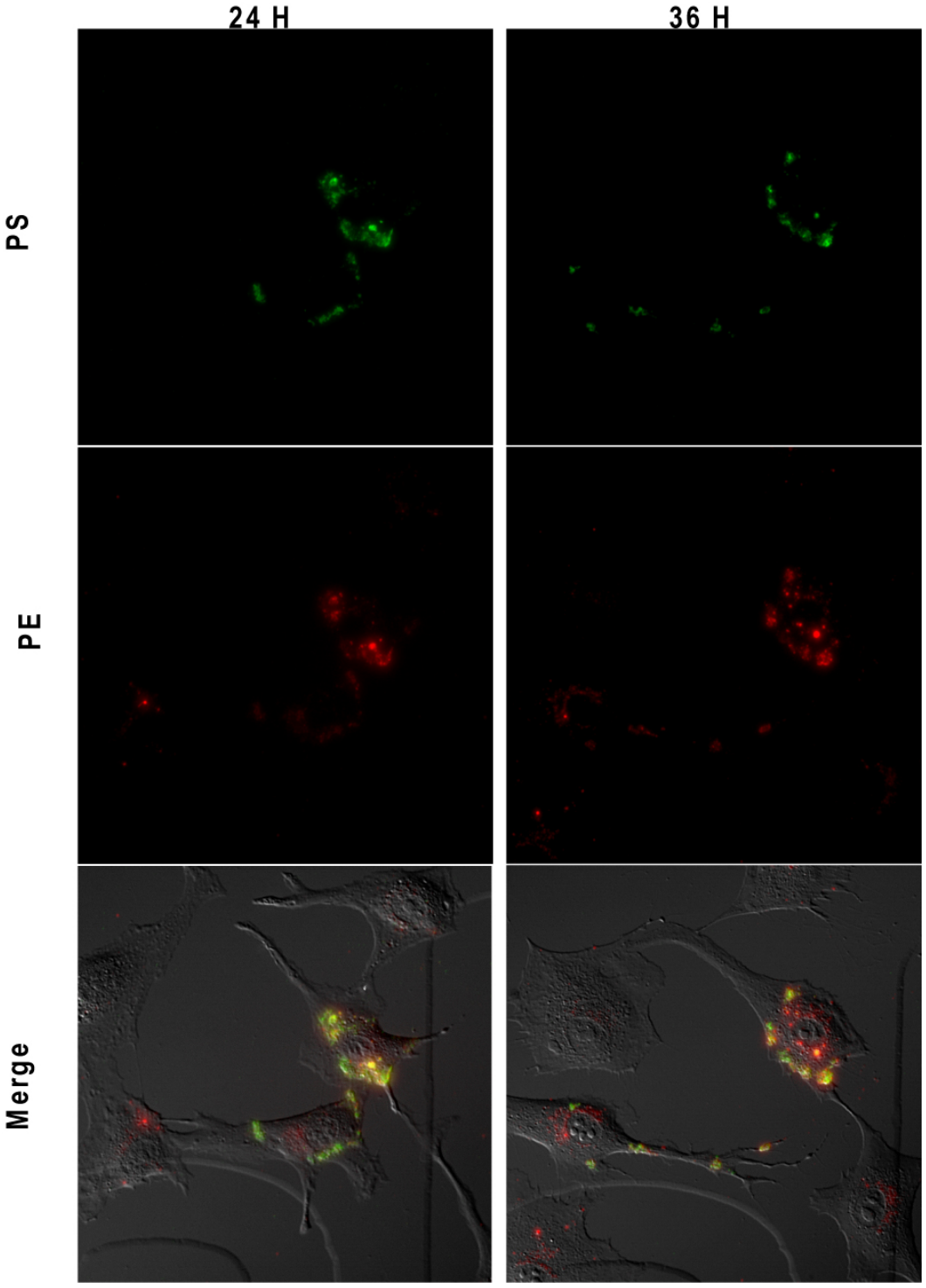
24 H
36 H
PS
PE
Merge

Fig. 5_11: PS and PE double positive areas drift on the cell surface and are escaped from the cytoskeleton anchorage

ABAE cells were plated on graded dishes, irradiated and stained for PS (green) and PE (red) 24 hours later. The cells were imaged at 24 hours and 36 hours after irradiation using a fluorescence microscope equipped with DIC filters. The pictures show colocalized PS and PE areas that look like membrane blebs. The lower positive cell is moving toward left of the field and a dendritic like protrusion remains on the back of the cell. The positive blebs drift from the perinuclear region to the tip of the membrane extension

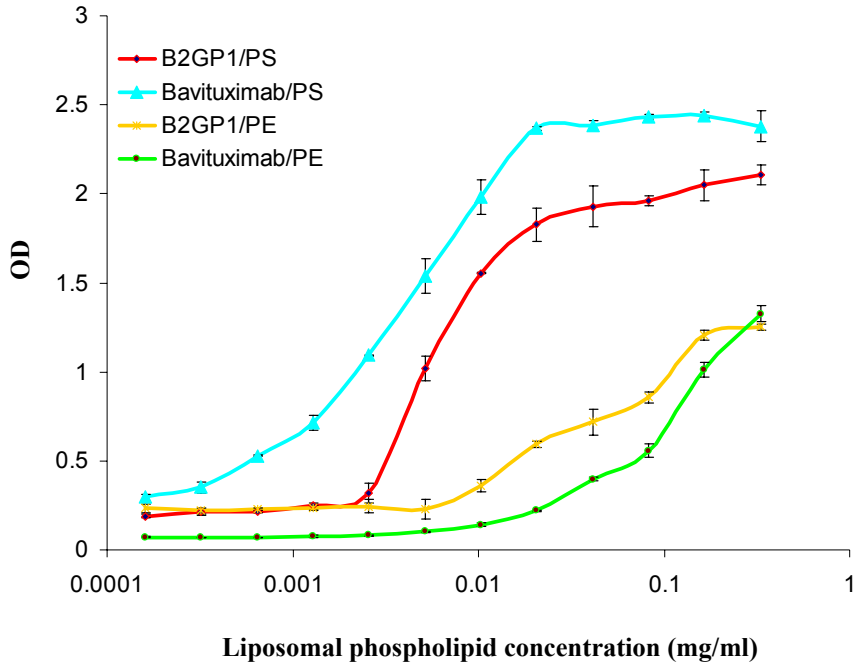

Fig. 5_12: β2GP1-liposomes have similar binding properties to bavituximab-liposomes

The wells of ELISA plates were coated with PS or PE and incubated with serial dilutions of biotinylated bavituximab conjugated liposomes and β2GP1 conjugated liposomes. The liposomes were detected using HRP conjugated streptavidin. β2GP1 liposomes bound to PS similarly to bavituximab ones. Both liposome types had only background binding to PE.

A)

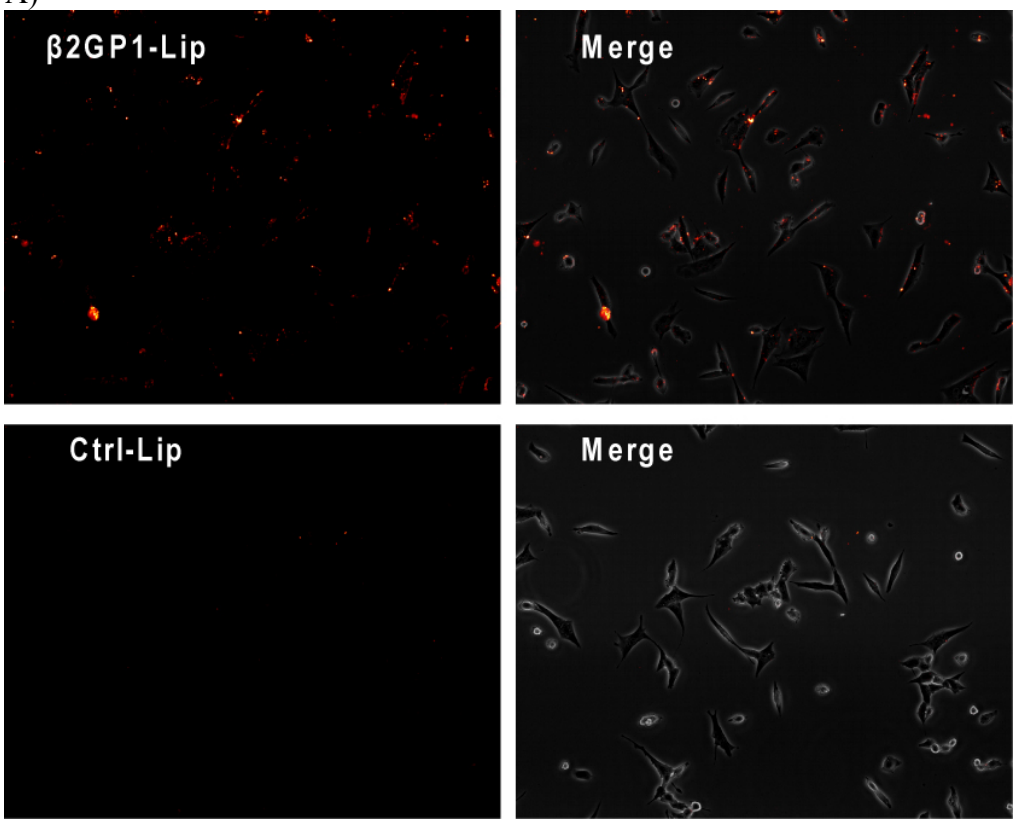
β2GP1-Lip
Merge
Ctrl-Lip
Merge

B)

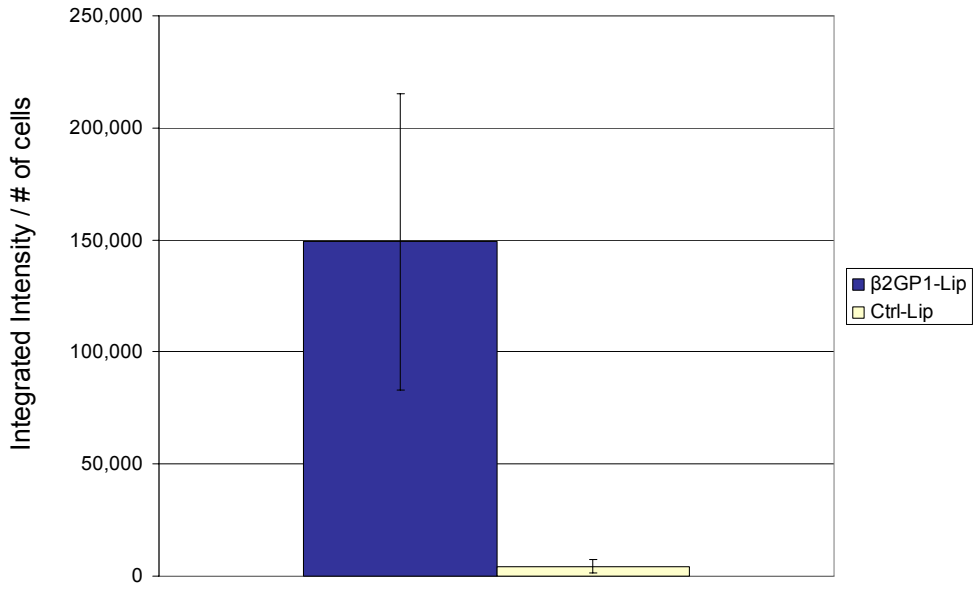
250,000
200,000
150,000
100,000
50,000
0
Integrated Intensity / # of cells
β2GP1-Lip
Ctrl-Lip

Fig. 5_13: β2GP1 conjugated liposomes bind to PS expressing endothelial cells

A) ABAE cells were treated with 200 μM l-PC for 30 minutes and immediately stained using sulphorhodamine filled liposomes conjugated to β2GP1 or with control liposomes. The cells were washed and immediately imaged using a fluorescence microscope. β2GP1 liposomes yield an intense staining on the majority of the cells. B) The staining on ABAE cells was quantified using Image J software. The histograms show the ratio of fluorescence units / cell +/- SEM. β2GP1 liposomes lead to ~ 30 times more staining intensity compared with the control liposomes.

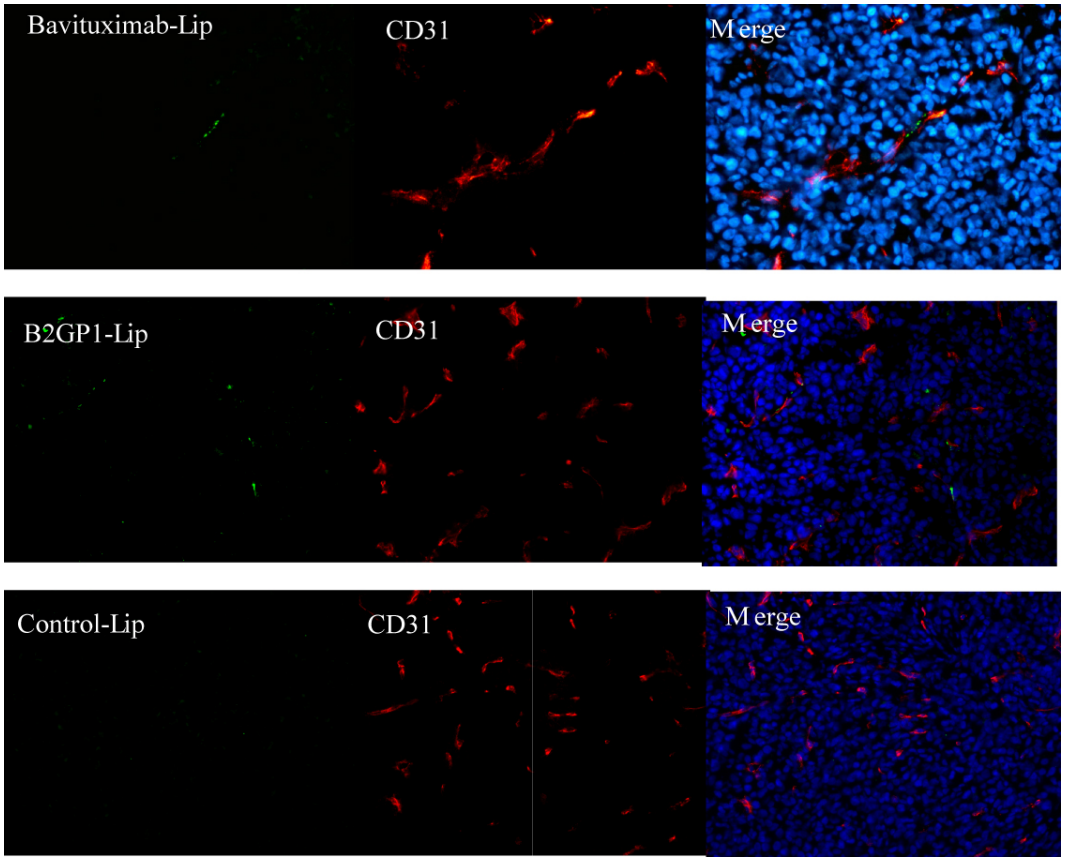

Fig. 5_14: **Tumor endothelial cell localization of PS binding liposomes**

Human breast cancer cells MDA-MB-231 were grown in the MFP of nude mice (nu/nu). A suspension of biotinylated PS targeting liposomes (0.2 mg phospholipids) were injected i.v. 4 hours later the mice were heparinized and sacrificed by perfusion through the left ventricle after general anesthesia. Tumors were harvested, sectioned and subjected to IHC. Liposomes were detected with FITC conjugated streptavidin (green) and blood vessels were detected by anti CD31 staining (red). Bavituximab and β2GP1 liposomes were detected on endothelial cells of the capillaries within the tumor.

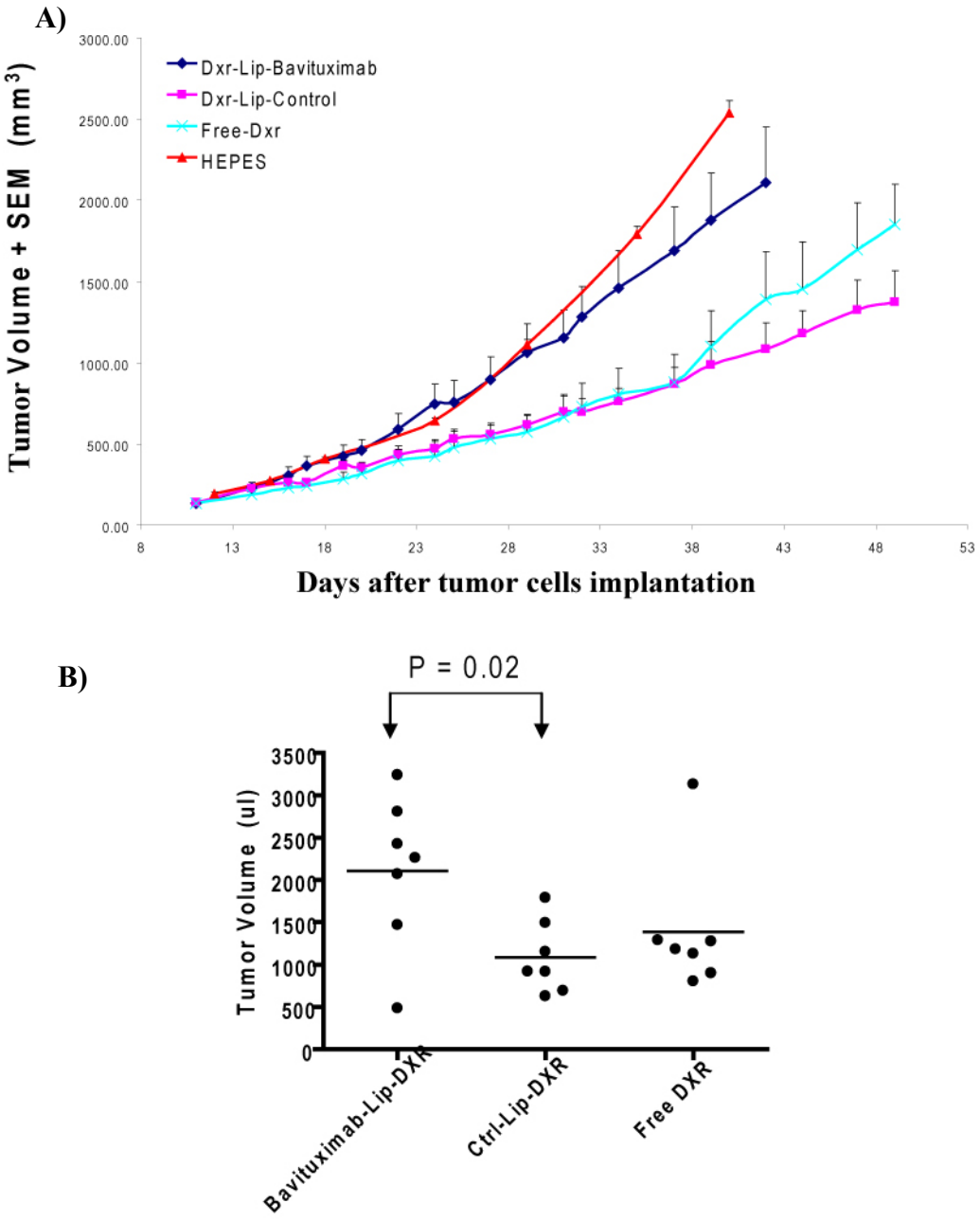

Fig. 5_15: Lack of therapeutic effect of bavituximab-liposomes against MDA-MB-231 tumors in mice

$3.5x10^6$ human breast cancer cells (MDA-MB-231) were injected into the MFP of female nude mice (nu/nu). When tumors grew at 100 µl, the mice were randomized to receive either bavituximab targeted liposomal DXR, control targeted liposomal DXR, free DXR, or buffer only. DXR was administered i.v. at

a dose of 4 mg/kg/injection every 5 days. The tumors were measured with a caliper and the tumor volume was calculated as (small diameter x large diameter^2)/2. A) The time evolution of the average tumor volume after cell implantation. B) Individual tumor volumes were plotted for each treatment group at the end of the experiment (day 49). The bavituximab treated group average tumor volume is statistically significant larger than the average in the control liposomes treated group.

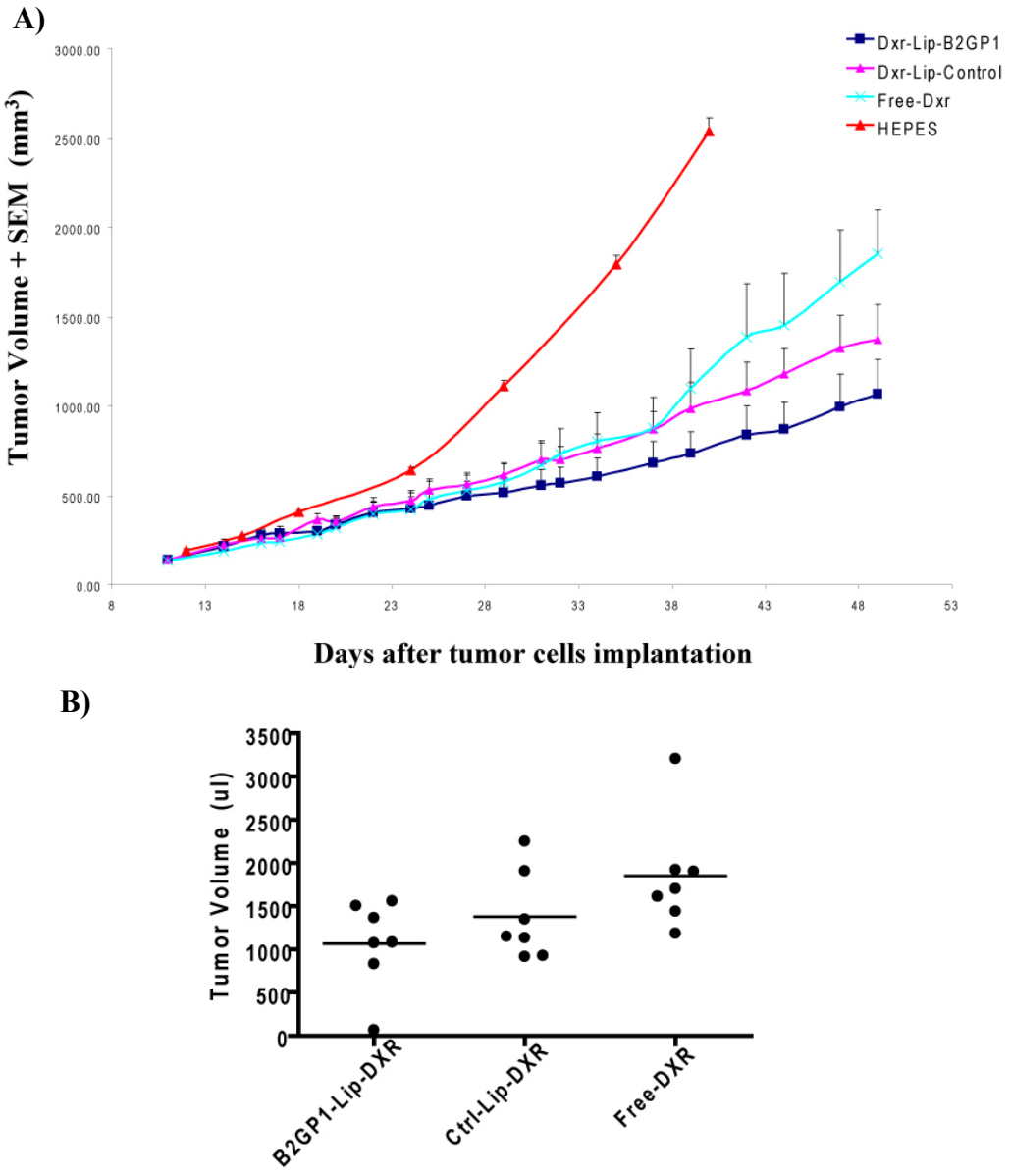

Fig. 5_16: Lack of therapeutic effect of β2GP1-liposomes against MDA-MB-231 tumors in mice

$3.5x10^6$ human breast cancer cells (MDA-MB-231) were injected into the MFP of female nude mice (nu/nu). When tumors grew at 100 µl, the mice were randomized to receive either β2GP1-targeted liposomal DXR, control targeted liposomal DXR, free DXR, or buffer only. DXR was administered i.v. at a dose of 4 mg/kg/injection every 5 days. The tumors were measured with a caliper and the tumor volume was calculated as (small diameter x large diameter^2)/2. A) The time

evolution of the average tumor volume after cell implantation. B) Individual tumor volumes were plotted for each treatment group at the end of the experiment (day 49). The β2GP1 treated group average tumor volume is not different from average in the control liposomes treated group.

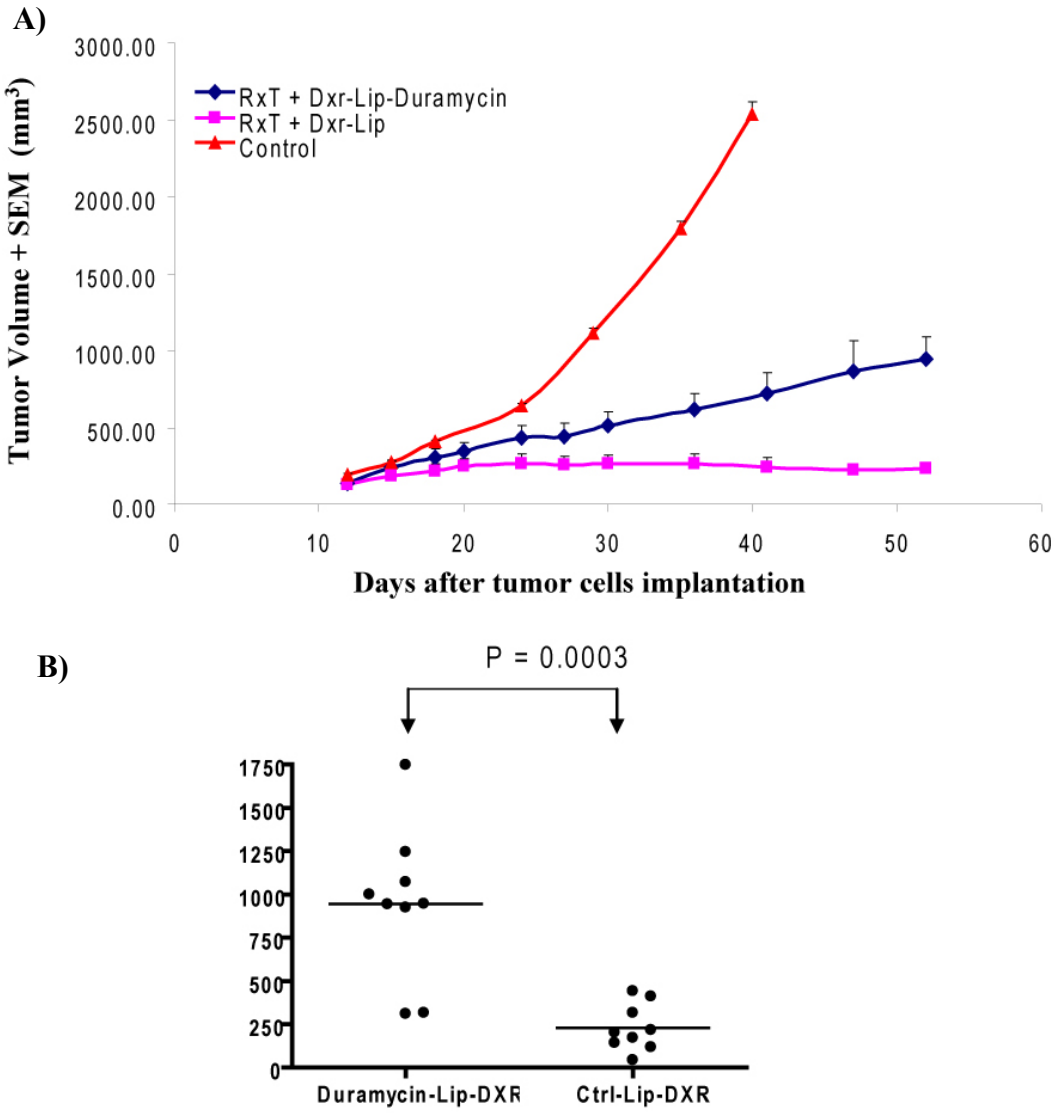

Fig. 5_17: Lack of therapeutic effect of duramycin-liposomes against MDA-MB-231 tumors in mice

$3.5x10^6$ human breast cancer cells (MDA-MB-231) were injected into the MFP of female nude mice (nu/nu). When tumors grew at 100 µl, the mice were randomized to receive local radiotherapy (2 Gy/session x 5 times) in combination with either duramycin targeted liposomal DXR or control targeted liposomal DXR. Another group of mice received only buffer treatment. DXR was administered i.v. at a dose of 4 mg/kg/injection every 5 days. The tumors were measured with a caliper and the tumor volume was calculated as (small diameter

x large diameter^2)/2. A) The time evolution of the average tumor volume after cell implantation. B) Individual tumor volumes were plotted for each treatment group at the end of the experiment (day 52). The average volume in the treatment with duramycin targeted liposomes is statistically significant larger than in the treatment with control liposomes.

Targeting agent	Tumor capillaries	Liver	Kidney glomeruli	Spleen
Bavituximab-Lip	+	-	-	-
β2GP1-Lip	+	+	-	+ +
Control-Lip	-	+/-	-	+

Table 5_1: **Biodistribution of PS targeting liposomes to the capillaries of organs known to trap liposomes.**

Cryosections of tumors, kidney, liver and spleen were obtained during the experiments described in the previous figure. The liposomes were detected with HRP-conjugated streptavidin and developed with DAB. The intensity of the staining was observed under the microscope and quantified as (-) for no clear staining above background, (+) 1-4 scattered, low intensity vessel-like structures, and (++) intensely stained > 5 vessels/field. Bavituximab liposomes were detected only on the tumor capillaries while β2GP1 liposomes were detected on tumor capillaries, liver and very intensely on spleen. Control liposomes were detected only in the liver and spleen. None of the liposomes was detected on the kidney glomeruli.

CHAPTER VI

CONCLUSIONS

My project was initiated with the purpose of enhancing the antitumor effects of previously developed vascular targeting antibodies. Targeting drug loaded liposomes to the tumor vessels using the antibodies against VEGFR-2 or PS constitutes a proof of principle that can be expanded to a variety of other therapeutic methods. Nanoparticles, and liposomes in particular, are attractive tools due to their flexibility to be used as carriers for drugs, imaging agents, radioisotopes, or even emerging technologies such as neutron capture therapy or near infra red energy capture.

In this project I have constructed and tested liposomes targeted toward three molecules known to be present on the surface of the endothelial cells within tumors: VEGFR-2, PS, and PE. Two of the targeting ligands were Fab' fragments (RAFL and bavituximab) which are already classical types of molecules for liposomal conjugation. Duramycin has been conjugated to an antibody backbone and used for PE targeting (unpublished data from Thorpe laboratory) but it was never conjugated to a nanoparticle. The use of β2GP1 is also a new concept for creating targeted nanoparticles.

Liposomes bound to the purified target in solid phase assays and to endothelial cells *in vitro* and *in vivo*. Bavituximab and duramycin conjugated

liposomes were used to determine the coincidence of PS and PE on the surface of irradiated cells [submitted paper]. This is the first time that PS and PE have been simultaneously detected on the surface of live cells. These two types of liposomes allowed me to study the distribution and time course of the externalization of PS and PE on the surface of irradiated cells.

The therapeutic benefit of targeting was tested by loading the liposomes with DXR and treating mice in orthotropic breast cancer models. No benefit was noted with any of the targets, while in some conditions targeting itself proved to be disadvantageous for the antitumor effect of the drug loaded liposome.

Vascular targeting with liposomes is a relative new field of study, with no formulation being in clinical use yet. Studies in animal models have been done only with cytotoxic drugs loaded in either cationic liposomes or PEG coated liposomes. The liposomes have been targeted with one of the four ligands only: RGD peptides, NGR peptides, MT1-MMP binding molecules, and PRP sequence containing peptides. Compared with the multitude of targets used by other classes of VTAs the liposomal targeting has not been widely developed.

The limited success in this field until now may be explained either by the general characteristics of the liposomes that makes them less suitable for tumor vascular targeting or by the wrong type of ligands being tested. PEG coated, long circulating liposomes have a spontaneous accumulation in tumor tissue. This phenomenon was named “passive targeting” because it appears without specific

interaction of a ligand with a target. A particle has to fulfill two conditions in order to be able to do passive targeting: large size (macromolecules or nanoparticles of 10-150 nm) and long circulation time.

The large size is necessary because it can take advantage of the "enhanced permeability and retention" (EPR) phenomenon in the tumor interstitium. A combination of chemical and morphological factors determines a high permeability of the tumor vessels. The tumor environment is enriched in humoral factors that promote vasodilatation and extravasation of the plasma: VEGF, bradikynin, and nitric oxide [206]. Also, the endothelial cells of the tumor vessels only provide an imperfect barrier due to the presence of gaps between them or within their cell body [49]. Another factor contributing to the EPR is the intratumoral blood circulation, with slow speed and occasional complete stop or reversal [207]. The result of these factors is that plasma components are leaking out of the tumor vessels abundantly. The insufficient lymphatic drainage of the tumor interstitium makes it more difficult for macromolecules than small molecules to be cleared from site. The increased permeability associated with deficient drainage leads to an overall higher tumor accumulation of macromolecules (or liposomes) compared with small molecules, i.e. passive targeting.

The second condition, the long circulation time of nanoparticles, depends on a minimal interaction with most organs and structures of the body. Classical

liposomes had a very short half life due to binding to the RES. It is only when they were coated with PEG, that they were found to have long half life and be able to do passive targeting; this lead to their extensive use. The PEG contributes little to the particle size or mass, it only decreases its interaction with other molecules and structures [123].

Use of PEG grafted liposomal technology represented an advancement in chemotherapy, because small molecules, such as DXR, behaved pharmacologically as large molecules upon encapsulation and were subjected to passive targeting [Fig. 6_1]

The concept of ligand targeted liposomes brings advantages to PEG coated liposomes only if the active targeting does not preclude the passive targeting. By definition, coating a PEG liposome with a ligand it will increase the interaction of the liposomes with the receptor. Since the liposomes are multivalent, usually their interaction with a target has a very high avidity, helping them bind and remain bound even to low density targets. If the receptor is expressed on various organs then the liposomes can be easily trapped, they will have a decreased circulation time, and the second condition for passive targeting (long circulation) will be broken. Even low expression can be sufficient to dramatically affect the long circulation time. A good example is the conjugation to endoglin binding single-chain Fv fragments, which decreased the half life of PEG liposomes to 3 minutes, less than even a non-PEG coated liposome would have [85].

We can assume that liposomes could be actively targeted to the tumor endothelial cells only if the target molecule is extremely specific for the tumor vessels with no expression on other structures. Simply having a relatively higher cell surface density does not suffice. Most tumor endothelial cell markers are not exclusively expressed there; they are expressed more at the tumor site but are not undetectable on other structures. This is most likely the reason why there are very few vascular targeting liposomes and why they are not successful, compared to tumor cell targeted liposomes.

Conjugation to ligands of molecules expressed directly on tumor cells has the advantage that it does not decrease the passive targeting. When liposomes have the opportunity to bind to the target, they are already in the tumor interstitium and passive targeting has already occurred. Successful experiments with anti-HER2 immunoliposomes showed that the therapeutic benefit does not rely on the increase of the amount of liposomes that accumulates inside the tumors, but only on the internalization into the tumor cells [208].

The liposomes designed for this project were targeted to VEGFR-2, PS, and PE. None of these targets is perfectly specific to the tumor endothelial cells. VEGFR-2 was detected by IHC on the intima layer of the aorta and by western blot in the liver, kidney, adipose tissue, and lungs of adult mice [136]. The density of the receptors in these organs is relatively lower than on the tumor capillaries, but due to the high vascularization, the absolute amount of receptor presented

may be very large. Due to their high avidity, liposomes can bind very well even to scattered receptors. The consequence is that PEG coated VEGFR-2 binding liposomes do not behave as non-reactive PEG coated liposomes do in circulation and the advantage of passive targeting is decreased. Additionally, this targeting disadvantage is not compensated by a higher toxicity on the endothelial cells, since our *in vitro* data shows that internalization into the endothelial cells via VEGFR-2 engaging only minimally enhances the toxicity against these cells.

The phospholipid targets, PS and PE, are also not perfectly specific to tumor vessels. Because the liver, kidney, and gut are able to trap a large amount of intravenously injected annexin V, it is likely that PS or PE are available for the binding by liposomes as well in the vasculature of these organs [199, 200]. Un-targeted liposomes have little accumulation in the kidney or the gut. Similar to VEGFR-2 targeted liposomes, the interaction between the liposomes and PS/PE in other organs would negatively affect the passive targeting. Supplementary, phospholipid targeting liposomes may be affected by a variety of blood components that can also expose PS and PE such as senescent red blood cells [197, 198], activated platelets [201-203], and circulating microparticles [194]. The circulating microparticles may be of increased significance because it has been found that they are more prevalent in cancer patients [204]. Passive targeting of liposomes in the tumor interstitium depends on their ability to extravasate through the leaky tumor vessels. Binding to aging erythrocytes, activated

platelets, and circulating microparticles would preclude the liposomes to get outside vasculature because all these structures are larger than the optimal particulate size for EPR, which is below 150 nm [206].

My hypothesis for why VEGFR-2, PS, and PE targeting liposomes bring a disadvantage to DXR filled liposomes is illustrated in Fig. 6_1. Non-targeted, long circulating liposomes have an optimal accumulation rate in the tumor environment due to minimal interaction with vessels in the normal organs or with blood cells. The possible supplemental interaction sites of the targeted liposomes are presented. From this model, I can conclude that an ideal vascular targeting liposome would target a ligand expressed exclusively on tumor cells, and will not interact with any molecule on the normal vasculature. Additionally, it could encapsulate a drug for which cytotoxicity is highly dependent on intracellular delivery. Intracellular delivery of DXR does not significantly decrease its IC50. A much more toxic drug that is cell impermeable would be more suitable. A toxin could also be enclosed into a liposome and released after encapsulation.

In the pseudometastatic model, the VEGFR-2 targeted liposomes extended the survival of the mice, in spite of the lack of the success in the orthotropic tumors. Two factors may contribute to the discrepancy of the effect in the two models. The first one is represented by the microcirculation of the incipient metastatic foci that is not yet as disorganized as the one in the established tumors, therefore the EPR effect is not yet as strong and the liposomes do not present the

passive targeting phenomenon. The second factor may be related to a higher receptor density of the VEGFR-2 on the endothelial cells in the small metastatic foci compared to the large tumors. As shown by Park et al. the target cell should present at least $1x10^5$ receptors to control tumor growth using targeted liposomes. In these conditions VEGFR-2 targeting of liposomes may be therapeutically useful if they are used for the prevention of metastasis in combination with other forms of treatment that would address the growth of the initial tumor or the larger metastatic foci.

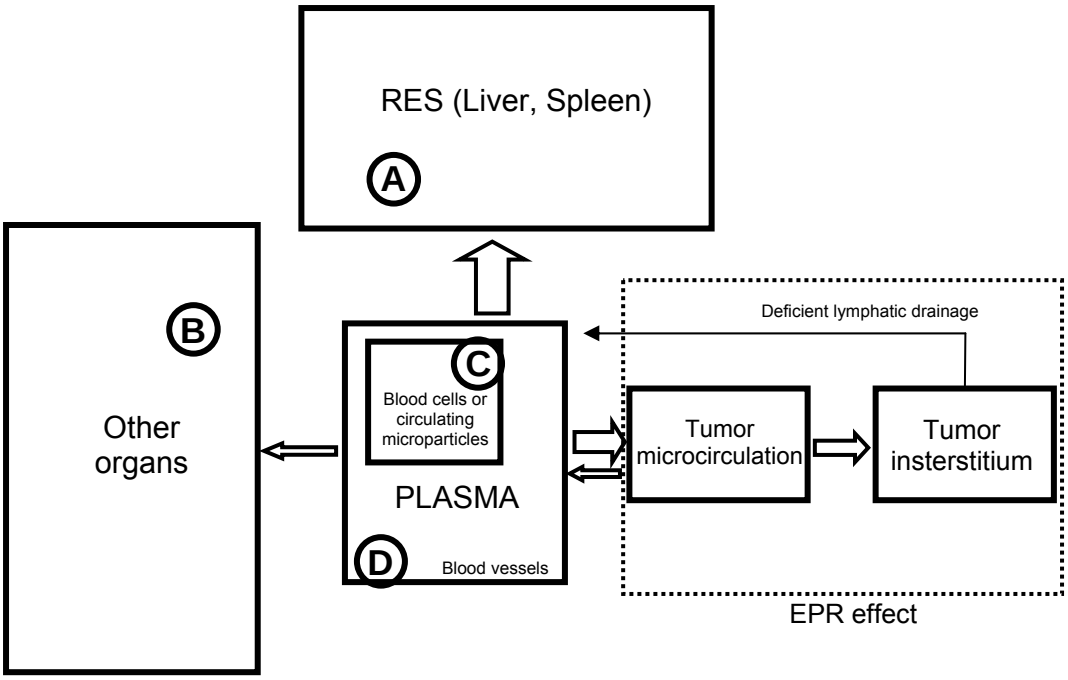

Fig. 6_1: Long circulating liposomes and targeting them to the tumor environment

The advantage of encapsulating drugs in PEG coated liposomes derives from the pharmacokinetics and biodistribution modification. The liposomes are long circulating and restricted to the intravascular space and the drugs are not distributed anymore to the whole body. Due to the EPR effect the liposomes passively homed to the tumor interstitium. The EPR effect is due to a leakiness of the tumor microcirculation and a deficient lymphatic drainage. The price for this advantage is a higher accumulation of the drug into the RES (liver, spleen) compared with free drug administration.

A-D = Possible interaction sites that have influenced negatively the passive targeting of the liposomes when conjugated to VEGFR-2, PS, or PE binding ligands. All these interactions decrease the amount of liposomes available to penetrate into the tumor interstitium.

A) – VEGFR-2 in the liver
   – PS and PE in the liver and spleen
B) – VEGFR-2 in the lungs and kidney
   – PS and PE in lungs, gut
C) – PS and PE on aged RBCs, activated platelets, circulating microparticles
D) – VEGFR-2 on normal vasculature

BIBLIOGRAPHY

[1] J. Denekamp, Vascular attack as a therapeutic strategy for cancer, Cancer Metastasis Rev 9 (1990) 267-282.

[2] F.J. Burrows, P.E. Thorpe, Eradication of large solid tumors in mice with an immunotoxin directed against tumor vasculature, Proc Natl Acad Sci U S A 90 (1993) 8996-9000.

[3] S.P. Cooke, G.M. Boxer, L. Lawrence, R.B. Pedley, D.I. Spencer, R.H. Begent, K.A. Chester, A strategy for antitumor vascular therapy by targeting the vascular endothelial growth factor: receptor complex, Cancer Res 61 (2001) 3653-3659.

[4] L. Ke, H. Qu, J.A. Nagy, I.A. Eckelhoefer, E.M. Masse, A.M. Dvorak, H.F. Dvorak, Vascular targeting of solid and ascites tumours with antibodies to vascular endothelial growth factor, Eur J Cancer 32A (1996) 2467-2473.

[5] M. Prewett, J. Huber, Y. Li, A. Santiago, W. O'Connor, K. King, J. Overholser, A. Hooper, B. Pytowski, L. Witte, P. Bohlen, D.J. Hicklin, Antivascular endothelial growth factor receptor (fetal liver kinase 1) monoclonal antibody inhibits tumor angiogenesis and growth of several mouse and human tumors, Cancer Res 59 (1999) 5209-5218.

[6] Z. Zhu, L. Witte, Inhibition of tumor growth and metastasis by targeting tumor-associated angiogenesis with antagonists to the receptors of vascular endothelial growth factor, Invest New Drugs 17 (1999) 195-212.

[7] R.A. Brekken, J.P. Overholser, V.A. Stastny, J. Waltenberger, J.D. Minna, P.E. Thorpe, Selective inhibition of vascular endothelial growth factor (VEGF) receptor 2 (KDR/Flk-1) activity by a monoclonal anti-VEGF antibody blocks tumor growth in mice, Cancer Res 60 (2000) 5117-5124.

[8] L. Huminiecki, M. Gorn, S. Suchting, R. Poulsom, R. Bicknell, Magic roundabout is a new member of the roundabout receptor family that is endothelial specific and expressed at sites of active angiogenesis, Genomics 79 (2002) 547-552.

[9] B. Carnemolla, E. Balza, A. Siri, L. Zardi, M.R. Nicotra, A. Bigotti, P.G. Natali, A tumor-associated fibronectin isoform generated by alternative splicing of messenger RNA precursors, J Cell Biol 108 (1989) 1139-1148.

[10] J. Kaczmarek, P. Castellani, G. Nicolo, B. Spina, G. Allemanni, L. Zardi, Distribution of oncofetal fibronectin isoforms in normal, hyperplastic and neoplastic human breast tissues, Int J Cancer 59 (1994) 11-16.

[11] B. Carnemolla, D. Neri, P. Castellani, A. Leprini, G. Neri, A. Pini, G. Winter, L. Zardi, Phage antibodies with pan-species recognition of the oncofoetal angiogenesis marker fibronectin ED-B domain, Int J Cancer 68 (1996) 397-405.

[12] P. Castellani, L. Borsi, B. Carnemolla, A. Biro, A. Dorcaratto, G.L. Viale, D. Neri, L. Zardi, Differentiation between high- and low-grade astrocytoma using a human recombinant antibody to the extra domain-B of fibronectin, Am J Pathol 161 (2002) 1695-1700.

[13] S. Christian, H. Ahorn, A. Koehler, F. Eisenhaber, H.P. Rodi, P. Garin-Chesa, J.E. Park, W.J. Rettig, M.C. Lenter, Molecular cloning and characterization of endosialin, a C-type lectin-like cell surface receptor of tumor endothelium, J Biol Chem 276 (2001) 7408-7414.

[14] M. Friedlander, P.C. Brooks, R.W. Shaffer, C.M. Kincaid, J.A. Varner, D.A. Cheresh, Definition of two angiogenic pathways by distinct alpha v integrins, Science 270 (1995) 1500-1502.

[15] J.D. Hood, M. Bednarski, R. Frausto, S. Guccione, R.A. Reisfeld, R. Xiang, D.A. Cheresh, Tumor regression by targeted gene delivery to the neovasculature, Science 296 (2002) 2404-2407.

[16] S.S. Chang, V.E. Reuter, W.D. Heston, N.H. Bander, L.S. Grauer, P.B. Gaudin, Five different anti-prostate-specific membrane antigen (PSMA) antibodies confirm PSMA expression in tumor-associated neovasculature, Cancer Res 59 (1999) 3192-3198.

[17] H. Liu, P. Moy, S. Kim, Y. Xia, A. Rajasekaran, V. Navarro, B. Knudsen, N.H. Bander, Monoclonal antibodies to the extracellular domain of prostate-specific membrane antigen also react with tumor vascular endothelium, Cancer Res 57 (1997) 3629-3634.

[18] J.M. Wang, S. Kumar, D. Pye, A.J. van Agthoven, J. Krupinski, R.D. Hunter, A monoclonal antibody detects heterogeneity in vascular endothelium of tumours and normal tissues, Int J Cancer 54 (1993) 363-370.

[19] Y. Wakai, J. Matsui, K. Koizumi, S. Tsunoda, H. Makimoto, I. Ohizumi, K. Taniguchi, S. Kaiho, H. Saito, N. Utoguchi, Y. Tsutsumi, S. Nakagawa, Y. Ohsugi, T. Mayumi, Effective cancer targeting using an anti-tumor tissue vascular endothelium-specific monoclonal antibody (TES-23), Jpn J Cancer Res 91 (2000) 1319-1325.

[20] P.K. Borjesson, E.J. Postema, J.C. Roos, D.R. Colnot, H.A. Marres, M.H. van Schie, G. Stehle, R. de Bree, G.B. Snow, W.J. Oyen, G.A. van Dongen, Phase I therapy study with (186)Re-labeled humanized monoclonal antibody BIWA 4 (bivatuzumab) in patients with head and neck squamous cell carcinoma, Clin Cancer Res 9 (2003) 3961S-3972S.

[21] Y. Sato, Role of aminopeptidase in angiogenesis, Biol Pharm Bull 27 (2004) 772-776.

[22] D.C. Sullivan, L. Huminiecki, J.W. Moore, J.J. Boyle, R. Poulsom, D. Creamer, J. Barker, R. Bicknell, EndoPDI, a novel protein-disulfide

isomerase-like protein that is preferentially expressed in endothelial cells acts as a stress survival factor, J Biol Chem 278 (2003) 47079-47088.

[23] S. Ran, B. Gao, S. Duffy, L. Watkins, N. Rote, P.E. Thorpe, Infarction of solid Hodgkin's tumors in mice by antibody-directed targeting of tissue factor to tumor vasculature, Cancer Res 58 (1998) 4646-4653.

[24] S. Ran, A. Downes, P.E. Thorpe, Increased exposure of anionic phospholipids on the surface of tumor blood vessels, Cancer Res 62 (2002) 6132-6140.

[25] S. Ran, J. He, X. Huang, M. Soares, D. Scothorn, P.E. Thorpe, Antitumor effects of a monoclonal antibody that binds anionic phospholipids on the surface of tumor blood vessels in mice, Clin Cancer Res 11 (2005) 1551-1562.

[26] S. Ran, P.E. Thorpe, Phosphatidylserine is a marker of tumor vasculature and a potential target for cancer imaging and therapy, Int J Radiat Oncol Biol Phys 54 (2002) 1479-1484.

[27] P. Oh, Y. Li, J. Yu, E. Durr, K.M. Krasinska, L.A. Carver, J.E. Testa, J.E. Schnitzer, Subtractive proteomic mapping of the endothelial surface in lung and solid tumours for tissue-specific therapy, Nature 429 (2004) 629-635.

[28] B. St Croix, C. Rago, V. Velculescu, G. Traverso, K.E. Romans, E. Montgomery, A. Lal, G.J. Riggins, C. Lengauer, B. Vogelstein, K.W. Kinzler, Genes expressed in human tumor endothelium, Science 289 (2000) 1197-1202.

[29] R. Pasqualini, E. Koivunen, E. Ruoslahti, Alpha v integrins as receptors for tumor targeting by circulating ligands, Nat Biotechnol 15 (1997) 542-546.

[30] D.A. Daniels, H. Chen, B.J. Hicke, K.M. Swiderek, L. Gold, A tenascin-C aptamer identified by tumor cell SELEX: systematic evolution of ligands by exponential enrichment, Proc Natl Acad Sci U S A 100 (2003) 15416-15421.

[31] A.D. Ellington, J.W. Szostak, Selection *in vitro* of single-stranded DNA molecules that fold into specific ligand-binding structures, Nature 355 (1992) 850-852.

[32] S.B. Shuker, P.J. Hajduk, R.P. Meadows, S.W. Fesik, Discovering high-affinity ligands for proteins: SAR by NMR, Science 274 (1996) 1531-1534.

[33] S. Melkko, J. Scheuermann, C.E. Dumelin, D. Neri, Encoded self-assembling chemical libraries, Nat Biotechnol 22 (2004) 568-574.

[34] S. Ran, K.A. Mohamedali, T.A. Luster, P.E. Thorpe, M.G. Rosenblum, The vascular-ablative agent VEGF(121)/rGel inhibits pulmonary metastases of MDA-MB-231 breast tumors, Neoplasia 7 (2005) 486-496.

[35] L.M. Veenendaal, H. Jin, S. Ran, L. Cheung, N. Navone, J.W. Marks, J. Waltenberger, P. Thorpe, M.G. Rosenblum, *In vitro* and *in vivo* studies of a VEGF121/rGelonin chimeric fusion toxin targeting the neovasculature of solid tumors, Proc Natl Acad Sci U S A 99 (2002) 7866-7871.

[36] G. Gregoriadis, P.D. Leathwood, B.E. Ryman, Enzyme entrapment in liposomes, FEBS Lett 14 (1971) 95-99.

[37] G. Gregoriadis, B.E. Ryman, Liposomes as carriers of enzymes or drugs: a new approach to the treatment of storage diseases, Biochem J 124 (1971) 58P.

[38] N. Emanuel, E. Kedar, E.M. Bolotin, N.I. Smorodinsky, Y. Barenholz, Targeted delivery of doxorubicin via sterically stabilized immunoliposomes: pharmacokinetics and biodistribution in tumor-bearing mice, Pharm Res 13 (1996) 861-868.

[39] N. Emanuel, E. Kedar, E.M. Bolotin, N.I. Smorodinsky, Y. Barenholz, Preparation and characterization of doxorubicin-loaded sterically stabilized immunoliposomes, Pharm Res 13 (1996) 352-359.

[40] A. Schnyder, S. Krahenbuhl, J. Drewe, J. Huwyler, Targeting of daunomycin using biotinylated immunoliposomes: pharmacokinetics, tissue distribution and *in vitro* pharmacological effects, J Drug Target 13 (2005) 325-335.

[41] H. Song, J. Zhang, Z. Han, X. Zhang, Z. Li, L. Zhang, M. Fu, C. Lin, J. Ma, Pharmacokinetic and cytotoxic studies of pegylated liposomal daunorubicin, Cancer Chemother Pharmacol 57 (2006) 591-598.

[42] A. Gabizon, R. Isacson, E. Libson, B. Kaufman, B. Uziely, R. Catane, C.G. Ben-Dor, E. Rabello, Y. Cass, T. Peretz, et al., Clinical studies of liposome-encapsulated doxorubicin, Acta Oncol 33 (1994) 779-786.

[43] A. Gabizon, R. Catane, B. Uziely, B. Kaufman, T. Safra, R. Cohen, F. Martin, A. Huang, Y. Barenholz, Prolonged circulation time and enhanced accumulation in malignant exudates of doxorubicin encapsulated in polyethylene-glycol coated liposomes, Cancer Res 54 (1994) 987-992.

[44] A. Eberhard, S. Kahlert, V. Goede, B. Hemmerlein, K.H. Plate, H.G. Augustin, Heterogeneity of angiogenesis and blood vessel maturation in human tumors: implications for antiangiogenic tumor therapies, Cancer Res 60 (2000) 1388-1393.

[45] D.M. McDonald, P.L. Choyke, Imaging of angiogenesis: from microscope to clinic, Nat Med 9 (2003) 713-725.

[46] G.M. Tozer, S.M. Ameer-Beg, J. Baker, P.R. Barber, S.A. Hill, R.J. Hodgkiss, R. Locke, V.E. Prise, I. Wilson, B. Vojnovic, Intravital imaging of tumour vascular networks using multi-photon fluorescence microscopy, Adv Drug Deliv Rev 57 (2005) 135-152.

[47] G.M. Tozer, S. Lewis, A. Michalowski, V. Aber, The relationship between regional variations in blood flow and histology in a transplanted rat fibrosarcoma, Br J Cancer 61 (1990) 250-257.
[48] H. Hashizume, P. Baluk, S. Morikawa, J.W. McLean, G. Thurston, S. Roberge, R.K. Jain, D.M. McDonald, Openings between defective endothelial cells explain tumor vessel leakiness, Am J Pathol 156 (2000) 1363-1380.
[49] E. Ruoslahti, Specialization of tumour vasculature, Nat Rev Cancer 2 (2002) 83-90.
[50] F. Yuan, M. Dellian, D. Fukumura, M. Leunig, D.A. Berk, V.P. Torchilin, R.K. Jain, Vascular permeability in a human tumor xenograft: molecular size dependence and cutoff size, Cancer Res 55 (1995) 3752-3756.
[51] J.W. McLean, E.A. Fox, P. Baluk, P.B. Bolton, A. Haskell, R. Pearlman, G. Thurston, E.Y. Umemoto, D.M. McDonald, Organ-specific endothelial cell uptake of cationic liposome-DNA complexes in mice, Am J Physiol 273 (1997) H387-404.
[52] G. Thurston, J.W. McLean, M. Rizen, P. Baluk, A. Haskell, T.J. Murphy, D. Hanahan, D.M. McDonald, Cationic liposomes target angiogenic endothelial cells in tumors and chronic inflammation in mice, J Clin Invest 101 (1998) 1401-1413.
[53] R.B. Campbell, D. Fukumura, E.B. Brown, L.M. Mazzola, Y. Izumi, R.K. Jain, V.P. Torchilin, L.L. Munn, Cationic charge determines the distribution of liposomes between the vascular and extravascular compartments of tumors, Cancer Res 62 (2002) 6831-6836.
[54] S. Krasnici, A. Werner, M.E. Eichhorn, M. Schmitt-Sody, S.A. Pahernik, B. Sauer, B. Schulze, M. Teifel, U. Michaelis, K. Naujoks, M. Dellian, Effect of the surface charge of liposomes on their uptake by angiogenic tumor vessels, Int J Cancer 105 (2003) 561-567.
[55] R. Kunstfeld, G. Wickenhauser, U. Michaelis, M. Teifel, W. Umek, K. Naujoks, K. Wolff, P. Petzelbauer, Paclitaxel encapsulated in cationic liposomes diminishes tumor angiogenesis and melanoma growth in a "humanized" SCID mouse model, J Invest Dermatol 120 (2003) 476-482.
[56] S. Strieth, M.E. Eichhorn, B. Sauer, B. Schulze, M. Teifel, U. Michaelis, M. Dellian, Neovascular targeting chemotherapy: encapsulation of paclitaxel in cationic liposomes impairs functional tumor microvasculature, Int J Cancer 110 (2004) 117-124.
[57] M.E. Eichhorn, S. Becker, S. Strieth, A. Werner, B. Sauer, M. Teifel, H. Ruhstorfer, U. Michaelis, J. Griebel, G. Brix, K.W. Jauch, M. Dellian, Paclitaxel encapsulated in cationic lipid complexes (MBT-0206) impairs functional tumor vascular properties as detected by dynamic contrast enhanced magnetic resonance imaging, Cancer Biol Ther 5 (2006) 89-96.

[58] H.G. Augustin, K. Braun, I. Telemenakis, U. Modlich, W. Kuhn, Ovarian angiogenesis. Phenotypic characterization of endothelial cells in a physiological model of blood vessel growth and regression, Am J Pathol 147 (1995) 339-351.
[59] H. Jin, J. Varner, Integrins: roles in cancer development and as treatment targets, Br J Cancer 90 (2004) 561-565.
[60] A.P. Janssen, R.M. Schiffelers, T.L. ten Hagen, G.A. Koning, A.J. Schraa, R.J. Kok, G. Storm, G. Molema, Peptide-targeted PEG-liposomes in anti-angiogenic therapy, Int J Pharm 254 (2003) 55-58.
[61] R.M. Schiffelers, G.A. Koning, T.L. ten Hagen, M.H. Fens, A.J. Schraa, A.P. Janssen, R.J. Kok, G. Molema, G. Storm, Anti-tumor efficacy of tumor vasculature-targeted liposomal doxorubicin, J Control Release 91 (2003) 115-122.
[62] G.A. Koning, M.M. Fretz, U. Woroniecka, G. Storm, G.C. Krijger, Targeting liposomes to tumor endothelial cells for neutron capture therapy, Appl Radiat Isot 61 (2004) 963-967.
[63] W. Arap, R. Pasqualini, E. Ruoslahti, Cancer treatment by targeted drug delivery to tumor vasculature in a mouse model, Science 279 (1998) 377-380.
[64] R. Pasqualini, E. Koivunen, R. Kain, J. Lahdenranta, M. Sakamoto, A. Stryhn, R.A. Ashmun, L.H. Shapiro, W. Arap, E. Ruoslahti, Aminopeptidase N is a receptor for tumor-homing peptides and a target for inhibiting angiogenesis, Cancer Res 60 (2000) 722-727.
[65] H. Fujii, M. Nakajima, I. Saiki, J. Yoneda, I. Azuma, T. Tsuruo, Human melanoma invasion and metastasis enhancement by high expression of aminopeptidase N/CD13, Clin Exp Metastasis 13 (1995) 337-344.
[66] F. Pastorino, C. Brignole, D. Marimpietri, M. Cilli, C. Gambini, D. Ribatti, R. Longhi, T.M. Allen, A. Corti, M. Ponzoni, Vascular damage and anti-angiogenic effects of tumor vessel-targeted liposomal chemotherapy, Cancer Res 63 (2003) 7400-7409.
[67] P. Osenkowski, M. Toth, R. Fridman, Processing, shedding, and endocytosis of membrane type 1-matrix metalloproteinase (MT1-MMP), J Cell Physiol 200 (2004) 2-10.
[68] N.E. Sounni, E.N. Baramova, C. Munaut, E. Maquoi, F. Frankenne, J.M. Foidart, A. Noel, Expression of membrane type 1 matrix metalloproteinase (MT1-MMP) in A2058 melanoma cells is associated with MMP-2 activation and increased tumor growth and vascularization, Int J Cancer 98 (2002) 23-28.
[69] K. Holmbeck, P. Bianco, J. Caterina, S. Yamada, M. Kromer, S.A. Kuznetsov, M. Mankani, P.G. Robey, A.R. Poole, I. Pidoux, J.M. Ward, H. Birkedal-Hansen, MT1-MMP-deficient mice develop dwarfism,

osteopenia, arthritis, and connective tissue disease due to inadequate collagen turnover, Cell 99 (1999) 81-92.
[70] V. Chiarugi, L. Magnelli, P. Dello Sbarba, M. Ruggiero, Tumor angiogenesis: thrombin and metalloproteinases in focus, Exp Mol Pathol 69 (2000) 63-66.
[71] M.A. Lafleur, M.M. Handsley, D.R. Edwards, Metalloproteinases and their inhibitors in angiogenesis, Expert Rev Mol Med 5 (2003) 1-39.
[72] M.A. Lafleur, M.M. Handsley, V. Knauper, G. Murphy, D.R. Edwards, Endothelial tubulogenesis within fibrin gels specifically requires the activity of membrane-type-matrix metalloproteinases (MT-MMPs), J Cell Sci 115 (2002) 3427-3438.
[73] M. Kondo, T. Asai, Y. Katanasaka, Y. Sadzuka, H. Tsukada, K. Ogino, T. Taki, K. Baba, N. Oku, Anti-neovascular therapy by liposomal drug targeted to membrane type-1 matrix metalloproteinase, Int J Cancer 108 (2004) 301-306.
[74] H. Hatakeyama, H. Akita, E. Ishida, K. Hashimoto, H. Kobayashi, T. Aoki, J. Yasuda, K. Obata, H. Kikuchi, T. Ishida, H. Kiwada, H. Harashima, Tumor targeting of doxorubicin by anti-MT1-MMP antibody-modified PEG liposomes, Int J Pharm 342 (2007) 194-200.
[75] J.A. Madri, D. Graesser, Cell migration in the immune system: the evolving inter-related roles of adhesion molecules and proteinases, Dev Immunol 7 (2000) 103-116.
[76] M.V. Gulubova, Expression of cell adhesion molecules, their ligands and tumour necrosis factor alpha in the liver of patients with metastatic gastrointestinal carcinomas, Histochem J 34 (2002) 67-77.
[77] A.J. Staal-van den Brekel, F.B. Thunnissen, W.A. Buurman, E.F. Wouters, Expression of E-selectin, intercellular adhesion molecule (ICAM)-1 and vascular cell adhesion molecule (VCAM)-1 in non-small-cell lung carcinoma, Virchows Arch 428 (1996) 21-27.
[78] Y.B. Ding, G.Y. Chen, J.G. Xia, X.W. Zang, H.Y. Yang, L. Yang, Association of VCAM-1 overexpression with oncogenesis, tumor angiogenesis and metastasis of gastric carcinoma, World J Gastroenterol 9 (2003) 1409-1414.
[79] B. Hemmerlein, J. Scherbening, A. Kugler, H.J. Radzun, Expression of VCAM-1, ICAM-1, E- and P-selectin and tumour-associated macrophages in renal cell carcinoma, Histopathology 37 (2000) 78-83.
[80] S. Gosk, T. Moos, C. Gottstein, G. Bendas, VCAM-1 directed immunoliposomes selectively target tumor vasculature *in vivo*, Biochim Biophys Acta 1778 (2008) 854-863.
[81] M. Voinea, I. Manduteanu, E. Dragomir, M. Capraru, M. Simionescu, Immunoliposomes directed toward VCAM-1 interact specifically with

activated endothelial cells--a potential tool for specific drug delivery, Pharm Res 22 (2005) 1906-1917.

[82] F.J. Burrows, E.J. Derbyshire, P.L. Tazzari, P. Amlot, A.F. Gazdar, S.W. King, M. Letarte, E.S. Vitetta, P.E. Thorpe, Up-regulation of endoglin on vascular endothelial cells in human solid tumors: implications for diagnosis and therapy, Clin Cancer Res 1 (1995) 1623-1634.

[83] M. Jerkic, A. Rodriguez-Barbero, M. Prieto, M. Toporsian, M. Pericacho, J.V. Rivas-Elena, J. Obreo, A. Wang, F. Perez-Barriocanal, M. Arevalo, C. Bernabeu, M. Letarte, J.M. Lopez-Novoa, Reduced angiogenic responses in adult Endoglin heterozygous mice, Cardiovasc Res 69 (2006) 845-854.

[84] C. Li, I.N. Hampson, L. Hampson, P. Kumar, C. Bernabeu, S. Kumar, CD105 antagonizes the inhibitory signaling of transforming growth factor beta1 on human vascular endothelial cells, FASEB J 14 (2000) 55-64.

[85] T. Volkel, P. Holig, T. Merdan, R. Muller, R.E. Kontermann, Targeting of immunoliposomes to endothelial cells using a single-chain Fv fragment directed against human endoglin (CD105), Biochim Biophys Acta 1663 (2004) 158-166.

[86] N. Oku, T. Asai, K. Watanabe, K. Kuromi, M. Nagatsuka, K. Kurohane, H. Kikkawa, K. Ogino, M. Tanaka, D. Ishikawa, H. Tsukada, M. Momose, J. Nakayama, T. Taki, Anti-neovascular therapy using novel peptides homing to angiogenic vessels, Oncogene 21 (2002) 2662-2669.

[87] T. Asai, S. Miyazawa, N. Maeda, K. Hatanaka, Y. Katanasaka, K. Shimizu, S. Shuto, N. Oku, Antineovascular therapy with angiogenic vessel-targeted polyethyleneglycol-shielded liposomal DPP-CNDAC, Cancer Sci 99 (2008) 1029-1033.

[88] S. Yonezawa, T. Asai, N. Oku, Effective tumor regression by anti-neovascular therapy in hypovascular orthotopic pancreatic tumor model, J Control Release 118 (2007) 303-309.

[89] P. Roth, C. Hammer, A.C. Piguet, M. Ledermann, J.F. Dufour, E. Waelti, Effects on hepatocellular carcinoma of doxorubicin-loaded immunoliposomes designed to target the VEGFR-2, J Drug Target 15 (2007) 623-631.

[90] P. Vajkoczy, M.D. Menger, B. Vollmar, L. Schilling, P. Schmiedek, K.P. Hirth, A. Ullrich, T.A. Fong, Inhibition of tumor growth, angiogenesis, and microcirculation by the novel Flk-1 inhibitor SU5416 as assessed by intravital multi-fluorescence videomicroscopy, Neoplasia 1 (1999) 31-41.

[91] A.D. Laird, P. Vajkoczy, L.K. Shawver, A. Thurnher, C. Liang, M. Mohammadi, J. Schlessinger, A. Ullrich, S.R. Hubbard, R.A. Blake, T.A. Fong, L.M. Strawn, L. Sun, C. Tang, R. Hawtin, F. Tang, N. Shenoy, K.P. Hirth, G. McMahon, Cherrington, SU6668 is a potent antiangiogenic and

antitumor agent that induces regression of established tumors, Cancer Res 60 (2000) 4152-4160.
[92] S. Ran, X. Huang, A. Downes, P.E. Thorpe, Evaluation of novel antimouse VEGFR2 antibodies as potential antiangiogenic or vascular targeting agents for tumor therapy, Neoplasia 5 (2003) 297-307.
[93] T.A. Luster, J. He, X. Huang, S.N. Maiti, A.J. Schroit, P.G. de Groot, P.E. Thorpe, Plasma protein beta-2-glycoprotein 1 mediates interaction between the anti-tumor monoclonal antibody 3G4 and anionic phospholipids on endothelial cells, J Biol Chem 281 (2006) 29863-29871.
[94] K. Emoto, N. Toyama-Sorimachi, H. Karasuyama, K. Inoue, M. Umeda, Exposure of phosphatidylethanolamine on the surface of apoptotic cells, Exp Cell Res 232 (1997) 430-434.
[95] T. Ishida, M.J. Kirchmeier, E.H. Moase, S. Zalipsky, T.M. Allen, Targeted delivery and triggered release of liposomal doxorubicin enhances cytotoxicity against human B lymphoma cells, Biochim Biophys Acta 1515 (2001) 144-158.
[96] M.B. Bally, R. Nayar, D. Masin, M.J. Hope, P.R. Cullis, L.D. Mayer, Liposomes with entrapped doxorubicin exhibit extended blood residence times, Biochim Biophys Acta 1023 (1990) 133-139.
[97] A.A. Gabizon, Y. Barenholz, M. Bialer, Prolongation of the circulation time of doxorubicin encapsulated in liposomes containing a polyethylene glycol-derivatized phospholipid: pharmacokinetic studies in rodents and dogs, Pharm Res 10 (1993) 703-708.
[98] E. Mayhew, Y.M. Rustum, F. Szoka, D. Papahadjopoulos, Role of cholesterol in enhancing the antitumor activity of cytosine arabinoside entrapped in liposomes, Cancer Treat Rep 63 (1979) 1923-1928.
[99] T.M. Allen, L.G. Cleland, Serum-induced leakage of liposome contents, Biochim Biophys Acta 597 (1980) 418-426.
[100] D. Needham, T.J. McIntosh, D.D. Lasic, Repulsive interactions and mechanical stability of polymer-grafted lipid membranes, Biochim Biophys Acta 1108 (1992) 40-48.
[101] T.M. Allen, A. Chonn, Large unilamellar liposomes with low uptake into the reticuloendothelial system, FEBS Lett 223 (1987) 42-46.
[102] D. Papahadjopoulos, T.M. Allen, A. Gabizon, E. Mayhew, K. Matthay, S.K. Huang, K.D. Lee, M.C. Woodle, D.D. Lasic, C. Redemann, et al., Sterically stabilized liposomes: improvements in pharmacokinetics and antitumor therapeutic efficacy, Proc Natl Acad Sci U S A 88 (1991) 11460-11464.
[103] M.C. Woodle, D.D. Lasic, Sterically stabilized liposomes, Biochim Biophys Acta 1113 (1992) 171-199.

[104] A. Gabizon, D. Papahadjopoulos, Liposome formulations with prolonged circulation time in blood and enhanced uptake by tumors, Proc Natl Acad Sci U S A 85 (1988) 6949-6953.
[105] A.L. Klibanov, K. Maruyama, V.P. Torchilin, L. Huang, Amphipathic polyethyleneglycols effectively prolong the circulation time of liposomes, FEBS Lett 268 (1990) 235-237.
[106] T.M. Allen, C. Hansen, F. Martin, C. Redemann, A. Yau-Young, Liposomes containing synthetic lipid derivatives of poly(ethylene glycol) show prolonged circulation half-lives *in vivo*, Biochim Biophys Acta 1066 (1991) 29-36.
[107] M.S. Webb, D. Saxon, F.M. Wong, H.J. Lim, Z. Wang, M.B. Bally, L.S. Choi, P.R. Cullis, L.D. Mayer, Comparison of different hydrophobic anchors conjugated to poly(ethylene glycol): effects on the pharmacokinetics of liposomal vincristine, Biochim Biophys Acta 1372 (1998) 272-282.
[108] D.C. Drummond, O. Meyer, K. Hong, D.B. Kirpotin, D. Papahadjopoulos, Optimizing liposomes for delivery of chemotherapeutic agents to solid tumors, Pharmacol Rev 51 (1999) 691-743.
[109] F. Szoka, Jr., D. Papahadjopoulos, Procedure for preparation of liposomes with large internal aqueous space and high capture by reverse-phase evaporation, Proc Natl Acad Sci U S A 75 (1978) 4194-4198.
[110] M.H. Milsmann, R.A. Schwendener, H.G. Weder, The preparation of large single bilayer liposomes by a fast and controlled dialysis, Biochim Biophys Acta 512 (1978) 147-155.
[111] D. Papahadjopoulos, J.C. Watkins, Phospholipid model membranes. II. Permeability properties of hydrated liquid crystals, Biochim Biophys Acta 135 (1967) 639-652.
[112] F. Olson, C.A. Hunt, F.C. Szoka, W.J. Vail, D. Papahadjopoulos, Preparation of liposomes of defined size distribution by extrusion through polycarbonate membranes, Biochim Biophys Acta 557 (1979) 9-23.
[113] L.D. Mayer, M.J. Hope, P.R. Cullis, Vesicles of variable sizes produced by a rapid extrusion procedure, Biochim Biophys Acta 858 (1986) 161-168.
[114] D.D. Lasic, P.M. Frederik, M.C. Stuart, Y. Barenholz, T.J. McIntosh, Gelation of liposome interior. A novel method for drug encapsulation, FEBS Lett 312 (1992) 255-258.
[115] D.D. Lasic, B. Ceh, M.C. Stuart, L. Guo, P.M. Frederik, Y. Barenholz, Transmembrane gradient driven phase transitions within vesicles: lessons for drug delivery, Biochim Biophys Acta 1239 (1995) 145-156.

[116] R.M. Straubinger, D. Papahadjopoulos, K.L. Hong, Endocytosis and intracellular fate of liposomes using pyranine as a probe, Biochemistry 29 (1990) 4929-4939.
[117] C.M. Biegel, J.M. Gould, Kinetics of hydrogen ion diffusion across phospholipid vesicle membranes, Biochemistry 20 (1981) 3474-3479.
[118] R.M. Straubinger, N.G. Lopez, R.J. Debs, K. Hong, D. Papahadjopoulos, Liposome-based therapy of human ovarian cancer: parameters determining potency of negatively charged and antibody-targeted liposomes, Cancer Res 48 (1988) 5237-5245.
[119] C.B. Hansen, G.Y. Kao, E.H. Moase, S. Zalipsky, T.M. Allen, Attachment of antibodies to sterically stabilized liposomes: evaluation, comparison and optimization of coupling procedures, Biochim Biophys Acta 1239 (1995) 133-144.
[120] F.J. Martin, W.L. Hubbell, D. Papahadjopoulos, Immunospecific targeting of liposomes to cells: a novel and efficient method for covalent attachment of Fab' fragments via disulfide bonds, Biochemistry 20 (1981) 4229-4238.
[121] F.J. Martin, D. Papahadjopoulos, Irreversible coupling of immunoglobulin fragments to preformed vesicles. An improved method for liposome targeting, J Biol Chem 257 (1982) 286-288.
[122] A. Desormeaux, M.G. Bergeron, Lymphoid tissue targeting of anti-HIV drugs using liposomes, Methods Enzymol 391 (2005) 330-351.
[123] O. Garbuzenko, Y. Barenholz, A. Priev, Effect of grafted PEG on liposome size and on compressibility and packing of lipid bilayer, Chem Phys Lipids 135 (2005) 117-129.
[124] O. Tirosh, Y. Barenholz, J. Katzhendler, A. Priev, Hydration of polyethylene glycol-grafted liposomes, Biophys J 74 (1998) 1371-1379.
[125] P. Carmeliet, VEGF as a key mediator of angiogenesis in cancer, Oncology 69 Suppl 3 (2005) 4-10.
[126] M.A. Konerding, E. Fait, A. Gaumann, 3D microvascular architecture of pre-cancerous lesions and invasive carcinomas of the colon, Br J Cancer 84 (2001) 1354-1362.
[127] N. Ferrara, H.P. Gerber, J. LeCouter, The biology of VEGF and its receptors, Nat Med 9 (2003) 669-676.
[128] Y. Harada, Y. Ogata, K. Shirouzu, Expression of vascular endothelial growth factor and its receptor KDR (kinase domain-containing receptor)/Flk-1 (fetal liver kinase-1) as prognostic factors in human colorectal cancer, Int J Clin Oncol 6 (2001) 221-228.
[129] F. Pastorino, C. Brignole, D. Marimpietri, P. Sapra, E.H. Moase, T.M. Allen, M. Ponzoni, Doxorubicin-loaded Fab' fragments of anti-disialoganglioside immunoliposomes selectively inhibit the growth and

dissemination of human neuroblastoma in nude mice, Cancer Res 63 (2003) 86-92.
[130] P. Sapra, T.M. Allen, Internalizing antibodies are necessary for improved therapeutic efficacy of antibody-targeted liposomal drugs, Cancer Res 62 (2002) 7190-7194.
[131] J.N. Moreira, C.B. Hansen, R. Gaspar, T.M. Allen, A growth factor antagonist as a targeting agent for sterically stabilized liposomes in human small cell lung cancer, Biochim Biophys Acta 1514 (2001) 303-317.
[132] J.N. Moreira, R. Gaspar, T.M. Allen, Targeting Stealth liposomes in a murine model of human small cell lung cancer, Biochim Biophys Acta 1515 (2001) 167-176.
[133] J.N. Moreira, R. Gaspar, Antagonist G-mediated targeting and cytotoxicity of liposomal doxorubicin in NCI-H82 variant small cell lung cancer, Braz J Med Biol Res 37 (2004) 1185-1192.
[134] K.R. Gehlsen, G.E. Davis, P. Sriramarao, Integrin expression in human melanoma cells with differing invasive and metastatic properties, Clin Exp Metastasis 10 (1992) 111-120.
[135] G. Conforti, C. Dominguez-Jimenez, A. Zanetti, M.A. Gimbrone, Jr., O. Cremona, P.C. Marchisio, E. Dejana, Human endothelial cells express integrin receptors on the luminal aspect of their membrane, Blood 80 (1992) 437-446.
[136] A.S. Maharaj, M. Saint-Geniez, A.E. Maldonado, P.A. D'Amore, Vascular endothelial growth factor localization in the adult, Am J Pathol 168 (2006) 639-648.
[137] T. Inai, M. Mancuso, H. Hashizume, F. Baffert, A. Haskell, P. Baluk, D.D. Hu-Lowe, D.R. Shalinsky, G. Thurston, G.D. Yancopoulos, D.M. McDonald, Inhibition of vascular endothelial growth factor (VEGF) signaling in cancer causes loss of endothelial fenestrations, regression of tumor vessels, and appearance of basement membrane ghosts, Am J Pathol 165 (2004) 35-52.
[138] L.F. Brown, A.J. Guidi, S.J. Schnitt, L. Van De Water, M.L. Iruela-Arispe, T.K. Yeo, K. Tognazzi, H.F. Dvorak, Vascular stroma formation in carcinoma in situ, invasive carcinoma, and metastatic carcinoma of the breast, Clin Cancer Res 5 (1999) 1041-1056.
[139] J.W. Park, K. Hong, P. Carter, H. Asgari, L.Y. Guo, G.A. Keller, C. Wirth, R. Shalaby, C. Kotts, W.I. Wood, et al., Development of anti-p185HER2 immunoliposomes for cancer therapy, Proc Natl Acad Sci U S A 92 (1995) 1327-1331.
[140] X. Huang, M. Bennett, P.E. Thorpe, A monoclonal antibody that binds anionic phospholipids on tumor blood vessels enhances the antitumor

effect of docetaxel on human breast tumors in mice, Cancer Res 65 (2005) 4408-4416.
[141] J.C. Holthuis, T.P. Levine, Lipid traffic: floppy drives and a superhighway, Nat Rev Mol Cell Biol 6 (2005) 209-220.
[142] K. Balasubramanian, A.J. Schroit, Aminophospholipid asymmetry: A matter of life and death, Annu Rev Physiol 65 (2003) 701-734.
[143] D.L. Daleke, Regulation of transbilayer plasma membrane phospholipid asymmetry, J Lipid Res 44 (2003) 233-242.
[144] C.C. Paulusma, R.P. Oude Elferink, The type 4 subfamily of P-type ATPases, putative aminophospholipid translocases with a role in human disease, Biochim Biophys Acta 1741 (2005) 11-24.
[145] G. Morrot, P. Herve, A. Zachowski, P. Fellmann, P.F. Devaux, Aminophospholipid translocase of human erythrocytes: phospholipid substrate specificity and effect of cholesterol, Biochemistry 28 (1989) 3456-3462.
[146] P.F. Devaux, I. Lopez-Montero, S. Bryde, Proteins involved in lipid translocation in eukaryotic cells, Chem Phys Lipids 141 (2006) 119-132.
[147] T. Pomorski, J.C. Holthuis, A. Herrmann, G. van Meer, Tracking down lipid flippases and their biological functions, J Cell Sci 117 (2004) 805-813.
[148] Y. Hamon, C. Broccardo, O. Chambenoit, M.F. Luciani, F. Toti, S. Chaslin, J.M. Freyssinet, P.F. Devaux, J. McNeish, D. Marguet, G. Chimini, ABC1 promotes engulfment of apoptotic cells and transbilayer redistribution of phosphatidylserine, Nat Cell Biol 2 (2000) 399-406.
[149] A. Pohl, P.F. Devaux, A. Herrmann, Function of prokaryotic and eukaryotic ABC proteins in lipid transport, Biochim Biophys Acta 1733 (2005) 29-52.
[150] S.K. Sahu, S.N. Gummadi, N. Manoj, G.K. Aradhyam, Phospholipid scramblases: an overview, Arch Biochem Biophys 462 (2007) 103-114.
[151] P. Williamson, E.M. Bevers, E.F. Smeets, P. Comfurius, R.A. Schlegel, R.F. Zwaal, Continuous analysis of the mechanism of activated transbilayer lipid movement in platelets, Biochemistry 34 (1995) 10448-10455.
[152] P. Williamson, A. Christie, T. Kohlin, R.A. Schlegel, P. Comfurius, M. Harmsma, R.F. Zwaal, E.M. Bevers, Phospholipid scramblase activation pathways in lymphocytes, Biochemistry 40 (2001) 8065-8072.
[153] F.W. Orr, H.H. Wang, R.M. Lafrenie, S. Scherbarth, D.M. Nance, Interactions between cancer cells and the endothelium in metastasis, J Pathol 190 (2000) 310-329.
[154] L. Jin, R.Q. Yuan, A. Fuchs, Y. Yao, A. Joseph, R. Schwall, S.J. Schnitt, A. Guida, H.M. Hastings, J. Andres, G. Turkel, P.J. Polverini, I.D.

Goldberg, E.M. Rosen, Expression of interleukin-1beta in human breast carcinoma, Cancer 80 (1997) 421-434.
[155] S.G. Shaughnessy, M.R. Buchanan, S. Turple, M. Richardson, F.W. Orr, Walker carcinosarcoma cells damage endothelial cells by the generation of reactive oxygen species, Am J Pathol 134 (1989) 787-796.
[156] J.K. Leach, G. Van Tuyle, P.S. Lin, R. Schmidt-Ullrich, R.B. Mikkelsen, Ionizing radiation-induced, mitochondria-dependent generation of reactive oxygen/nitrogen, Cancer Res 61 (2001) 3894-3901.
[157] S.W. Ryter, H.P. Kim, A. Hoetzel, J.W. Park, K. Nakahira, X. Wang, A.M. Choi, Mechanisms of cell death in oxidative stress, Antioxid Redox Signal 9 (2007) 49-89.
[158] R.J. Musters, J.A. Post, A.J. Verkleij, The isolated neonatal rat-cardiomyocyte used in an *in vitro* model for 'ischemia'. I. A morphological study, Biochim Biophys Acta 1091 (1991) 270-277.
[159] R.J. Musters, E. Probstl-Biegelmann, T.A. van Veen, K.H. Hoebe, J.A. Op den Kamp, A.J. Verkleij, J.A. Post, Sarcolemmal phosphatidylethanolamine reorganization during simulated ischaemia and reperfusion: reversibility and ATP dependency, Mol Membr Biol 13 (1996) 159-164.
[160] H.A. Andree, C.P. Reutelingsperger, R. Hauptmann, H.C. Hemker, W.T. Hermens, G.M. Willems, Binding of vascular anticoagulant alpha (VAC alpha) to planar phospholipid bilayers, J Biol Chem 265 (1990) 4923-4928.
[161] J. He, T.A. Luster, P.E. Thorpe, Radiation-enhanced vascular targeting of human lung cancers in mice with a monoclonal antibody that binds anionic phospholipids, Clin Cancer Res 13 (2007) 5211-5218.
[162] K. Iwamoto, T. Hayakawa, M. Murate, A. Makino, K. Ito, T. Fujisawa, T. Kobayashi, Curvature-dependent recognition of ethanolamine phospholipids by duramycin and cinnamycin, Biophys J (2007).
[163] J. Navarro, J. Chabot, K. Sherrill, R. Aneja, S.A. Zahler, E. Racker, Interaction of duramycin with artificial and natural membranes, Biochemistry 24 (1985) 4645-4650.
[164] E.M. Bevers, R.F. Zwaal, G.M. Willems, The effect of phospholipids on the formation of immune complexes between autoantibodies and beta2-glycoprotein I or prothrombin, Clin Immunol 112 (2004) 150-160.
[165] E.M. Bevers, M.P. Janssen, P. Comfurius, K. Balasubramanian, A.J. Schroit, R.F. Zwaal, G.M. Willems, Quantitative determination of the binding of beta2-glycoprotein I and prothrombin to phosphatidylserine-exposing blood platelets, Biochem J 386 (2005) 271-279.
[166] G.M. Willems, M.P. Janssen, M.M. Pelsers, P. Comfurius, M. Galli, R.F. Zwaal, E.M. Bevers, Role of divalency in the high-affinity binding of

anticardiolipin antibody-beta 2-glycoprotein I complexes to lipid membranes, Biochemistry 35 (1996) 13833-13842.
[167] H. Kato, K. Enjyoji, Amino acid sequence and location of the disulfide bonds in bovine beta 2 glycoprotein I: the presence of five Sushi domains, Biochemistry 30 (1991) 11687-11694.
[168] M. Hoshino, Y. Hagihara, I. Nishii, T. Yamazaki, H. Kato, Y. Goto, Identification of the phospholipid-binding site of human beta(2)-glycoprotein I domain V by heteronuclear magnetic resonance, J Mol Biol 304 (2000) 927-939.
[169] B. Bouma, P.G. de Groot, J.M. van den Elsen, R.B. Ravelli, A. Schouten, M.J. Simmelink, R.H. Derksen, J. Kroon, P. Gros, Adhesion mechanism of human beta(2)-glycoprotein I to phospholipids based on its crystal structure, Embo J 18 (1999) 5166-5174.
[170] E. Matsuura, M. Igarashi, Y. Igarashi, H. Nagae, K. Ichikawa, T. Yasuda, T. Koike, Molecular definition of human beta 2-glycoprotein I (beta 2-GPI) by cDNA cloning and inter-species differences of beta 2-GPI in alternation of anticardiolipin binding, Int Immunol 3 (1991) 1217-1221.
[171] Y. Sheng, S.W. Reddel, H. Herzog, Y.X. Wang, T. Brighton, M.P. France, S.A. Robertson, S.A. Krilis, Impaired thrombin generation in beta 2-glycoprotein I null mice, J Biol Chem 276 (2001) 13817-13821.
[172] K. Emoto, M. Umeda, Membrane lipid control of cytokinesis, Cell Struct Funct 26 (2001) 659-665.
[173] K. Emoto, T. Kobayashi, A. Yamaji, H. Aizawa, I. Yahara, K. Inoue, M. Umeda, Redistribution of phosphatidylethanolamine at the cleavage furrow of dividing cells during cytokinesis, Proc Natl Acad Sci U S A 93 (1996) 12867-12872.
[174] K. Emoto, M. Umeda, An essential role for a membrane lipid in cytokinesis. Regulation of contractile ring disassembly by redistribution of phosphatidylethanolamine, J Cell Biol 149 (2000) 1215-1224.
[175] V. Hinkovska-Galcheva, D. Petkova, K. Koumanov, Changes in the phospholipid composition and phospholipid asymmetry of ram sperm plasma membranes after cryopreservation, Cryobiology 26 (1989) 70-75.
[176] R.O. Calderon, G.H. DeVries, Lipid composition and phospholipid asymmetry of membranes from a Schwann cell line, J Neurosci Res 49 (1997) 372-380.
[177] P. Zhang, M. Castedo, Y. Tao, D. Violot, D. Metivier, E. Deutsch, G. Kroemer, J. Bourhis, Caspase independence of radio-induced cell death, Oncogene 25 (2006) 7758-7770.
[178] R. Kolesnick, Z. Fuks, Radiation and ceramide-induced apoptosis, Oncogene 22 (2003) 5897-5906.

[179] P. Santana, L.A. Pena, A. Haimovitz-Friedman, S. Martin, D. Green, M. McLoughlin, C. Cordon-Cardo, E.H. Schuchman, Z. Fuks, R. Kolesnick, Acid sphingomyelinase-deficient human lymphoblasts and mice are defective in radiation-induced apoptosis, Cell 86 (1996) 189-199.
[180] L.A. Pena, Z. Fuks, R.N. Kolesnick, Radiation-induced apoptosis of endothelial cells in the murine central nervous system: protection by fibroblast growth factor and sphingomyelinase deficiency, Cancer Res 60 (2000) 321-327.
[181] A. Morales, H. Lee, F.M. Goni, R. Kolesnick, J.C. Fernandez-Checa, Sphingolipids and cell death, Apoptosis 12 (2007) 923-939.
[182] D.L. Daleke, W.H. Huestis, Incorporation and translocation of aminophospholipids in human erythrocytes, Biochemistry 24 (1985) 5406-5416.
[183] B. Verhoven, R.A. Schlegel, P. Williamson, Mechanisms of phosphatidylserine exposure, a phagocyte recognition signal, on apoptotic T lymphocytes, J Exp Med 182 (1995) 1597-1601.
[184] D.L. Daleke, Phospholipid flippases, J Biol Chem 282 (2007) 821-825.
[185] R.D. Kornberg, H.M. McConnell, Inside-outside transitions of phospholipids in vesicle membranes, Biochemistry 10 (1971) 1111-1120.
[186] Y. Taniguchi, T. Ohba, H. Miyata, K. Ohki, Rapid phase change of lipid microdomains in giant vesicles induced by conversion of sphingomyelin to ceramide, Biochim Biophys Acta 1758 (2006) 145-153.
[187] J.D. Lane, V.J. Allan, P.G. Woodman, Active relocation of chromatin and endoplasmic reticulum into blebs in late apoptotic cells, J Cell Sci 118 (2005) 4059-4071.
[188] X.L. An, Y. Takakuwa, S. Manno, B.G. Han, P. Gascard, N. Mohandas, Structural and functional characterization of protein 4.1R-phosphatidylserine interaction: potential role in 4.1R sorting within cells, J Biol Chem 276 (2001) 35778-35785.
[189] X. An, X. Zhang, G. Debnath, A.J. Baines, N. Mohandas, Phosphatidylinositol-4,5-biphosphate (PIP2) differentially regulates the interaction of human erythrocyte protein 4.1 (4.1R) with membrane proteins, Biochemistry 45 (2006) 5725-5732.
[190] S. Manno, Y. Takakuwa, N. Mohandas, Identification of a functional role for lipid asymmetry in biological membranes: Phosphatidylserine-skeletal protein interactions modulate membrane stability, Proc Natl Acad Sci U S A 99 (2002) 1943-1948.
[191] J. Dai, M.P. Sheetz, Membrane tether formation from blebbing cells, Biophys J 77 (1999) 3363-3370.
[192] M.P. Sheetz, Cell control by membrane-cytoskeleton adhesion, Nat Rev Mol Cell Biol 2 (2001) 392-396.

[193] J.A. McIntyre, D.R. Wagenknecht, W.P. Faulk, Antiphospholipid antibodies: discovery, definitions, detection and disease, Prog Lipid Res 42 (2003) 176-237.
[194] V. Combes, A.C. Simon, G.E. Grau, D. Arnoux, L. Camoin, F. Sabatier, M. Mutin, M. Sanmarco, J. Sampol, F. Dignat-George, *In vitro* generation of endothelial microparticles and possible prothrombotic activity in patients with lupus anticoagulant, J Clin Invest 104 (1999) 93-102.
[195] H.L. Staub, E.N. Harris, M.A. Khamashta, G. Savidge, W.H. Chahade, G.R. Hughes, Antibody to phosphatidylethanolamine in a patient with lupus anticoagulant and thrombosis, Ann Rheum Dis 48 (1989) 166-169.
[196] T. Sugi, J. Katsunuma, S. Izumi, J.A. McIntyre, T. Makino, Prevalence and heterogeneity of antiphosphatidylethanolamine antibodies in patients with recurrent early pregnancy losses, Fertil Steril 71 (1999) 1060-1065.
[197] J. Connor, C.C. Pak, A.J. Schroit, Exposure of phosphatidylserine in the outer leaflet of human red blood cells. Relationship to cell density, cell age, and clearance by mononuclear cells, J Biol Chem 269 (1994) 2399-2404.
[198] R.A. Schlegel, P. Williamson, Phosphatidylserine, a death knell, Cell Death Differ 8 (2001) 551-563.
[199] H.H. Boersma, I.H. Liem, G.J. Kemerink, P.W. Thimister, L. Hofstra, L.M. Stolk, W.L. van Heerde, M.T. Pakbiers, D. Janssen, A.J. Beysens, C.P. Reutelingsperger, G.A. Heidendal, Comparison between human pharmacokinetics and imaging properties of two conjugation methods for 99mTc-annexin A5, Br J Radiol 76 (2003) 553-560.
[200] P.W. Thimister, L. Hofstra, I.H. Liem, H.H. Boersma, G. Kemerink, C.P. Reutelingsperger, G.A. Heidendal, *In vivo* detection of cell death in the area at risk in acute myocardial infarction, J Nucl Med 44 (2003) 391-396.
[201] C. Kunzelmann-Marche, J.M. Freyssinet, M.C. Martinez, Regulation of phosphatidylserine transbilayer redistribution by store-operated Ca2+ entry: role of actin cytoskeleton, J Biol Chem 276 (2001) 5134-5139.
[202] B.R. Lentz, Exposure of platelet membrane phosphatidylserine regulates blood coagulation, Prog Lipid Res 42 (2003) 423-438.
[203] N.O. Solum, Procoagulant expression in platelets and defects leading to clinical disorders, Arterioscler Thromb Vasc Biol 19 (1999) 2841-2846.
[204] S.F. Lynch, C.A. Ludlam, Plasma microparticles and vascular disorders, Br J Haematol 137 (2007) 36-48.
[205] A. Piccin, W.G. Murphy, O.P. Smith, Circulating microparticles: pathophysiology and clinical implications, Blood Rev 21 (2007) 157-171.
[206] H. Maeda, J. Fang, T. Inutsuka, Y. Kitamoto, Vascular permeability enhancement in solid tumor: various factors, mechanisms involved and its implications, Int Immunopharmacol 3 (2003) 319-328.

[207] K. Hori, M. Suzuki, S. Tanda, S. Saito, M. Shinozaki, Q.H. Zhang, Fluctuations in tumor blood flow under normotension and the effect of angiotensin II-induced hypertension, Jpn J Cancer Res 82 (1991) 1309-1316.

[208] D.B. Kirpotin, D.C. Drummond, Y. Shao, M.R. Shalaby, K. Hong, U.B. Nielsen, J.D. Marks, C.C. Benz, J.W. Park, Antibody targeting of long-circulating lipidic nanoparticles does not increase tumor localization but does increase internalization in animal models, Cancer Res 66 (2006) 6732-6740.